MASTER THESIS

ENERGY TECHNOLOGY FOR SUSTAINABLE DEVELOPMENT

Techno-economic Analysis and Market Potential Study of Solar Heat in Industrial Processes

A Fresnel Direct Steam Generation case study

AUTHOR: **GUILLERMO DE SANTOS LÓPEZ**

TUTOR: RAFAEL GUÉDEZ MATA

Academic Year: 2020-21

"May 2021"

KTH Industrial Engineering and Management

Master of Science Thesis

Department of Energy Technology

KTH 2020

Techno-economic Analysis and Market Potential Study of Solar Heat in Industrial Processes

A Fresnel Direct Steam Generation case study

TRITA: ITM-EX 2021:86

Guillermo de Santos López

Approved	Examiner	Supervisor
Date 19/04/2021	Björn Laumert	Rafael Guédez Mata
	Industrial Supervisor	Contact person

Abstract

The industrial sector not only has a big contribution to global emissions but also a low share of renewable energy for heat demand. Knowing that most of the energy consumption in industry is heat and that half of it is at medium-low temperature (below 400 ºC), it is a great market for the integration of solar thermal technologies.

Following the criteria of high heat demand and low-temperature requirements, five promising industrial sectors and their processes have been analysed: food and beverage, paper and pulp, chemical, textile and mining. Steam generation at supply level has been considered one of the most promising systems considering its integration advantages and the potential of direct steam generation plants.

The market potential study has been geographically determined performing an MCA; countries all over the world have been assessed considering their heat consumption in the promising sectors and other conditions that enhance the SHIP feasibility such as solar radiation levels, favourable energy policies, previous experience in SHIP plants, ease of doing business, etc. The price of natural gas has been also considered after selecting Europe as a suitable market. The potential heat demand that this technology could cover has been estimated considering limitations as the competitiveness with other renewable heat sources, the expected heat recovery potential for some sectors, the solar fraction of the region and roof space of the factories. The results show that the five countries with bigger potential are Germany, France, Netherlands, Italy, and Spain, while the sectors with the most suitable market are food and beverage, and chemical.

A case study has been selected based on the previous conclusions: a Fresnel direct steam generation plant in Sevilla (Spain) characterized thanks to the data provided by the company Solatom. The plant has been modelled using the software TRNSYS, taking special consideration in the Fresnel performance, the dynamic steam drum behaviour and its influence on the start-up time of the plant.

The results achieved through the techno-economic analysis show that parameters such as solar radiation, conventional fuel prices and EU ETS prices have a major impact on the economic indicators. A sensitivity analysis shows that locations with radiation levels above 1750 kWh/m² have positive values for NPV, and above 2250 kWh/m² the cost of generating solar heating (LCOH) is under European natural gas prices. In addition to this, fuel prices above 50 €/MWh, which are common for SMEs, results in payback periods under 10 years. Future trends depict favourable scenarios as current European policies are causing a rapid growth of the ETS.

Therefore, solar heat in industrial processes can be a feasible alternative, or work as a complement, to conventional systems. Its deployment is driven by supportive policies, high radiation levels, costly fuels prices (such as the ones for SMEs) and the necessity of reducing GHG emissions and decrease the independence on fossil energies.

Keywords:

Solar heat in industrial processes, techno-economic analysis, market potential, direct steam generation, Fresnel technology.

Sammanfattning

Industrisektorn har inte bara ett stort bidrag till globala utsläpp utan också en låg andel förnybar energi för värmebehov. Att veta att det mesta av energiförbrukningen i industrin är värme och att hälften av den är vid medelhög låg temperatur (under 400ºC), är det en fantastisk marknad för integration av solvärmeteknik.

Enligt kriterierna för högt värmebehov och lågtemperaturkrav har fem lovande industrisektorer och deras processer analyserats: mat och dryck, papper och massa, kemikalier, textil och gruvdrift. Ånggenerering på leveransnivå har ansetts vara ett av de mest lovande systemen med tanke på dess integrationsfördelar och potentialen hos direkta ånggenereringsanläggningar.

Marknadspotentialstudien har fastställts geografiskt med en MCA; länder över hela världen har bedömts med tanke på deras värmeförbrukning i de lovande sektorerna och andra förhållanden som förbättrar SHIP-genomförbarheten, såsom solstrålningsnivåer, gynnsam energipolitik, tidigare erfarenhet av SHIP-anläggningar, lätt att göra affärer etc. Priset på naturgas har också övervägs efter valet av Europa som en lämplig marknad. Det potentiella värmebehovet som denna teknik kan täcka har uppskattats med tanke på begränsningar som konkurrenskraft med andra förnybara värmekällor, den förväntade värmeåtervinningspotentialen för vissa sektorer, solfraktionen i regionen och fabrikernas takutrymme. Resultaten visar att de fem länderna med större potential är Tyskland, Frankrike, Nederländerna, Italien och Spanien, medan de sektorer som har den mest lämpliga marknaden är mat och dryck samt kemikalier.

En fallstudie har valts utifrån de tidigare slutsatserna: en Fresnel-ångproduktionsanläggning i Sevilla (Spanien) som kännetecknas av uppgifterna från företaget. Anläggningen har modellerats med hjälp av programvaran TRNSYS, med särskild hänsyn till Fresnel-prestanda, det dynamiska ångtrummans beteende och dess inflytande på anläggningens starttid.

De resultat som uppnåtts genom den tekno-ekonomiska analysen visar att parametrar som solstrålning, konventionella bränslepriser och EU: s ETS-priser har stor inverkan på de ekonomiska indikatorerna. En känslighetsanalys visar att platser med strålningsvärden över 1750 kWh/m² har positiva värden för NPV och över 2250 kWh/m² är kostnaden för att generera solvärme (LCOH) under europeiska naturgaspriser. Utöver detta leder bränslepriser över 50 €/MWh, som är vanliga för små och medelstora företag, till återbetalningsperioder under tio år. Framtida trender visar gynnsamma scenarier eftersom europeisk politik orsakar en snabb tillväxt på ETS.

Därför kan solvärme i industriella processer vara ett genomförbart alternativ eller fungera som ett komplement till konventionella system. Dess utplacering drivs av stödjande politik, höga strålningsnivåer, dyra bränslepriser (som de för små och medelstora företag) och behovet av att minska växthusgasutsläppen och minska självständigheten för fossila energier.

Acknowledgements

First of all, I want to express how grateful I am for the opportunity that the Erasmus program has given to me, this period in Stockholm at the KTH has brought me a unique experience of expansion in the engineering field; a motivation to believe and contribute to the sustainable path which is, from my point of view, the only solution nowadays.

I want to give a special thanks to my tutor Rafael Guédez, for providing me with the chance of working in the promising field of solar heat in industry, guiding me through the thesis and introducing me to the SHC task and the Solatom company. I also appreciate the selfless help of Miguel Frasquet who has advised me and clear my doubts. I want to mention as well the contribution of Antonio Cazorla to this thesis, providing me useful resources and helpful opinion.

I could not have done my thesis without the previous work of researchers from which I have learnt and based part of this project. As it is a long list, I especially thanks Christoph Lauterbach, Soteris Kalogirou, Antoine Frein and Marwan M. Mokhtar.

La experiencia vivida a lo largo de estos meses realizando la tesis ha sido única y si la llevaré siempre conmigo es gracias a las maravillosas personas que he conocido en Estocolmo. Quiero recordar también a con quien inicié este camino y a quienes les agradezco cada momento compartido; desde mis amigos de toda y para toda la vida de Mairena, a aquellos que se fueron uniendo en mi formación como ingeniero en Sevilla y Valencia, y en especial a Alberto, Michelle, Álvaro y Maciej, con quienes mantengo el sueño conjunto de un cambio social y energético por un mundo mejor.

Quiero agradecer a Isabella su apoyo incondicional, ayuda y amor durante este proyecto; nada sería igual sin ella.

Para finalizar, dedico este trabajo a mi familia y en especial, a mis padres. He sentido vuestro apoyo y energía incesante durante toda mi carrera, me habéis dado todo para que hoy pueda estar aquí, convirtiéndome en ingeniero y pensando en qué puedo hacer para dejar el mundo mejor de cómo lo encontré.

Nomenclature

Abbreviations

AFPC	Advanced Flat Plate Collectors
BAU	Business-as-Usual
CAPEX	Capital Expenditures
CC	Composite Curve
CCUS	Carbon Capture, Utilization and Storage
COP	Conference of the Parties
CPC	Compound Parabolic Collectors
DNI	Direct Normal Irradiation
DSG	Direct Steam Generation
ECCP	European Climate Change Programme
ETC	Evacuated Tube Collectors
ETS	Emissions Trading System
EU	European Union
FPC	Flat Plate Collectors
GCC	Grand Composite Curve
GHG	Green House Gases
HFR	Heliostat Field Reflector
HTF	Heat Transfer Fluid
IAM	Incidence Angle Modifier
IEA	International Energy Agency
IPC	Index of Perceived Corruption
IRR	Internal Rate of Return
LCOH	Levelized Cost of Heat
LFR	Linear Fresnel Reflector
MCA	Multi-Criteria Analysis
MPC	Model Predictive Control
NG	Natural Gas
NPV	Net Present Value
OECD	Organisation for Economic Co-operation and Development
OPEX	Operational Expenditures
PB	Payback
PCM	Phase Change Material
PDR	Parabolic Dish Reflector
PTC	Parabolic Trough Collector
SDR	System Degradation Rate
SF	Solar Fraction
SGD	Sustainable Development Goal
SHC TCP	The Solar Heating and Cooling Technology Collaboration Programme
SHIP	Solar Heat for Industrial Process
SHW	Sanitary Hot Water
SME	Small and Medium Enterprise
SWH	Solar Water Heating
TFHC	Total Final Heat Consumption
TFEC	Total Final Energy Consumption
TMY	Typical Meteorological Year

TRNSYS	Transient Systems Simulation Program
US	United States
WACC	Weighted Average Capital Cost

Latin Symbols

C_p	Specific heat capacity	[J/kgK]
$Debt_{\%}$	Debt share	
E_L	longwave irradiance	W/m²
$Eq_{\%}$	Equity share of the investment	
F_R	Collector heat removal factor	
IRR_{eq}	Equity rate of return	
T_{corp}	Corporation tax	
a_0	Intercept efficiency	
a_1	First-order coefficient of the efficiency	[W/m²K]
a_2	Second-order coefficient of the efficiency	[W/m²K²]
b_0, b_1	Incidence angle modifier constants	
c_1	Heat loss coefficient for $T_m - T_{amb} = 0$	[W/m²K]
c_2	Temperature dependant heat loss coefficient	[W/m²K²]
c_3	Wind dependency coefficient	[J/m³K]
c_4	Longwave irradiance coefficient	[W/m²K]
c_5	Effective thermal capacity coefficient	[J/m²K]
c_6	Wind dependant optical losses coefficient	[s/m]
i_{debt}	Debt interest rate	
Δ	Increment or difference	
ΔT	Temperature difference	[K]
h	Specific enthalpy	[J/kg]
$\dot{m}$	Mass flow rate	[Kg/s]
p	Weight factor for c_5	
θ	Incident angle	[rad]
A	Area	[m²]
C	Cost	[€]
Ce	Effective thermal capacity	[J/K]
F	Collector's fine efficiency factor	
G	Solar radiation	[W/m²]
H	Heat	[Wh]
M	Mass	[kg]
P	Pressure	[bar]
$Price$	Price	[€/Wh]
Q	Heat power	[W]
T	Temperature	[K]
U	Overall thermal losses	[W/ m²K]
V	Volume	[m³]
i	Inflation rate	
t	time	[s]
u	Wind velocity	[m/s]
v	Specific volume	[m³/kg]

Greek Symbols

α	Steam title	
η	Collector's efficiency	
σ	Stefan-Boltzmann constant	[W/m² K⁴]
$\tau\alpha$	Absorptance-transmittance product	
φ	Incident radiation on the solar field	[Wh]

Subscripts

amb	Ambient
aux	Auxiliaries
b	Beam
cont	Contingency
d	Steam drum
eq	Equivalent
ETS	Emissions Trading System
f	Saturated liquid
factor	factor
fresnel	Fresnel
fw	Feedwater
g	Saturated steam
gained	Gained
gl	Global
in	Inlet
load	Load
loss	Loss
m	medium
net	Annual yield
opt	Optical
out	Outlet
pp	Piping
r	Receiver
rec	Recirculation
s	Steam
sat	Saturated
saved	Saved
sf	Solar field
solar	Solar
test	Test
th	Thermal
w	Water
fuel	Fuel

Table of Contents

Tables

Figures

1 INTRODUCTION

"Solar power has the potential to more than meet todays' energy needs, allowing us to leave the fossil fuel in the ground, if only we would choose to do so"

– Mike Berners-Lee –

Nowadays the world is facing one of its biggest challenge, climate change. An obsolete energy system based on fossil fuels is leading to an environmental crisis with extreme impacts on life on Earth. Moreover, the growth of economy and population is leading to an increase in the energy demand and consequently, the related emissions. The energy sector is the major contributor to global Green House Gases (GHG) emissions; in the year 2016, 70% (around 35.8 Gt $CO_{2,eq}$) were generated due to fossil fuel combustion, cement production and other industrial processes [1]. Having analysed the effect of high GHG emissions due to anthropogenic activity in global warming, governments from all over the world decided the goal of limiting the raise of our planet temperature to 2ºC with the Paris Agreement (December 2015) [2]. At the same time, United Nations Agenda and the Sustainable Developments Goals (SDG) have as one of their main targets the task of decarbonizing the energy sector and power human development with clean energy [1].

Global heat consumption accounted for half of the total final energy consumed in 2018, meaning that heat is the largest energy end-use and contributes to 40% of the GHG emissions. Particularly, the case of industrial processes is essential for understanding the world´s heat consumption since a third of this energy is used in the sector. Even though fossil fuels are the most common energy source in industry and cover more than three-quarters of the world heat demand, renewable systems for heat generation is expected to expand a 22% during the period 2019-2024, which makes this market an interesting focus for reducing carbon emissions towards the 7th SDG. Even though heat demand might increase a 9% during that period, the use of clean technologies such as bioenergy (which currently accounts for 86% of the renewable heat consumed), renewable electricity and solar thermal are expected to lead the industry to a low-carbon scenario [3].

Solar heat for industrial process (SHIP) has a significant potential to cover useful heat demand, especially for those sectors which require heat at low and medium temperature. In developed economies, half of this energy consumption in industrial and agricultural food processes could be technically cover with solar thermal systems supplying hot water and steam in a temperature range of up to 400°C [4].

The integration of solar thermal energy in industry is still in progress, only 0.02% of the heat consumption is supplied thanks to this technology [3]. To enhance the deployment of solar heat, international cooperation programmes have a key role; The Solar Heating and Cooling Technology Collaboration Programme (SHC TCP) is one of the first programmes created by the International Energy Agency (IEA) and its main mission is *"to increase the deployment rate of solar heating and cooling systems by breaking down the technical and non-technical barriers"* [5].

This Master Thesis aims to identify the potential of solar thermal energy in industry by performing a market assessment of this technology and verifying with a case of study the feasibility of integrating SHIP in the most promising industrial sectors.

1.1 Objective of the project

The first aim of this study is to analyse the solar thermal market for industrial processes as well as the state of the art of the technology and its integration in the sector. After identifying market trends and the potential of solar energy in this field a deeper study of suitable industrial sectors and processes is developed to assess the feasibility of this technology and the main parameters that should be taken into consideration to pursue the deployment of these systems. A techno-economic analysis is performed for a case study based on the identified market and it is analysed the competitiveness of solar thermal technologies in comparison with the current conventional solutions for industrial heat requirements.

The next steps are defined to structure the project and reach the objective:

- To describe the state of solar thermal technologies and their integration in industrial processes.
- To review the design and modelling of solar thermal technologies.
- To identify the most promising industrial sectors, their processes and the potential for SHIP.
- To determine the most suitable customers and regions for implementing solar thermal technologies.
- To perform a techno-economic analysis model to assess the feasibility of SHIP integration in the selected process and technology with a case study.

1.2 Structure of the project

The report is divided into different chapters which follow the objective steps. An overview is described below:

1. **Introduction:** the context of the project and its purpose.
2. **Current background:** the framework of the study, giving notions of the current environmental and energy crisis which are a driver for renewable technologies. The heat consumption in industry is characterized and the solar thermal technology is overviewed.
3. **Methodology:** the steps to reach the objective of the study and the procedure to assess SHIP potential with a Multi-Criteria Analysis (MCA) and apply the case study.
4. **Solar integration in industrial processes:** a review of the heat in industry, the conditions under solar thermal systems are deployed and the integration of this technology for different processes requirements.
5. **Key costumers and market:** an analysis of the potential market of SHIP for different industrial sectors and processes. An MCA is performed under geographical conditions.
6. **Techno-economic analysis:** a case study based on the previous conclusions is modelled with the software TRNSYS and the techno-economic indicators and parameters are selected.
7. **Results and discussion:** an assessment of the boundary conditions for a feasible solar heat integration based on the results for the case study simulation and a sensibility analysis.
8. **Conclusions**
9. **Further research**

2 CURRENT BACKGROUND

This chapter is dedicated to describing the current situation when this study is made in order to have a better knowledge of the worldwide heat consumption, the conventional systems which supply it, its repercussion on the environment and the role it has in industrial processes. Finally, the main solar thermal technologies are reviewed.

2.1 Environmental and energy crisis

The environmental crisis that the world must face is caused by anthropogenic activities and, among other causes, the great dependency on fossil fuels for the energy supply. The emissions generated in the last decades have led to global warming with a rise in the Earth temperature and huge impacts on the ecosystems of the planet. Moreover, recent reports have estimated that 75% of the terrestrial environment and 66% of the marine has been severely altered; the loss of wildlife biodiversity is putting nearly 25% of species to the edge of extinction [6].

Climate change is driven by the GHG emissions of the last decades, for which the energy sector has a major role as it generates nearly 70% of those emissions [1]. As it is shown in the figure below, electricity and heat producers, transport and industry are the main sectors responsible for global GHG emissions, which makes them a suitable focus for humans to take action fighting climate change and follow the path towards a sustainable scenario. The growth of the emissions for most of the sectors is induced by the increase of fossil fuel consumption; only the coal related emissions have declined (1.3%) since 2018. On the other hand, natural gas and oil have increased globally since emerging economies have a greater energy demand each year. This is not the case for regions such as Europe and US, where the emissions in 2019 were reduced by near 150 Mt CO_2 and the power sector is integrating renewable energies achieving a decline of the carbon dioxide (CO_2) emissions intensity of electricity generation by nearly 6.5% in 2019 [7].

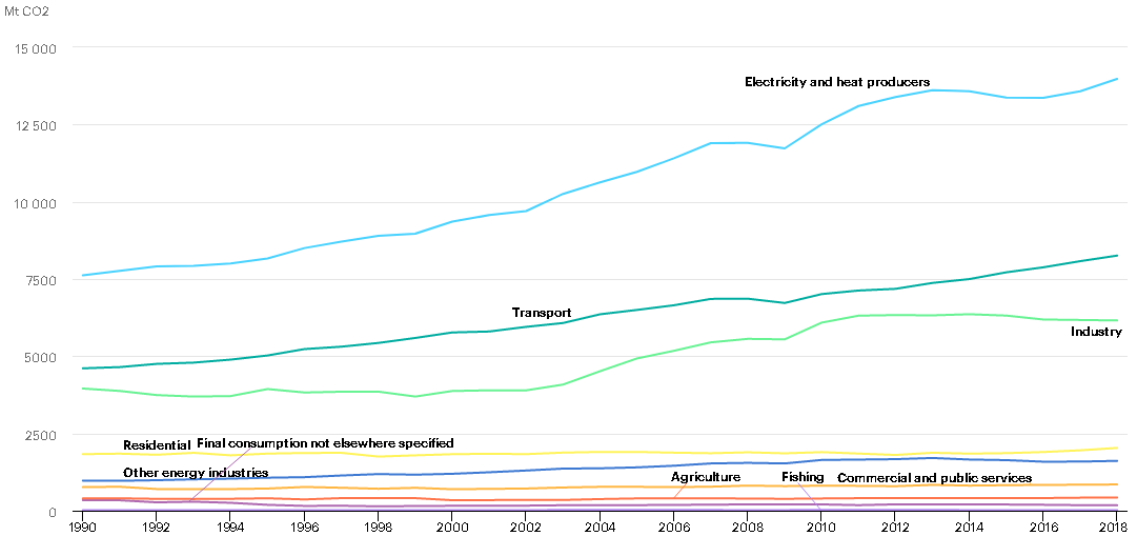

Figure 1. World CO_2 emissions by sector [8].

The efforts for reducing emissions in the energy sector has been motivated by events of international cooperation such as the Conference of the Parties (COP) in which the Paris Agreement was signed in 2015 [2]. Its main goal was to limit the Earth temperature increase to 2 degree Celsius (preferably 1.5ºC) compared to pre-industrial levels. This decision leads to an action plan for an economic and social transformation and the creation of the Sustainable Development Goals by the United Nations. These 17 goals aim to gather a global effort for ending poverty and other deprivations with strategies to improve health, education, equity, etc. Some goals related to the energy field is to ensure affordable

and clean energy (number 7), reduce health impacts due to air pollution (number 3) and take climate action (number 13) [9].

As the world is not on the correct path to meet the requirements of the SDGs related to energy, the International Energy Agency has designed the "Sustainable Development Scenario". This scenario is based on a reduction of the CO_2 equivalent emissions in the energy field to ensure that the increase of the planet temperature does not go over 1.8 ºC by 2100 with a 66% of probability [10].

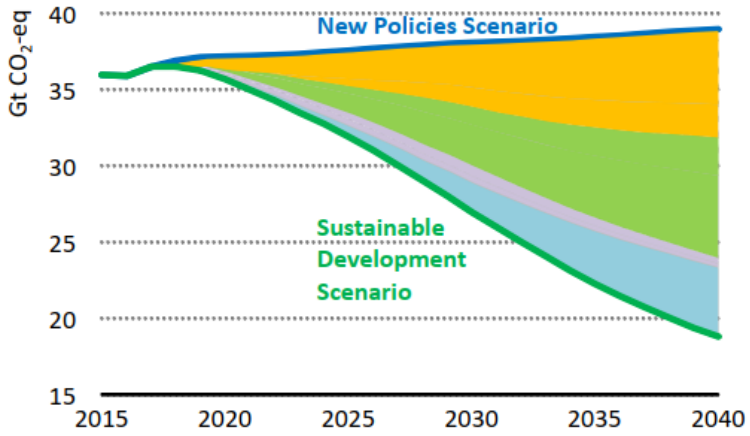

Figure 2. CO_2 emissions forecast for different policies scenarios [11].

The new policies scenario of the figure above represents the expected emissions until 2040 if the world continues with the existing and announced policies, way far from the Paris Agreement target. In order to reach the Sustainable Development Scenario four measures are proposed:

1. The yellow area represents 37% of the emissions reduction and it is based on improving end-use efficiency and making a fossil fuel subsidies reform.
2. The green area represents 36% and is related to the integration of renewable energies, hydrogen and bioenergy, and reducing the coal fired power.
3. The purple area accounts for 9% of the emissions reduction and is related to reducing upstream oil and gas methane.
4. Finally, a 20% (blue region) will be reduced thanks to nuclear power, fuel-switching and carbon capture, utilization, and storage (CCUS).

2.1.1 Covid-19 crisis

The most recent reports from the EIA shows that the covid-19 crisis has made a huge shock to the energy trends as the global economic activity has been affected. Energy demand and related emissions have dropped by 5% and 7% respectively in 2020 while the energy investment has suffered a reduction of 18%. Among the fossil fuel demand, natural gas has the lowest fall in (3%) while oil has decreased 8%. The global primary energy demand is set to reach pre-covid terms between the years 2023 and 2025, depending on the crisis duration [12].

Besides this, the resilience of renewable energies during the crisis is remarkable as its demand has kept growing, 1% in 2020. Solar energy will be the new leader in the electricity mix by 2024, surpassing natural gas and coal. Even though the investment and installed capacity of renewable technologies (especially wind and solar) keep a positive trend, energy policies in the next years will have a key role in ensuring its growth.

Anyway, the financing activity for utility-scale renewables is expected to increase as supportive policies for investors have not been abandoned, and regions with big renewable market such as the European Union (EU) or China have maintained their zero emissions goals. Moreover, stimulus

packages have ensured the solvency of major utilities and some small companies which invest in renewable projects, both in advanced and emerging economies.

Finally, industrial activity has been affected by the crisis with a decline of 4.2% in 2020 compared to 2019 in terms of heat demand. This shock may affect bioenergy intensive subsectors (such as pulp and paper) maintaining the share of renewable heat almost unchanged. Anyway, the industrial recovery during the years 2021 and 2022 is expected to increase again the heat demand, as well as the non-renewable heat consumption [13].

2.2 Heat industry overview

Nowadays the role of energy in modern society and its dependency on fossil fuels is leading humans to the depletion of these resources as well as to global warming. The industrial sector is responsible for a third of the energy consumption in our planet, which means that it is a suitable market to integrate renewable energies in order to achieve a reduction of GHG emissions [14].

Moreover, three-quarters of the final energy consumed by the industry worldwide is in form of heat; the rest corresponds to a share of mechanical and electrical work. This shows that contributing with renewable sources to supply heat for industrial processes might be an efficient way to reduce the use of fossil fuels in this sector, therefore, reducing as well the GHG emissions [15].

A key aspect for the integration of solar thermal energy systems that should be considered is the temperature at which the heat has to be supplied. The heat demand required in the world for the year 2014 is detailed in Figure 3, where it is possible to see that 30% of it is required below 150ºC, 22% is between 150 and 400ºC and the rest is above 400ºC (high-temperature heat). Most of the heat currently consumed in industries comes from coal (45%), natural gas (30%) and oil (15%), being only covered with renewable energies 9%.

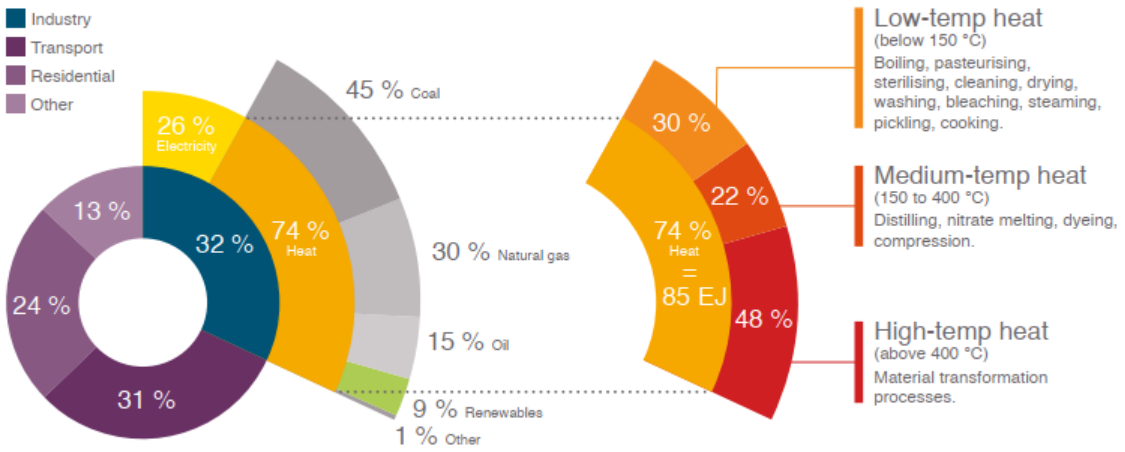

Figure 3. Breakdown of heat demand in industry [16].

Even though the industrial sector accounts for 32% of the heat consumed, transport has a similar share of consumption with 31%, followed by the residential sector [16]. The main use for buildings is heating spaces and water, followed by cooking; the remaining heat used is partially consumed by agriculture for greenhouse heating [3].

Nowadays the main sources that supply this heat demand, as mentioned before, are fossil fuels along with the traditional use of biomass (12%), which generally have negative impacts regarding human health, socioeconomic and environmental aspects [3]. Traditional biomass is low cost, do not require pre-treatment and is commonly used in countries with emerging economies causing deforestation and respiratory diseases when this type of fuel widely used [17]. On the other side, modern bioenergy

is the most common renewable source for heating and it is expected to grow with a 12% increase during the period 2019-2024 [3].

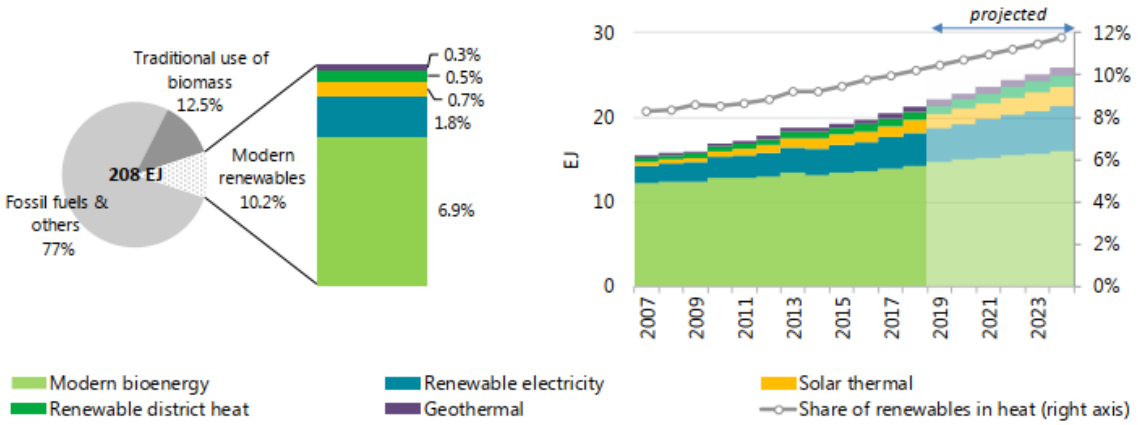

Figure 4. Energy sources shares in global heat consumption, 2018 (left). Global renewable heat consumption (right) [3].

Two-thirds of the bioenergy shown in Figure 4 is consumed by the industrial sector essentially in processes that demand heat. The second largest renewable source in industry is renewable electricity which makes electrification a promising option for industrial decarbonisation. Electricity for heat generation is mainly consumed in metallurgy industries such as iron, steel and aluminium [3].

Indeed, heat demand in industry is anticipated to rise almost 9% globally during 2019-2024, a good reason to make more urgent the transition to a renewable heat system. The regions which are contributing in a higher way to a sustainable change in the system are the EU, the United States, India and Brazil. The fast integration of renewable electricity in China is also significant.

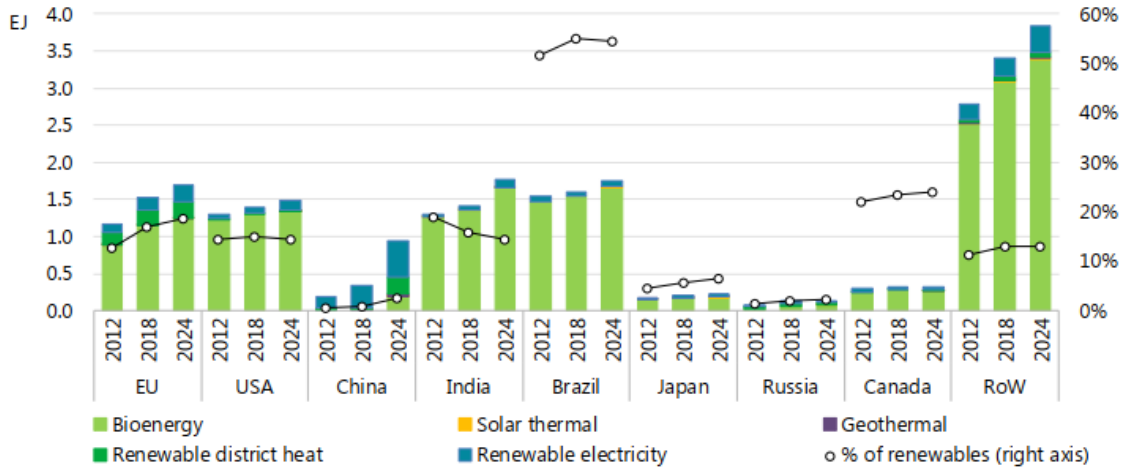

Figure 5. Historical and projected renewable heat consumption trends in industry for selected regions [3].

In this context, solar thermal technologies contribute less than 0.02% to the global share of industrial heat demand. Nevertheless, this technology is still in expansion with 7% of growth every year, which means a new capacity installed of 37.6 MW_{th} in 2018. Regarding this deployment, China was responsible for more than half of the collector area additions, followed by Mexico (13%), France (10%) and India (7%) [3].

Solar thermal energy is a promising alternative for those industrial processes which requires hot air or water, steam, etc. The integration of solar thermal technologies depends on the heat demand, the temperature needed and the space available. The design of the system must define the type of solar collector, the sun tracking, the storage if it is needed and other parameters [14].

2.3 Solar thermal technology

Solar thermal systems transform solar radiation into heat, which is transferred to the working fluid. This heat can be directly used to feed water, heat/cool equipment, other industrial processes, or can be stored to adapt a system to its demand and even work during hours with low or null radiation [4]. In this section, the main elements which integrate the solar thermal system are described and analysed in order to understand how it operates and what are the main selection and design criteria. Therefore, it is necessary to review the types of solar collector, storage systems, and working fluids [14].

2.3.1 Solar collectors

Solar collectors are a fundamental piece of solar thermal technology and their selection varies depending on multiple factors; therefore, assessing the current solar technologies will make it possible to identify the most suitable for the variety of industrial processes.

The selection of an appropriate solar collector depends mainly on five factors:

1. Operating temperatures.
2. Thermal efficiency.
3. Energy yield.
4. Cost.
5. Occupied space.

The solar collectors can be divided into two categories depending on whether solar radiation is concentrated or not. The non-concentrators do not generally have any tracking system because the temperature range demanded by the user is low, and their intercepting and absorbing zone is the same. On the other hand, concentrator collectors use reflective materials to focus a higher radiation flux in a reduced absorber area [4].

2.3.1.1 Non-concentrators

Three non-concentrators collectors are the most used nowadays:

Flat Plate Collectors (FPC)

This technology has been highly implemented in houses for supplying sanitary hot water (SHW) and it can reach temperatures up to 100ºC [4]. It harnesses both direct and diffusive solar radiation, which is absorbed by a dark material area and transmitted to the circulating liquid in the tubes. An isolation material is placed in the back part of the collector and a glass cover on the top tries to minimize the convection losses. This plate could be also unglazed, with the disadvantage of having higher convective losses and being not suitable for cold weather. On the other side, its optical performance is higher due to the absence of glass and its reduced cost makes it commonly used for heating swimming pools [14].

This collector is also applied for heating air in multiple activities such as drying. It has been studied the possibility of reducing its cost and changing absorber tubes for recycled materials such as aluminium cans, finding that thermal efficiency of 74% could be achieved [18].

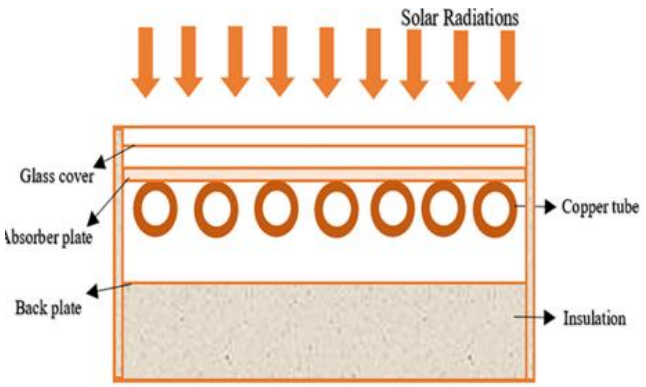

Figure 6. FPC technology scheme [14].

New types of collectors with different materials and manufacturing techniques are being developed, a good example is the Advanced Flat Plate Collector (AFPC). AFPCs are made via ultrasonic welding and usually have fins on the tubes to increase the heat conduction rate.

Evacuated Tube Collectors (ETC)

As well as FPC, this technology collects direct and diffusive radiation but, in this case,, using a vacuum glass pipe that covers the copper tube which contains the heat transfer fluid. When solar radiation is received, the fluid inside the tube evaporates and goes up to exchange heat to the external fluid as is shown in Figure 7. After this phase, the internal fluid turns into liquid and descend to the absorber part to receive solar radiation again.

One advantage of this type of collector is that at lower incidence angles presents very high efficiency and low losses. It has a better performance in cold climates than FPC and reaches temperatures up to 120ºC, resulting in a higher price.

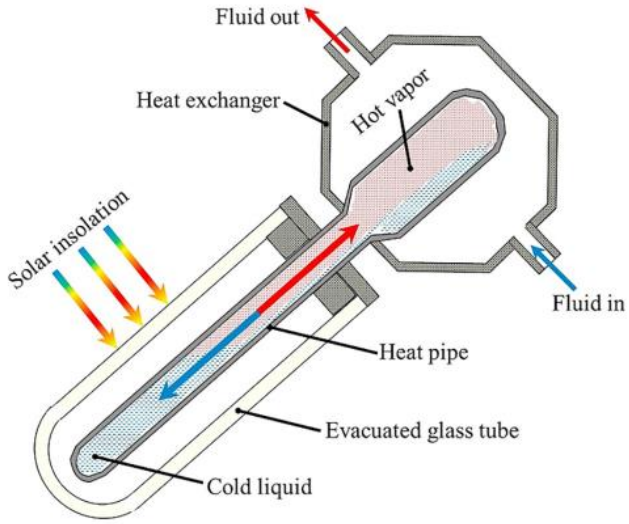

Figure 7. ETC technology scheme [18].

Stationary Compound Parabolic Collectors (CPC)

These collectors have a liner receptor and a low concentration ratio up to two, too low to be considered in the gru¡oup of concentrator collectors. This technology has the advantage of absorbing solar radiation over a wide range of angles even though it does not generally have any tracking system. CPCs are commonly shielded with glass aiming to protect the reflectance materials from dust and

external danger. The reflectance surface is fitted behind the vacuum tubes of the ETC, reflecting both direct and diffuse sunlight onto the absorber (also called CPC vacuum tubes) [14].

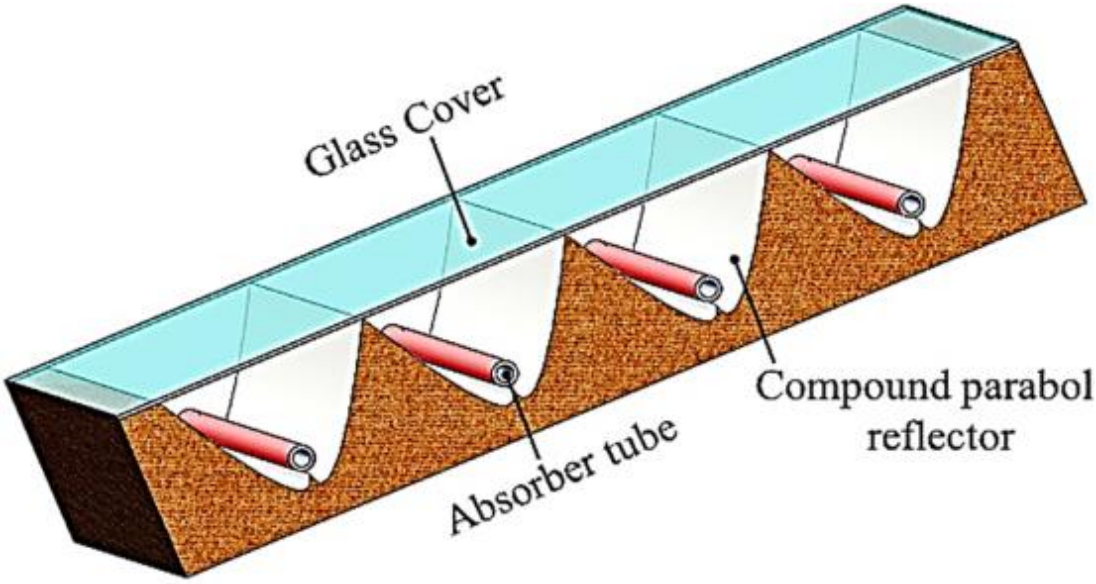

Figure 8. CPC technology scheme [18].

There are multiple new techniques to improve these technologies: triple glazed, ultra-high vacuum, transparent insulation, etc [4].

2.3.1.2 Concentrating collectors

Concentrators allow to capture the solar incident radiation of a big area and transmit it to a smaller collecting area where temperatures reach higher levels than the devices described previously. The concentrators can be refractors or reflectors, continuous or non-continuous and cylindrical or parabolic. In this case, a tracking system is needed to get a better position along the day following the Sun and achieve high efficiency, therefore, obtaining economical results which justify the initial investment [14].

Parabolic Trough Collector (PTC)

This device is a linear collector based on a reflective parabola shape that contains an absorber pipe in its focal line. This receiver is a black metal tube with high absorptivity and low thermal radiation dissipation. It is covered by an anti-reflective glass that ensures the vacuum and enhances the reduction of convective losses. A tracking mechanism is necessary, not only to follow the Sun and gain the maximum radiation each hour but also to protect the collector from dangerous environmental conditions. It is normally orientated north-south with an only axe that moves the PTC aperture from east to west along the day. The temperatures for the operational fluid (which is usually oil or water) do not go above 400ºC.

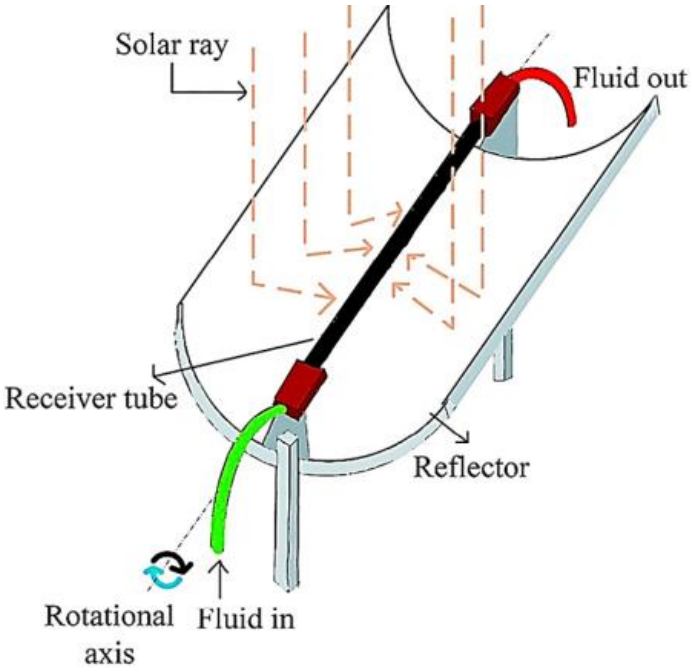

Figure 9. PTC technology scheme [18].

Linear Fresnel Reflector (LFR)

The main advantage of this technology is that the reflectors are cheaper than PTCs thanks to being plane or slightly rounded, which reduces the manufacturing costs. The reflectance material is mounted to the ground and seems like a broken-up parabolic as it is shown in Figure 10. The collector has a fixed linear absorber upon the concentrators.

The major drawbacks are that the system provides a lower concentration ratio and needs quite a big area to be implemented. It is suitable for applications with a large available space and demanded heat at temperatures as high as 300ºC.

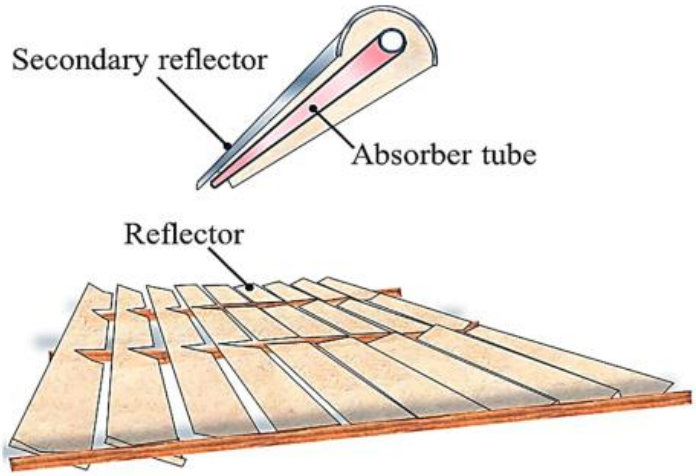

Figure 10. Linear Fresnel reflector [18].

Parabolic Dish Reflector (PDR)

This collector is similar in shape to a satellite dish antenna with a focal point and a receiver in its focus. It has two-axis tracking and reaches extremely high temperatures over 1500ºC. Moreover, its concentration ratio is between 600 and 2000 [14]. With the purpose of power generation, a Stirling

cycle is fixed in the focus of the dish to convert directly in the radiation into electricity. Nevertheless, parabolic dish reflectors are costly due to the high precision required in their manufacturing [18].

Heliostat Field Reflector (HFR)

This technology uses multiple flat mirrors (heliostats) that reflect beam radiation into a punctual focus, a tower, where temperatures up to 2000ºC are achieved thanks to a concentration ratio of 300-1500. The working fluid is typically water or molten salt and normally operates around 550ºC [14].

The heat transfer fluid selection depends on the temperature that the solar field reaches, the pressure demanded and the process itself. Generally, in open-loops it is water (with a low boiling point and corrosivity) or even air but, in close-loops, it is oil (hydrocarbons), molten salt. This last group shows several challenges such as danger of getting frozen, high viscosity, oxidation, etc [4].

2.3.2 Collectors' efficiency

The performance efficiency of solar collectors is a parameter created to compare, not only different types of collectors but also modifications in significant characteristics such as materials to develop the devices. The useful energy produced by the solar thermal collector is an energy balance of the difference between the solar radiation which reaches the absorber and the total thermal losses [19].

Figure 11 represents typical efficiency curves for various types of collector under standard environmental conditions and global radiation of 1000 W/m^2. The efficiency in this figure varies with the mean temperature between ambient air and the collector outlet fluid. When this mean temperature raises, thermal losses tend to be higher and the collectors which are less protected from environmental conditions (less isolated, absence of glass covers, etc) are susceptible to present worse performances. The maximum efficiency is reached by FPC when the ambient temperature is favourable, however, in extreme conditions the double-glazed FPC minimize the losses. ETC have lower losses but its performance is not suitable in comparison with FPC when T_M has values below 100 ºC. The case of concentrator technologies as PTC shows very low heat loss coefficients at the cost of optical efficiency [14].

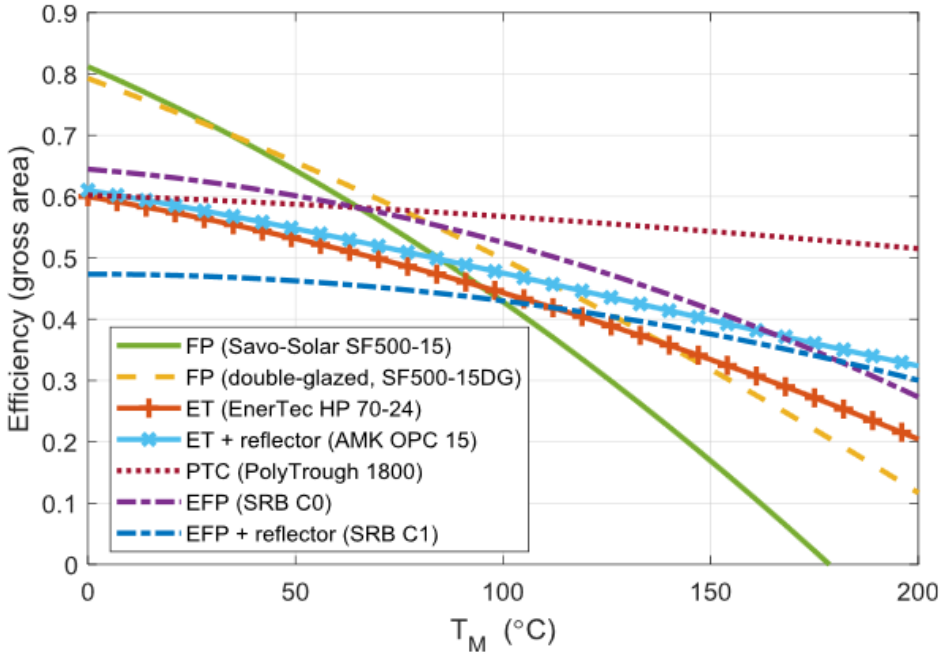

Figure 11. Efficiency curves at G = 1000 W/m2 for a variety of solar thermal collector [20]

As a summary of the collector technology main properties, the following table depicts the tracking system implemented in each collector, its absorber type, concentration ratio and the temperature range that operates with. This last parameter is fundamental for the collector selection in a specific heating process since there are multiple heating demands and temperature requirements.

Motion	Collector type	Absorber type	Concentration ratio	Temperature range (ºC)
Stationary	FPC	Flat	1	30-80
	ETC	Flat	1	50-200
	CPC	Tubular	1-5	60-240
One-axis tracking	PTC	Tubular	10-85	60-400
	LFR	Tubular	10-40	60-250
Two-axes tracking	PDR	Point	600-2000	100-1500
	HFR	Point	300-1500	150-2000

Table 1. Solar thermal devices classification [21].

2.3.3 Solar tracking

Different systems of solar tracking have been implemented in diverse solar technology, been especially important the ones for concentrating collectors. These systems could have one or two axes depending on the economical assessment, the type of technology and the degree of freedom movements needed. The types of tracking systems are listed as follows [14].

- **Active:** tracking with sensors to detect the solar path and send a signal to the motor of the collector.
- **Passive:** systems based on the thermal expansion of materials. A liquid is vaporised when the maximum radiation is achieved, ensuring the correct position of the collector. These tracking systems are more suitable in regions close to the equator and under favourable weather conditions.
- **Semi-passive:** the solar path is tracked by the concentrator ensuring sun rays to be horizontal to a cross-sectional area of the absorber.
- **Manual:** the angle of the collector is changed over the seasons using a manual gear.
- **Chronological:** based on the calculated location of the Sun for an exact time of the year, the motor rotates with a fixed speed along the day.

As it was mentioned in section 2.3.1, the tracking system as well as the number of axes has a high dependence on the type of collector selected. In summary, non-concentrator collectors do not need a tracking system that might make them economically unfeasible, while the case of concentrator collectors is different. One axis is mostly applied in parabolic through and linear Fresnel solar collectors, whereas two axes are fundamental for solar dish and tower collectors [14] which concentrates the flux in a focal point and must have a very accurate track of the Sun.

2.3.4 Modelling simulation tools

Modelling and simulation of solar thermal systems help design and ensure the proper behaviour of the technology. Even though there is not a standardized software to simulate these processes, some of the most common tools are described in this section [14]:

- **TRNSYS:** it is one of the most common tools to simulate solar energy systems nowadays. An information flow diagram is drawn and system components are displayed in boxes with time-dependent inputs and constant parameters. The results are given as time-dependent outputs and the mean error between the simulation and the real system is less than 10% as it is shown in various studies.
- **T*SOL:** used to design and optimize a solar thermal energy system for dynamic simulation, helps to dimension the components and performs economic and environmental calculations.
- **WATSUN:** this software can calculate system results for every hour but also long-term performance analysis. It also provides a cost-benefit assessment and has a synthetic weather generator.
- **Polysun:** a user-friendly tool that runs with dynamic time stages from 1s to 1h and is capable to compare the GHG emissions from different systems as well as economic analysis. Its accuracy has been validated as 5-10%.
- **F-chart method:** elementary, quick in results and without a detailed simulation scenario. It mainly uses two design variables (primary and secondary) and calculates based on correlations between thousands of TRNSYS simulation results.
- **Artificial neural networks:** it provides solutions for complex systems with specific requirements, and it has been used by many researchers. Nevertheless, it is not a user-friendly tool, and it is still in the development stage.

In a simplified analysis, there are some drawbacks such as deficiency of control over assumptions and limited flexibility of design, nevertheless, they are essential to assess the feasibility of solar thermal systems integration.

2.3.5 Thermal storage systems

Solar thermal storage collects and accumulates a part of the energy captured by the solar field during a day for later use when the solar radiation level is not able to reach heat demands. This technology provides the solar system with partial or full dispatchability [22] necessary in cases when the heat demand and the radiation and energy supplied by the collectors do not fix. Energy storage is generally needed due to the variability of solar radiation along the day, nevertheless, it is also common that a conventional system works to supply the peaks of demand [14].

Solar systems which seek to distribute the heat gained over time need to incorporate storage systems. This concept applied in the designing of solar heat integration aims to minimize capital costs as well as operating losses, reaching the lowest possible operating temperature in the collectors, and minimum heat waste from heat storages [23].

The main design parameters for a storage system could be listed as the following ones: Capacity and size, power, operating temperature, storage period and efficiency. The design of storage systems has some difficulties due to the limitations that must confront: Heat loss, leakage, supercooling (for Phase Change Materials, PCM), corrosion, safety, volume variation, steam pressure, etc [24].

A common classification for solar storage is described below and is related to the interaction between the storage material and the exchange of its energy with the system [14]:

- **Active direct:** the storage material and the heat transfer fluid of the collectors are similar.

- **Active indirect:** the storage material and the heat transfer are not the same and it is needed a heat exchanger between both systems.
- **Passive:** the heat transfer fluid must pass through the storage material that might be rocks, concrete, or PCM

2.3.5.1 Storage fluids and materials:

Storage materials are determined by a set of physical, chemical, environmental, and economic properties [22]:

- The energy density of the storage material.
- Heat transfer and mechanical properties.
- Chemical compatibility and stability.

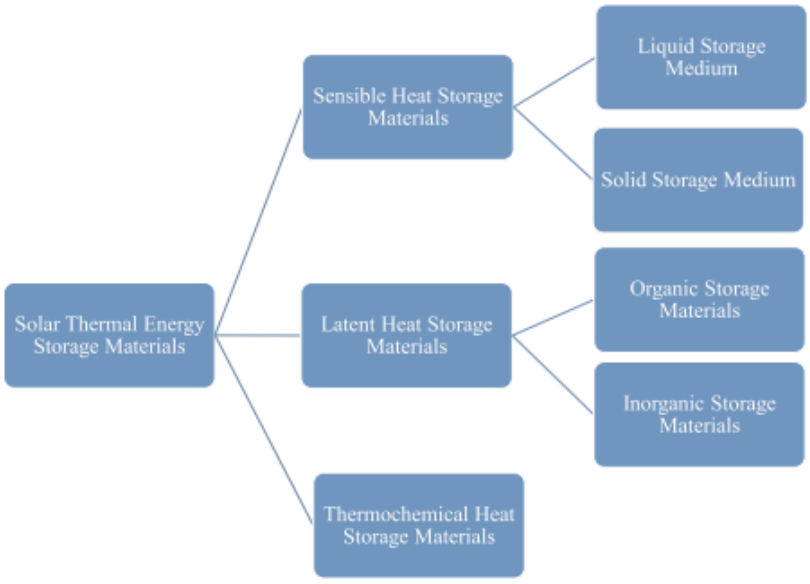

Figure 12. Classification of the storage materials used in SHIP [14].

Figure 12 shows a diagram with the types of storage materials [14]:

- **Sensible:** It is generally used in high-temperature applications and do the change its phase during the transference of heat. In the case of liquids (water, mineral oil and molten salt), the main benefit is that they can circulate easily as an active system and, inside a tank, hot and cold liquids are separated thanks to the density difference. Solid materials are also used due to their low cost and the absence of high-pressure problems that sometimes result in leakage. Nevertheless, solids (rocks, concreate…) cannot circulate so they are characterized as passive systems.
- **Latent:** These materials, known as Phase Change Materials, smelt during the heat absorption and achieve the "latent heat of fusion". Thanks to this change of phase, the temperature difference between the heat charge and discharge is small hence the losses. PCMs could be organic, which have the ability of congruent melting and are not used for high-temperature applications, or inorganic, that melt incongruently and have a high volumetric latent heat density.
- **Thermochemical:** A thermochemical reaction occurs to absorb heat during charging (endothermic) and supply it backwards when discharged is needed (exothermic). It is still at laboratory level meanwhile latent and sensible are currently used in industries.

3 METHODOLOGY

In this chapter the methodology developed and the approach selected to perform this study is explained in detail.

3.1 Overview of the methodology

Two main approaches have been performed to achieve the objectives:

1. A literature review of the solar heat technology and current methods applied to integrate it in industrial process. Moreover, a top-down study is made to identify the potential customers and regions for SHIP and a multi-criteria analysis is carried out.
2. The key parameters for SHIP integration and feasibility are identified within a case study. This case is modelled using the software TRNSYS and the results are analysed from a techno-economical perspective and a sensibility study.

The methodology applied through the study is explained with four main steps:

Step 1: Ideal customer type

This step of the study aims to review the current industrial processes which are suitable for solar thermal energy implementation and the main characteristics needed for succeeding in this integration. A classification regarding types of integration is made, as well as further analysis of industrial sectors where promising processes take place.

A SHIP integration method is studied and the tools and parameters needed for modelling this technology in the case of study.

Subsequently, the industrial sectors where SHIP with adequate heat temperature conditions and high demand are selected and used in later parts of the study to locate the regions where these sectors have a noticeable weight in industry and heat consumption.

Step 2: Analysing potential regions

A multi-criteria analysis is conducted to find which are the most promising countries or regions to integrate solar thermal technology in industrial processes. The MCA is utilized for assessing a finite number of alternatives (in this case, countries) by defining a range of conflicting criteria expressed in different forms of data.

A deeper study of the potential for the selected countries is performed. This potential is based on the heat consumption for promising customers and then limited by a series of factors such as roof availability, solar fraction, heat recovery potential, heat temperature, etc. These limitations are decided after a review of multiple studies which try to identify SHIP potential in a specific region or industrial sector.

Step 3: Case of study

The case study is identified thanks to the results given by the previous steps. The characterization of the system depends on the industrial sector, the type of integration, the technology applied and demand conditions. The data required to model the components might be provided by the task 49 of SCH, and TRNSYS the software selected for this purpose.

The results of this simulation are used to perform a techno-economic analysis.

Step 4: Techno-economic analysis

The feasibility of the solar heat integration into the industrial process is assessed using the results provided by the previous simulation of the case study. Various performance indicators are defined and calculated to identify the boundaries of SHIP feasibility and finally it is concluded with the conditions that make possible the deployment of this technology in the global industry.

3.2 Multi-criteria analysis

Based on the literature reviewed and the promising industrial sectors selected, an MCA is performed for ranking the countries with the highest SHIP integration potential and therefore, the most appealing market. It is important to clarify that the outcome of an MCA depends on the selected criteria which are used to assess the different alternatives (countries). Moreover, the weight assigned to each criterion and the methodology applied for ranking the alternatives have also a great impact on the outcome [25].

Qualitative and quantitative data was collected for the variety of criteria selected, relying on international sources such as the IEA and the Organisation for Economic Co-operation and Development (OECD). The weight of each criterion has been calculated with a binary comparison matrix (see appendix 11.1) and normalization has been made by assigning a value of 100 to the country with the best performance for each criterion.

This MCA does not only consider a ranking of countries regarding their performance for each criterion with a global perspective but also takes into account the relative importance of a criterion value within the country. As an example, for the criterion of heat consumption of a promising industrial sector in a specific country, it is determined not only the total amount of heat consumption but also the relative weight of this sector consumption regarding the total heat industrial consumption of the country.

After selecting a geographical scope based on the results from the MCA, the price of natural gas for the countries in the selected area is taken into account to provide a more accurate value of the potential for SHIP in each country. The high price of fossil fuels for heat generation in industry is one of the main drivers for companies to integrate solar systems [16].

A more detailed description of each criterion, how it is calculated, and its source could be found in the 11.1Appendix 1: Multi-Criteria Analysis. The list of criteria and weights is listed below and divided into three categories:

Potential industrial sectors

Having selected the promising sectors for SHIP, their energy consumption and relevance both from a global and a country perspective have been defined. The five industrial sectors have been analysed accounting for these criteria and, as they have a great impact on the results, their weights sum 37.1% of the total available score. The criteria are weight equally:

a. Final energy consumption in the chemical industry (weight=7.42%)
b. Final energy consumption in the food and beverage industry (weight=7.42%)
c. Final energy consumption in the paper and pulp industry (weight=7.42%)
d. Final energy consumption in the textile and leather industry (weight=7.42%)
e. Final energy consumption in the mining industry (weight=7.42%)

Energy situation and resources

Each country has a characteristic energy context where its natural resources are key. The solar resource, the dependence on fossil fuels imports and the pressure from international agreements are important motivations for a country to implement sustainable energy policies and deploy renewable energies. Due to the increase of electrification in industry for heat supply that competes with SHIP, a last criterion regarding the current power consumption is also considered. The following criteria have been chosen to define the energy situation:

a. Solar resource (weight=22.9%)
b. Renewable energy policies (weight=8.6%)
c. Investment trends in renewable energy (weight=8.1%)
d. Experience in SHIP (weight=7.5%)
e. Dependence rate on natural gas imports (weight=1.93%)
f. Power consumption in industry (weight=1.93%)

Macro-Environmental context

A comparison between economies is done to determine which regulatory environment is more suitable for local entrepreneurs. It is considered multiple economic, social and political indicators. Two criteria have been selected:

a. Easy of Doing Business (weight=9.7%)
b. Index of Perceived Corruption (weight= 2.3%)

4 SOLAR INTEGRATION IN INDUSTRIAL PROCESSES

This chapter shows a review of the heat in industry, suitable processes and integration methods for solar thermal systems and an introduction to the system modelling using the TRNSYS tool.

4.1 SHIP integration

One of the main drawbacks to implementing solar thermal technologies from an economic perspective is the high capital cost. From a technical point of view, the need for ensuring a continuous supply of heat even though the source of energy (solar radiation) is discontinuous is a great challenge too. Another important technical barrier is the available space and solar fraction, which varies a lot with the location of the solar plant.

As it is seen in Figure 13, there are three methods to integrate solar energy into industrial processes [26]:

1. Preheating of water that will go to a process (generally for low-temperature requirements).
2. Integration at the supply level (only for concentrating collectors due to the high temperature required, even steam).
3. Direct coupling to a process as a heat source for heating a circulating fluid (e.g. feed-up water, return of closed circuits, air preheating).

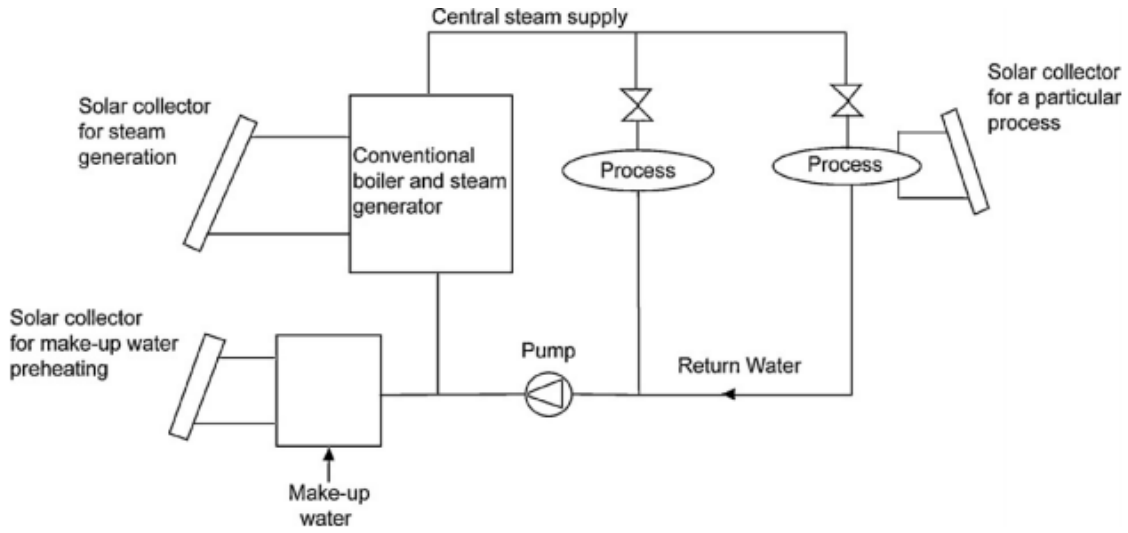

Figure 13. Integration of solar collectors for industrial processes [26]

The design of this integration should be focused on working at the lowest temperature (always in the range demanded by the industry) so the solar collectors maximize their efficiency. The steps needed to design and integrate solar energy in industry are three:

1. Describe the industrial sector, its heat demand and temperature range.
2. Determine the technical feasibility considering:
   - Type of process.
   - Available area for solar collectors.
   - Demand at various temperatures.
   - Use of thermal storage and recovery units.
3. Evaluate techno-economical potential considering energy cost trends [14].

4.1.1 Methodology for SHIP integration: Pinch Analysis

Different methodologies could be applied for designing the solar heat system integration in processes. These methods are used to achieve the following concepts for the integration [27]:

- An insight into the system and its specific bottlenecks.
- Solutions for energy and/or material efficiency.
- Help to plan process modifications.
- Optimize the design of a profitable energy mix for renewable energy supply in conjunction with heat recovery.

A popular tool for process integration is the Pinch Analysis which is also commonly used for SHIP integration. This methodology serves for analysing heat recovery potential for an industrial process or site and designing the heat recovery or utility mix based on a fixed utility system. The steps of the methodology are firstly defined for any generic process integration as follows:

Data collection and extraction: heating and cooling requirements are established for the industrial processes and each of these streams is defined based on their mass flow, specific heat and inlet and their target temperature (or phase change enthalpy).

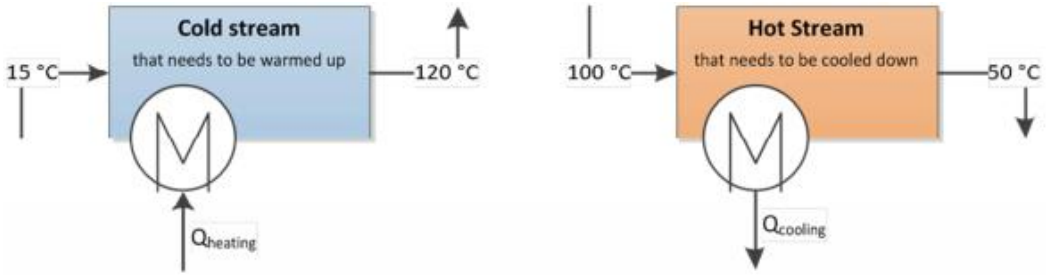

Figure 14. Defined streams for the Pinch Analysis [27].

Targeting: The two targets of this analysis are assessing the maximum heat recovery and the most efficient energy supply. For this purpose, two different graphs are drawn:

Composite Curve (CC): for determining the heat recovery potential, the temperature enthalpy profile of each stream (divided into hot or cold) in a temperature interval are combined as is shown in Figure 15. Cold Composite Curve composed of two cold streams .Figure 15.

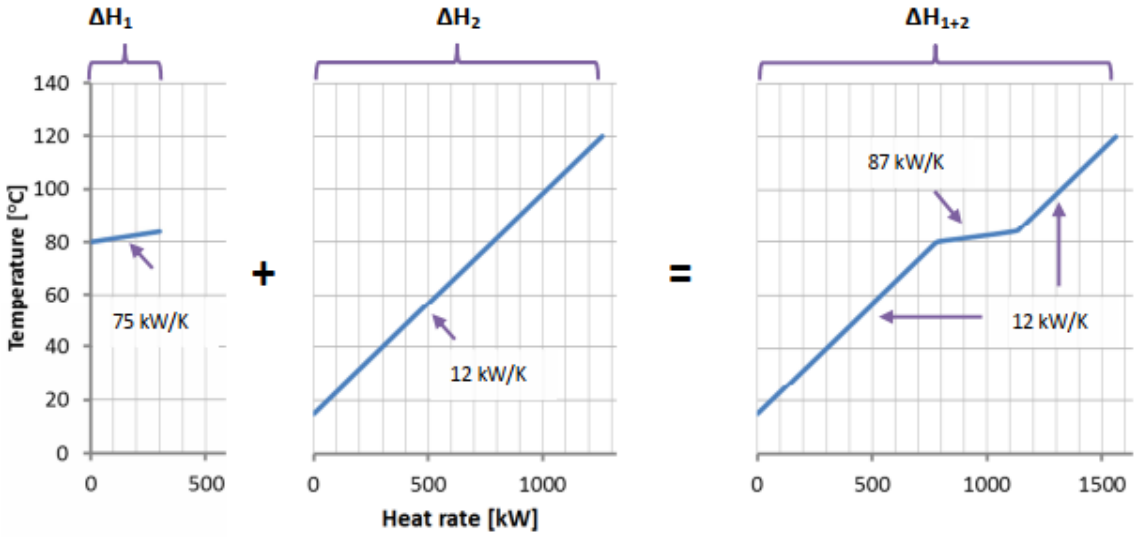

Figure 15. Cold Composite Curve composed of two cold streams [27].

After defining the cold and hot curve, both are displayed in the same graph always having the hot one above. It is generally necessary to move the curve along with the energy or the horizontal axis, which means that energy values are not absolute but a relative measurement. Then, a minimum temperature difference (ΔT_{min}) between both curves is selected based on the performance of the selected heat exchanger which aims to recover heat. This ΔT_{min} is an economical optimization between the savings thanks to the heat recovered and the heat exchanger high cost for the efficiency required to achieve a low ΔT_{min}. The curves are moved until the distance between them is the ΔT_{min}; that point defines the "Pinch point" and the "Pinch temperature" (see Figure 16).

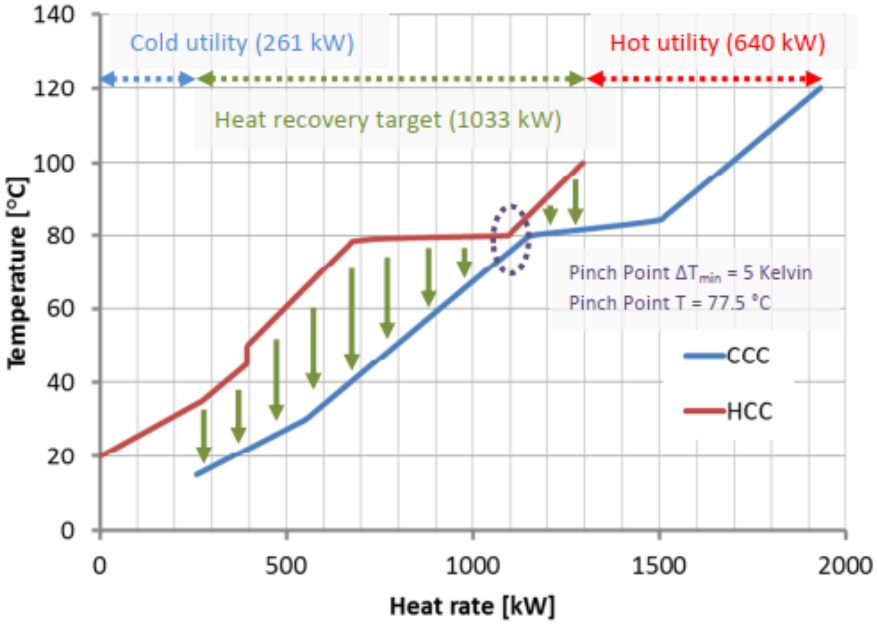

Figure 16. Hot and cold composite curves with a defined Pinch Point [27].

The horizontal overlap of the curves (green arrows) defined the theoretical maximum heat recovery that can be obtained. The minimum cooling and heating demand for processes are defined graphically in the top part of the figure (hot and cold utilities). The CCs give us information about the potential SHIP integration by defining three limitations:

- No external heating below the Pinch temperature (supposing that the waste heat available is going to be recovered).
- No external cooling above the Pinch temperature (cooling for the processes represented in this part of the curve can be achieved by heating other ones which are at a lower temperature).
- Do not transfer heat from heat sources above to heat sinks below the Pinch.

Processes with hot streams which are not feasible to transfer heat to colder ones do not have to be included in the composite curves.

Grand Composite Curve (GCC): this curve is created for implementing efficient energy supply and obtain useful information such as which is the lowest temperature heat demand in the processes (a relevant parameter to integrate solar systems). This curve is built from the hot and cold CCs as is depicted in Figure 17. First, the two CCs are shifted vertically so they touch each other in the middle of the ΔT_{min}, in the pinch (top left figure). Then, the GCC is drawn as the heat rate difference between hot and cold CCs and the minimal cold and hot utilities are represented in the extreme of the curve. Now the x-axis represents absolute values of heat rate.

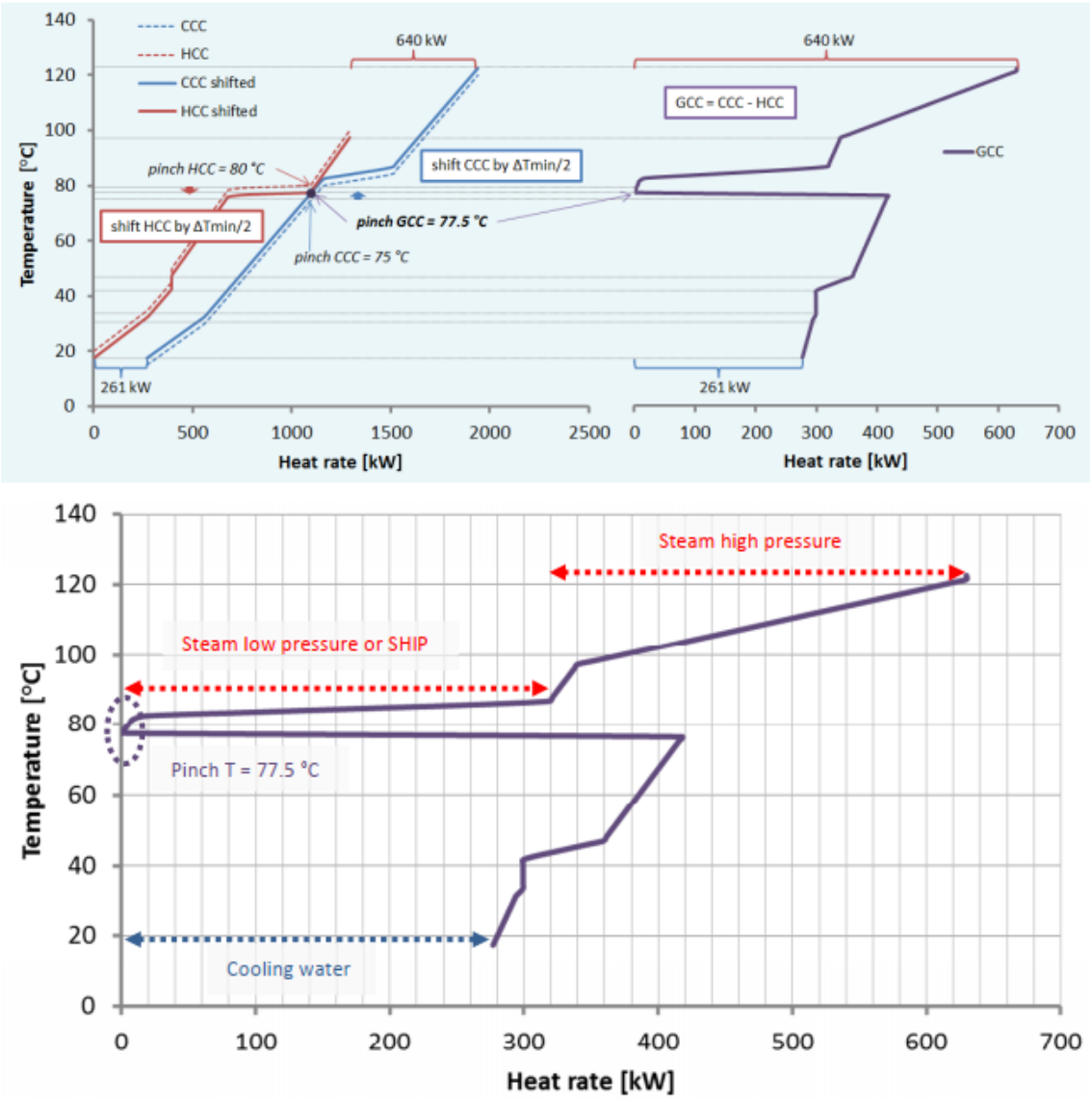

Figure 17. Construction steps for the GCC based on the hot and cold CCs (top) and final result (bottom) [27].

The GCC indicates the possible maximum heating rate contribution of the solar thermal system as a function of its operational temperatures. The final results for GCC in Figure 17 show that half of the hot utility is required below 90ºC, which is a very suitable heat temperature to be achieved by solar systems. For integrating SHIP using the graphs, two main concepts must be analysed:

1. Identification of the maximum heat that could be covered by solar energy at the minimum temperature (see GCC): Since the GCC represents several processes and the solar plant design is based on it, it should be considered that it might not be possible to cover all these processes due to techno-economic feasibility. Moreover, different supply temperatures may be needed so the selection of only one or two processes for the solar system is generally reasonable.
2. Listing the possible integration points for SHIP (see CCs): When the solar heat rate is defined in the GCC, it is added to the hot CCs. This action provides the possibility to evaluate different integration points for essentially continuous processes, highlighting cold process streams candidates and their heat rates.

Figure 18 represents possible solar integrations designed within the curves. On the right, the graphs show the case in which no heat waste is recovered so solar heat is integrated into any part of the curve. On the left, it is limited to the curve on the right side of the Pinch point.

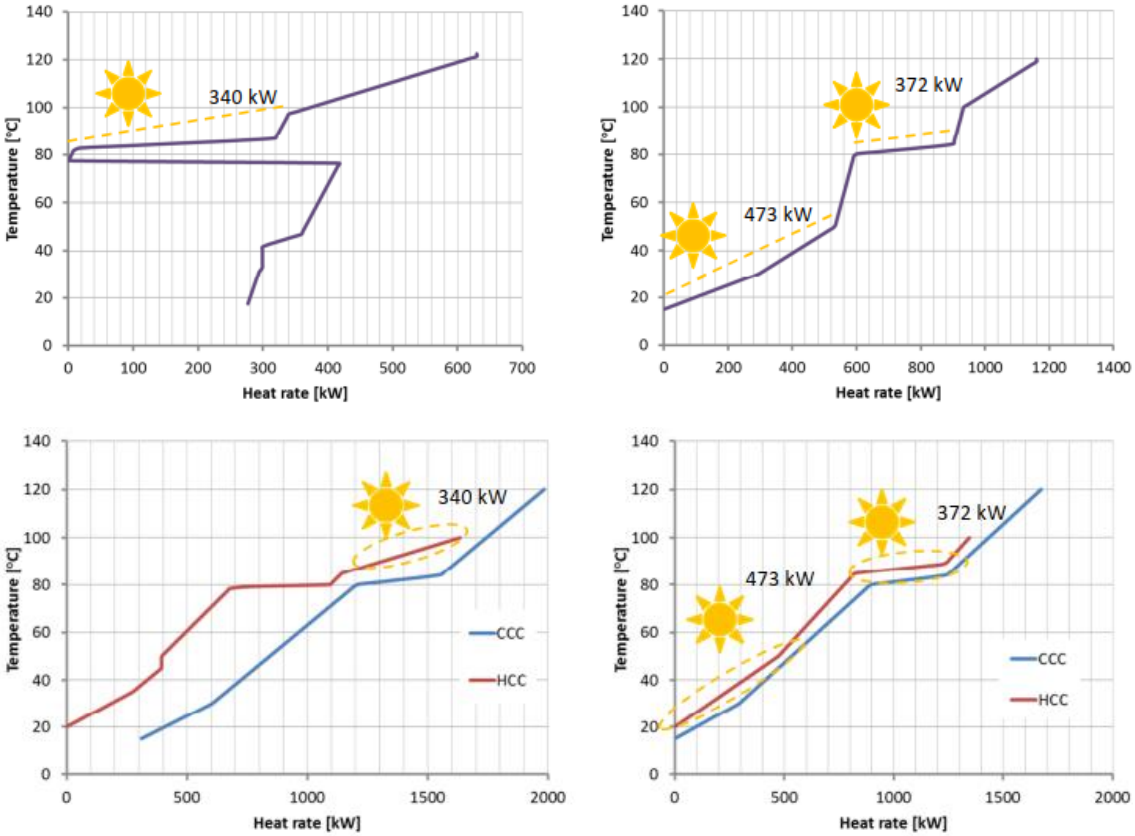

Figure 18. Solar heat integration in GCC (top) and CCs (bottom), considering heat recovery only in the left graphs [27].

Some challenges for integrating solar heat with the Pinch Analysis are:

- The difficulty in considering variable process streams.
- The time dependency of the solar resource.
- The solar heat gains cannot be known in detail until the technical concepts and temperature parameters of the solar design are defined.

Design: The heat exchanger location is analysed after integrating the utilities again in the composite curve. Optimization algorithms are commonly used for selecting the most energy-efficient and cost-effective place for the heat exchanger. A possible heat storage system, as well as the re-design of the streams network, might be necessary after taking into account the solar system.

The graphs and examples displayed in this section are based on a case study detailed in Appendix 2: Example of an industrial process integration using the Pinch analysis.

4.1.2 Classification of industrial heat consumers for solar integration

The multiple possibilities for the integration of solar thermal energy depend directly on the heat load, leading to a different suitable hydraulic concept for solar integration. It is proposed three different classifications for the use of solar heat:

- **Supply/Process level:** integration at the supply level consists of generating steam or hot water for a central distribution system that transfers these fluids to different heat consuming

process, generally inside a big factory. On the other side, the integration at the process level has the requirements of the specific application.

- In the case of supply level, the heat transfer medium is classified considering the characteristics of the solar system needed and its components.
- The process level can be subdivided depending on the heat load into two categories: "(pre)heating of fluid streams" or "heating and maintaining temperature of baths, machineries, or tanks".

Finally, it must be also considered the conventional heating equipment that is been used in the process because it determines the integration of the solar plant. A good example of this is the integration in Thermization (a process involved in pasteurization), where the product is conventionally heated by a heating jacket, making the integration a difficult work. On the other side, other processes facilitate the integration such as the tunnel pasteurization that is heated by an external exchanger [28].

The classification of the solar integration concepts is depicted in Table 2 both for supply and process level, distinguishing between the heat transfer medium and the conventional heating equipment respectively.

Level of Integration	Distinction		Solar Heat Integration Concept	
Supply Level	Heat Transfer Medium	Steam	SL_1	parallel integration (direct or indirect) of solar heat
			SL_2	solar (pre)heating of boiler feed water
			SL_3	solar (pre)heating of make-up water
		Liquid	SL_4	parallel integration (direct or indirect) of solar heat
			SL_5	solar return flow boost
			PL_6	solar heating of storages or cascades
Process Level	Conv. Heating Equipment	External Heat Exchanger	PL_1	solar heating of product, PM, intermediate hot water circuit or input streams
			PL_2	solar heating of bath, machinery, or tank
		Internal HEX	PL_3	solar heating with internal HEX
		Steam Supply	PL_4	solar steam supply at vacuum or low pressure

Table 2. Overview of the integration concepts for SHIP applications [28].

At the supply level, the heat transfer medium (steam or liquid) and the defined integration point leads directly to an integration concept. In the case of process level, an integration concept can have multiple approaches or technical solutions. In those cases, only the real process boundary conditions could decide which integration system is more appropriate. For example, for the process of "heating and maintaining temperature of baths, machineries, or tanks" with direct steam injection, four integration concepts could be applied:

- External bath heating
- Heating of input streams
- Internal heat exchanger
- Steam supply with low pressure

For the selection of the integration concept, the most important criterion would be the one that works with lower temperature demand. In the case that there is a large quantity of freshwater supplied to the scalding bath, the best option would be to heat this input stream. If the cold water must enter into the bath due to technical reasons (e.g. to cool down the product), this concept is not valid and the next ones with lower temperature requirements are considered. In this example, the limitation of removing the process heat medium to heat externally (external bath heating) or the availability of space to heat internally (internal heat exchanger) affects the integration selection. The possibility of a steam supply with low pressure is the easier integration thanks to not interfering with the existing process, with the disadvantage of requiring a higher temperature demand for the solar system and

affecting the collectors' design and performance. Another interesting option is the combination of two integration concepts: if the water input stream fed is discontinuous, it can be directly heated up when the stream is being supplied. Other way, an external heat exchanger is used when there is no freshwater input [27]. Some of the most common processes where solar heat systems have been integrated are described in section 4.1.4.

4.1.3 Trends for solar heat process design

The design methods and strategies for optimizing industrial processes are evolving, so as the solar process heat. Some specific future trends are indicated to be aware of the changes that occur in this field [27]:

- The solar yield can be increased thanks to flexible small-scale processes which adapts their curve of demand to the available solar resource. Moreover, new storage systems might have the chance of saving solar heat from summer to winter to exploit its potential.
- New conversion technologies include a drying process that might be feasible for solar heat with steam, increasing the overall efficiency.
- The deployment of advanced heat recovery systems would leave a heat demand for solar energy at higher temperatures, leading to greater use and research of concentrator collectors.
- On the other hand, the implementation of electricity for heat processes will eliminate current heat waste flows.

4.1.4 Low/medium temperature processes

The following Figure 19 shows, for the year 2006, that most of the processes which had integrated solar heat were those with operating temperature below 100ºC. For these processes, low-temperature collectors such as FPC are a more mature technology in comparison with concentring collectors and have been recognised generally as more suitable economically in the past years. Nevertheless, this reference is useful to understand the trends of the 2000s decade, new plants with higher temperature ranges have been implemented in recent years.

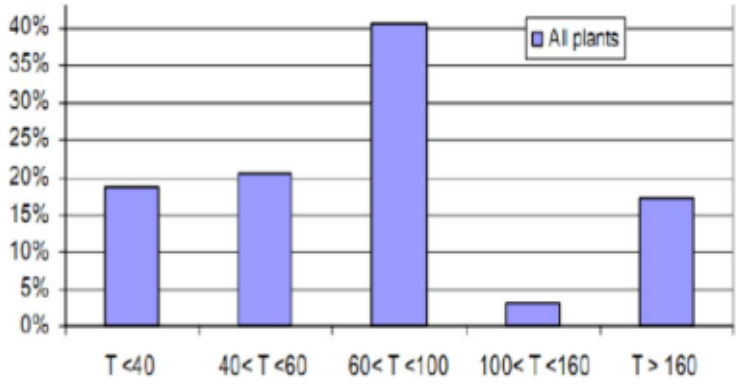

Figure 19. Temperature level for processes with existing solar heating systems (2006) [29].

Some of the main processes where solar energy has been successfully integrated are described below [29]:

- **Water heating:** constitute a major part of the solar thermal applications in industry.
- **Drying:** generally performed with hot air, eliminate the moisture from fruit, textile, mineral material and other products.
- **Preheating:** heating water for a process or as boiler feed water.

- **Steam heating:** this process requires high-temperature heat, therefore, it commonly involves the selection of concentrating collectors for this purpose.
- **Pasteurization and sterilization**: characteristic processes in the dairy and food industry.
- **Cooling and heating spaces**.
- **Washing:** it requires warm water and is generally used in all commercial sectors for the manufacturing of products such as bottles, barrels, containers, etc.

The most common of the industrial processes above which integrates solar thermal energy are explained in detail below:

4.1.4.1 Solar dryers

It is the most used method in the food and tobacco industry to dry and lengthen life. This technology is prepared for collecting the sun's radiation for drying application and it can be subdivided into two areas [4]:

- **Direct/Indirect:** this division depends on how solar rays reach the food, whether the radiation "sees" directly the product or there is a barrier. In a direct method occurs a loss of food properties, meanwhile, using the indirect method the food remains "protected" but usually requires a higher investment.
- **Active/Passive:** An active method forced the air circulation (controlled by fans) whilst the passive only uses natural convection.

In order to preheat the air, it has been generally used flat plate collectors and evacuated tube collectors.

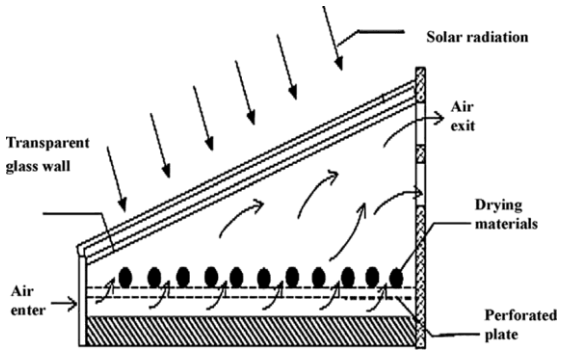

Figure 20. Solar dryer system [30].

4.1.4.2 Solar cooling

Cooling demand could be supplied in different ways: mechanical systems required electricity as their main source of energy while thermal systems can use solar radiation. This last technology uses absorption/adsorption chillers to substitute the need for a compressor, achieving high electricity savings. It is used water with ammonia or lithium-bromide requiring temperatures above 100ºC and commonly solar concentrators. Aiming to achieve higher efficiency in the process as it is quite lower than cooling with mechanical compressors, a double and triple effect is performed using higher temperatures on the hot source side [4].

Nevertheless, one great advantage of solar cooling is that the peak demand load usually happens when the sun is around its azimuth, therefore solar radiation levels are the highest of the day. It is also required a conventional heater (back-up) as an auxiliary [29].

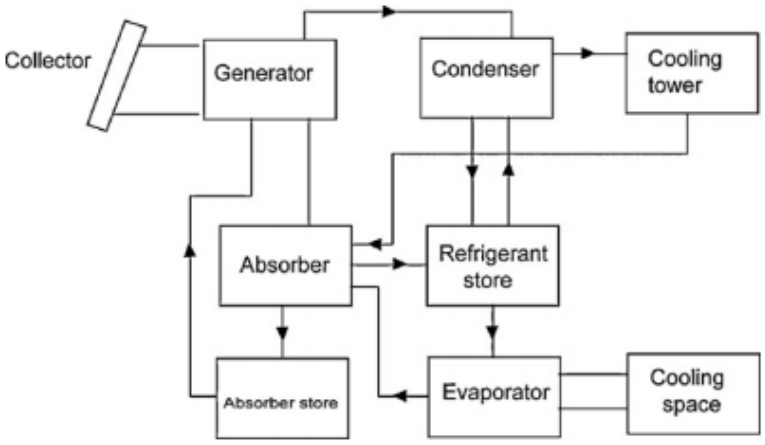

Figure 21. Block diagram of a typical solar cooling system with refrigerant storage [29].

4.1.4.3 Solar Water Heating (SWH)

SWH is considered one of the most cost-effective solar thermal technologies [29]. It is a mature technology and is mainly composed of solar collectors and a storage tank. It works thanks to the density inequality of hot and cold water which provokes natural segmentation inside the tank. Then, the water pumps are commanded by a differential thermostat in the solar loop which depends on the hot water demand. The system components and their configuration are shown in Figure 22:

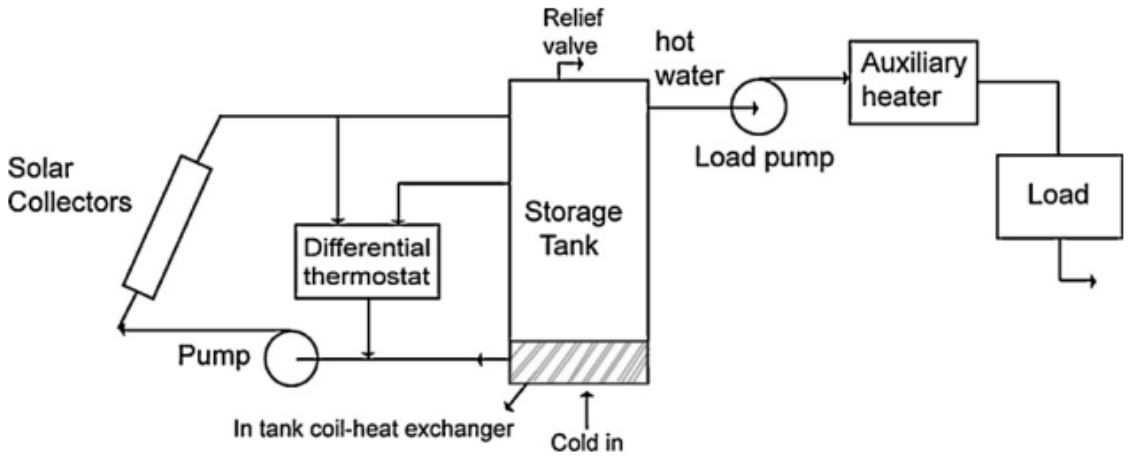

Figure 22. Block diagram of an SWH system [29]

4.1.4.4 Steam generation

Steam is a heat transfer fluid required in almost every industry and several processes demand it, which makes solar steam generation an appealing alternative in the global market. In the case of desalination and sterilization, it is used low-temperature steam showing that solar collectors are a suitable technology to generate it. PTC or Fresnel are efficient collectors used in this application with three main methods:

- **Steam-flash:** pressurized water is heated up through the solar field without losing its liquid phase. In the next step, it is depressurized with a flash valve generating steam at low temperature and pressure.

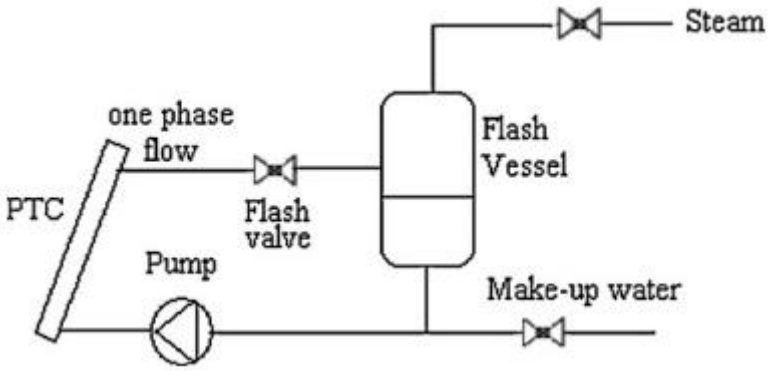

Figure 23. Steam flash generation system [29].

- **Direct or in situ boiling:** it is the same system as the steam flash but removing the flash valve, having return water from the collectors in form of steam and liquid at the same time. It has the disadvantage of instability problems.
- **Unfired boiler system:** the steam is generated thanks to a heat exchange located in the "steam boiler" which, instead of using fossil fuels, use as a hot source in the heat exchanger the fluid that comes from the solar field.

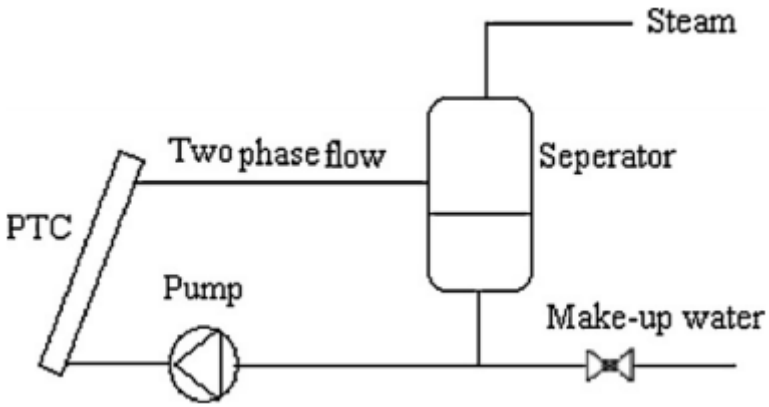

Figure 24. In situ generation system [29].

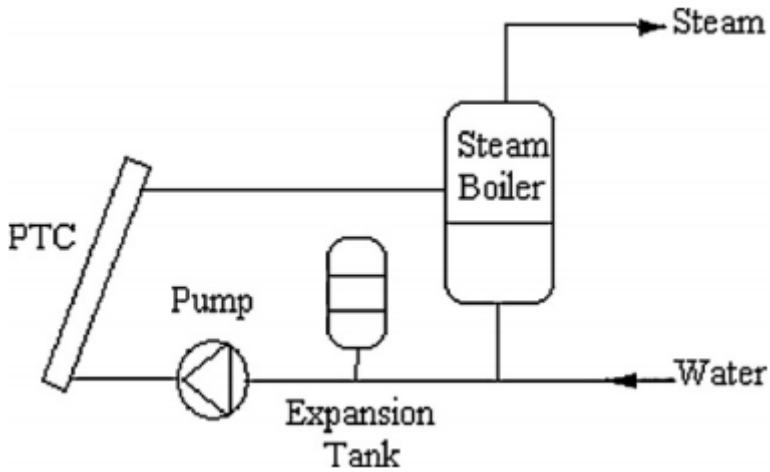

Figure 25. Unfired-boiler generation system [29].

4.2 Identification of suitable integration points

After performing the pinch analysis to know the potential for heat recovery and the possible solar heat cover in various processes, an assessment of the most suitable integration points should be done. It should be performed before the step of the techno-economic analysis.

A possible methodology for this task is explained in the next lines. A set of indicators are defined to create a decision matrix that includes all the possible integration points. Firstly, a pre-integration evaluation is made based on the data gathered from the heat demand of the processes, their schedule and the conventional technology that currently covers the thermal demand. Secondly, some criteria based on the future impacts of the SHIP integration are assessed, the post-integration matrix.

		Indicator name	Indicator variable	[unit]
pre- integration	Demand	process (return) temperature	T_p	[°C]
		tempearture lift	ΔT	[°C]
		annual heat demand	Q_a	[kWh/year]
		storage capacity	Q_{st}	[kWh]
		storage charging	$\dot{Q}_{st}$	[kW]
		operation time	t_{op}	[h/year]
		mean load	$P_{av} = Q_a/t_{op}$	[kW]
		recirculation	$1/rec$	[-]
	Schedule	daily demand coincidence	$C_d = Q_{mid}/Q_{day}$	[%]
		demand seasonality	$C_a = Q_{sum}/Q_a$	[%]
		demand uniformity	$unif = P_{av,day}/P_{max,day}$	[%]
		rescheduling	t_i	[h]
	Technology	equipment supply quality	$\pm\Delta T_e$	[°C]
		product supply quality	$\pm\Delta T_p$	[°C]

post-integration	Reliability	Process continuity
		Load balancing
		Control Hardware
		Control Software
		Fouling risk
	Cost	HX sizing
		Storage sizing
		Distance to solar
		Auxiliary energy
	Benefit	Estimated solar yield
		Multi-supply
		Modulation
		Dependency on radiation
	Efficiency	Replacement of CHP
		Replacement of WH/HR

Table 3. Pre (left) and pot-integration (right) criteria for selecting possible SHIP integration points [27].

The ranking of the integration points is made by assessing each indicator or criteria with a three-value scale: very suitable, moderately suitable and low suitable (it is graphically illustrated with green, yellow and red colour). The choice of these values is based on previous knowledge of the studied processes or of comparable sites. The final decision must consider that the indicators/criteria in the upper parts of Table 3 are the most significant [27].

4.3 Solar technology modelling

The design of a solar heat system and sizing it properly is a complex task that needs to use models of the different system components. The solar plant simulation is based on some characteristics from the heat industrial process:

- Load temperature range and flow rate.
- Use pattern or schedule (days per week and hours of the day).
- Collector to storage distance.
- Piping UA value.
- Relief valve set temperature.

The complexity of the analysis method selected affects the computational speed, time cost, flexibility for design optimization, accuracy of results, etc. For modelling a system, a structure is developed based on clear systems boundaries that have been established. This requires specifying which items, processes and effects are internal to the system. Generally, for non-standard systems, it is needed a detailed computer simulation such as the one provided by the software TRNSYS [26].

4.3.1 TRNSYS tool

TRNSYS program is an acronym from "transient simulation" because of its quasi-steady simulation model. It is considered one of the most used thermal process simulation tools and consists of many subroutines that model subsystem components which are defined by mathematical models (algebraic or differential equations). The software can interconnect components, solve differential equations and facilitate outputs. The modelling problem lies in the selection of these components for creating a proper mathematical description of the system. An information-flow diagram is built for the system to facilitate the identification of the components (represented by a box) and the information flow between them. Components work with constant parameters and time-dependent inputs to return outputs. An example of this diagram is shown in Figure 26 where the scheme of the generic solar thermal system is presented.

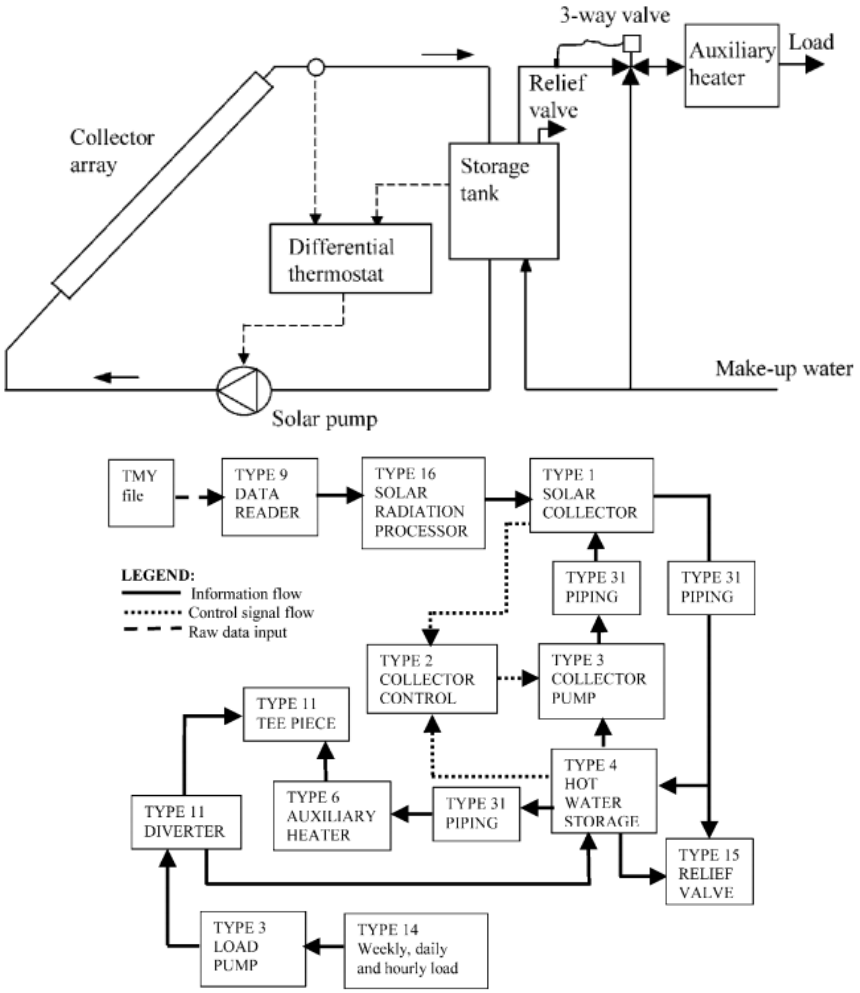

Figure 26. Scheme of a solar system model (top) and its TRNSYS information Flow diagram (bottom) [26].

Apart from the selection of the type of components that structure the model and the definition of their characteristics, it is crucial for the simulation the quality and reliability of the climatic conditions input. TRNSYS uses a Typical Meteorological Year (TMY) which characterize the climatic raw data input for the mean life of the system. The TMY is the average year climate and provides necessary information for determining the performance of the solar system such as solar radiation, ambient temperature, wind speed, humidity ratio, etc. The impact of this average year on the results depends on the sensitivity of the system performance to the hourly and daily weather sequences [26].

4.3.2 Solar field model

The solar collections performance and the useful heat supplied to the system depends on multiple properties that must be defined for each type of collector technology. The efficiency (η) of a collector Type 1 selected in TRNSYS (following the study [26]) is defined below:

$$\eta = a_0 IAM - a_1 \frac{\Delta T}{G} - a_2 (\frac{\Delta T^2}{G}) \quad (1)$$

The efficiency is calculated as a second-order function, nevertheless, for stationary collectors it is used a single-order equation (a_2=0). It is also possible to include the concept of effective thermal capacity in the equation as it is done in [31] for simulating the thermal performance of parabolic trough and flat plate collectors. The terms a_0, a_1 and a_2 are specific characteristics of the collector. The term ΔT is calculated as the difference between the collector inlet temperature and the ambient temperature. In the case of solar radiation, it could be considered the global (G_{gl}) or it can be divided into direct or beam and diffusive.

The incidence angle modifier (IAM) depends on the incident angle (θ) and two constants (b_0 and b_1) as is seen in equation (2). However, for stationary collectors only the factor b_0 is considered.

$$IAM = 1 - b_0 \left(\frac{1}{1 - cos(\theta)} - 1\right) - b_1 (\frac{1}{1 - cos(\theta)} - 1)^2 \quad (2)$$

The useful energy transferred from the collectors to the system is calculated with equation (3):

$$Q_{gained} = F_R A [IAM(\tau\alpha) G_{gl} - U(T_{in} - T_{amb})] \quad (3)$$

The term U represents the overall thermal losses and $\tau\alpha$ is the absorptance-transmittance product which characterizes the absorbed radiation by the solar collector [26].

The parameter F_R is essential as it represents the ratio between the actual useful thermal power gain (Qu) and the one that would be obtained if the collector-absorbing surface is considered at the local fluid temperature: This parameter is a function of the geometrical properties of the collector type [32].

The parameters needed to define the model of a collector vary with the type used (flat plate-FPC, evacuated tube-ETC, compound parabolic-CPC and parabolic-trough collectors-PTC) and the data required is different for concentrator and non-concentrator collectors (Table 4).

Collector technology	Parameter
Common for all	$\dot{m}_{test}$ -flow rate per unit area at test conditions [kg/s m²]
	a_0 - intercept efficiency
	a_1 - negative of the first-order coefficient of the efficiency
	b_0 - incidence angle modifier constant
FPC, ETC and CPC	Collector slope angle
FPC and ETC	Efficiency mode
FPC	Fixing of risers on the absorber plate
	Absorber coating
	Glazing

Collector technology	Parameter
ETC	Glass tube diameter
	Glass thickness
	Collector's length
	Absorber plate
	Coating
	Absorber area for each collector
CPC	**F** - collector's fine efficiency factor
	U - overall loss-coefficient of collector per unit aperture area
	Reflectivity of walls
	Half-acceptance angle
	Ratio of truncated to full height of CPC
	Axis orientation
	Absorbtance of the absorber plate
	Number of cover plates
	Index of refraction of cover material
	Product of extinction coefficient and the thickness of each cover plate
PTC	Collector rim angle
	Reflective surface
	Receiver material
	Collector aperture
	Receiver surface treatment – absorptance and emittance
	Glass envelope transmittance
	Absorber outside diameter
	$\mathbf{a_2}$ - negative of the second-order coefficient of the efficiency

Table 4. Characteristics of various solar collector systems for their TRNSYS modelling [26].

All these parameters must be determined for each of the collectors to model the solar field. Furthermore, other information is required to design the complete system such as the load curve, the control system, storage parameters, etc.

The final heat output from the solar field (H_{sf}) can be calculated for a specific period (Δt) following the next scheme and equation (4). The terms $\dot{m}_r$ refers the flow that gets through the receivers, C_p

term means specific heat capacity and $(T_{out} - T_{in})$ is the temperature jump induced by the solar system to the liquid heat carrier:

$$H_{sf} = \dot{m}_r * C_p * (T_{out} - T_{in}) * \Delta t \quad (4)$$

In the case of a steam generation system, it is commonly used the enthalpies of the fluid to perform this calculation. Moreover, this second equation is useful for any type of heat carrier [33]:

Figure 27. Direct steam production with a solar field [33].

$$H_{sf} = [\dot{m}_{w,out} * (h_{w,out} - h_{s,out}) - \dot{m}_{w,in} * (h_{w,in} - h_{s,out})] * temp \quad (5)$$

The equation (5) will be used in chapter 6 for the case study based on a direct steam generation system.

5 KEY CUSTOMERS AND MARKETS

In this chapter a thorough analysis of the solar thermal energy market is performed with the aim of finding the most suitable customer for integrating SHIP. The main industrial processes where solar heat is successfully integrated are reviewed, as well as the main sectors where heat demand is suitable for this integration. Furthermore, a geographical analysis is done to select the countries where SHIP has a potential expansion. Finally, the market of solar technologies is studied to select an adequate case study based on the selected customer characteristics for chapter 6.

The main characteristic of the ideal customer profile to determine the industrial sector potential for integrating SHIP are those with processes that require heat at low/medium temperature and have a great heat demand.

5.1 Conventional heat generation in industry

Conventional systems for heat generation around the world are mainly based on fossil fuels burning. Global industry sectors consumption in 2009 was 128 EJ of final energy, a total of 78 EJ were supplied by fuels to generate process heat via steam or direct heat. Another 9EJ were used for blast furnaces and coke ovens for iron and steel production and 16EJ for chemical and polymers fabrication. The use of natural gas (NG) for this purpose accounted for near 40% of this energy in OECD Americas and Europe, nevertheless, China and OECD Pacific met most of its demand with coal. This means that, even though renewable heat generation has increased in recent years, fossil fuels are still leading the heat supply in industry with a fuel mix that varies substantially between different regions [34].

Sources of energy	2006	2030
Liquids	34.6	28.6
Natural gas	24.1	25.6
Coal	24.8	24.3
Electricity	14.9	19.7
Renewable	1.5	1.8

Table 5. Global industrial energy consumption pattern by fuel in 2006 and 2030 (%) [29].

Nowadays, steam is one of the most important energy carriers along with electricity in industry, as well as a fundamental heat transfer fluid (HTF). Boilers are the most common way of producing steam, reaching a relatively high share capacity in industries such as chemical, paper, food, refining and metals industries. There are two main types of boilers, fire-tube or water-tube. The first one provides steam pressure at much as 30 bar and operates by heating a reservoir of water passing pipes with hot combustions gases through it. The water-pipe type heat with hot gases a set of pipes where water is running, reaching high pressures and temperature requirements. This technology has higher investment and maintenance costs [35].

The current HTF used in some of the main industrial sectors and the typical range of operating temperature are shown in the next table:

End-use	Temperature level (ºC)	Comment
Process cooling	<- 30	Mostly air separation in chemical industry
	- 30-0	Mostly refrigeration in food industry
	0-15	Mostly cooling in food industry
Process heating	<100	Low temperature heat (hot water) used in food industry and others
	100-200	Steam, of which much is paper, food and chemical industry
	200-500	Steam used mostly in chemical industry
	>500	Industrial furnaces in steel, cement, glass and other industries

Table 6.Temperature level and HTF in different industrial sectors [35].

5.2 Energy intensity and operation time

The heat demanded by processes may vary depending on the type of process but also on the operation time of the industry. Due to the variability of the solar availability, it is common that the heat load does not match with the solar heat supply (especially if the industry operates at night). Knowing this issue, the design of the solar system and the proper sizing of storage or back-up auxiliaries might be affected, as well as the feasibility of the integration.

Taken into account this consideration, industrial sectors operation time is usually related to the energy intensity. This term measures the quantity of energy used per unit output (e.g. manufactured product) and is widely used to analyse the energy consumption and energy efficiency in industries [36] dividing them into energy or non-energy intensive. As shown in Figure 28, energy-intensive industries are responsible for almost two-thirds of the world heat consumption and require mainly heat at temperatures higher than 400ºC. Non-energy intensive industries have temperature demands lower, mostly below 200ºC, which makes them an interesting focus for SHIP market.

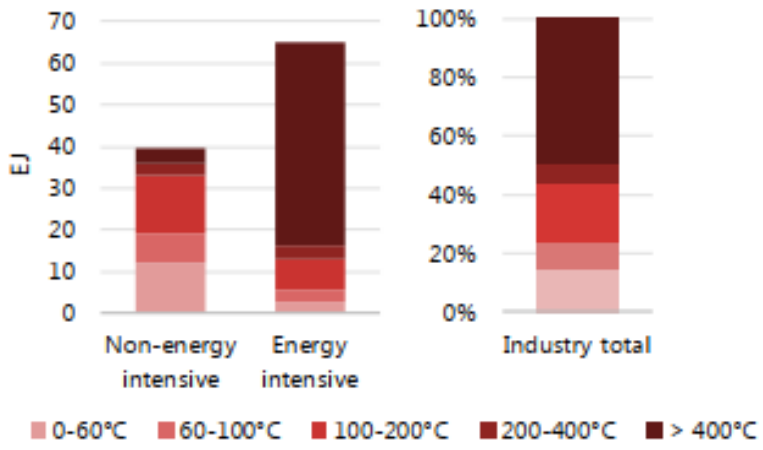

Figure 28. World heat demand by temperature range (2018) for both energy-intensive and non-energy intensive industries [3].

Nevertheless, this division does not only mean a different energy use but also imply different trends in operational time. Energy-intensive industries do not have cyclical short-term demand behaviour and tend to operate at full capacity all time. This means that, in general, these industries operate at the same load rate without seasonality to ensure the return of the intensive capital investment. On the other hand, non-energy intensive industries have a heat demand dependence on the production and working hours of employees [37]. A list of some industrial sectors divided by their energy intensity is depicted in Table 7:

Non-energy intensive industries	Energy-intensive industries
Food, beverage and tobacco	Iron and steel
Textile and leather	Non-ferrous metal
Ore extraction	Chemical (and refining)
Other metal products (machinery, electrical equipment …)	Non-metallic mineral products
Other chemicals (pharmaceutical, detergents…)	Paper and pulp

Table 7. Energy and non-energy intensive industries [37] [38].

Other industries such as mining are not considered as a manufacturing industry, therefore, it is not included in the table above. Moreover, the case of Food and Beverage could be analysed along with intensive industries as it is done by [37] since it has the higher energy consumption within the non-energy intensive industries, at least in the case of Europe.

5.3 Potential industrial sectors

The sectors analysed for showing a potential SHIP market are those with low/medium temperature heat demands, which, in the case of this study, is set under 400ºC. The temperature is also a key characteristic for selecting the solar collector, that is why some sectors tend to implement to a greater extent a type of collector.

The main sectors which deploy solar thermal technologies in their processes are described below:

Automobile industry: solar systems are integrated for heating water in processes as paint application, washing engine components, bodyworks pre-treatment line and bodyworks sheet surface preparation. The maximum temperature achieved with collectors in these processes are 120ºC and the countries which are leading this solar use are South Africa, India and Spain [39].

Food and beverage industry: it is estimated that more than 50% of the heat consumed by this sector is needed on a low-temperature level (less than 100ºC). It is one of the leading sectors in SHIP integration and many studies support its high potential. Typical processes with high thermal demand and the possibility of using solar thermal energy are cleaning, drying, evaporation and distillation, blanching, pasteurization, sterilization, etc [40].

Paper industry: 75% of the energy consumed in this sector is heating at low-intermediate temperature. The main processes that demand this heat are washing with hot water, pulping, drying and boiler feed. The case of India is especially notable because it is responsible for the production of 2.6% of the total paper consumed in the world [39].

Pharmaceutical industry: Production of bulk pharmaceutical products and final product formulation demands a high amount of steam, which is generally produced with a boiler using fossil fuels. This heat demanded reaches temperatures of 160-180ºC, so in this case concentrator collectors could be a suitable solution [41]. Pharmaceutical production is mainly located in Europe and North

America. Nevertheless, Greece, Egypt and Jordan are the main solar energy users for this industry [39].

Textile Industry: it is required a continuous supply of hot water in textile production, essentially in the dying process. Currently, this heat is provided by fossil fuels with conventional systems but, knowing that the temperature demanded is up to 80ºC, it seems like a suitable process for integrating solar thermal systems. The leader countries in applying SHIP in the textile industry are Greece, India and China, generally using non-concentrator collectors such as FPC [39].

Mineral processing: solar energy is an interesting option for remote mines. Multiple activities can integrate solar heating, the copper mining in Chile have implemented different solar technologies and represents an example of the potential for solar energy in this sector [42].

Manufacturing of chemical products: it is noticeable that, in some steps of the chemical production activity, preheating at low temperature is needed (which is suitable for solar thermal systems). Some of these processes are water heating, steam heating, cleaning and painting and the common solar technology implemented is flat-plate collectors, attaining a maximum temperature of 130 °C.

Agricultural industry: the main processes where SHIP is integrated is in drying and water heating. Both air and water collectors are used due to the variety of heat demand.

Manufacturing of leather products: Several countries in Asia such as Thailand, China and India have a large leather manufacturing production. In this sector the implementation of solar thermal energy is mainly in retanning process and water heating [39].

Figure 29 depicts the useful heat demand for some of the more extended industrial sectors in Europe. Even though Europe does not represent the market of the whole world, it gives a general idea of how the heat demand in industry is and which sectors require the most amount of energy at a low-medium temperature, the ideal for solar energy. The highest levels of heat with this condition come from the food, drink and tobacco sector followed by the paper and printing industry. The case of the chemical sector is also interesting as half of its demand is also low-medium temperature heat and, along with the machinery sector, is a target for SHIP implementation in metal processing. Textile processing shows a very high potential for SHIP integration for several regions in Southeast Asia and China [43].

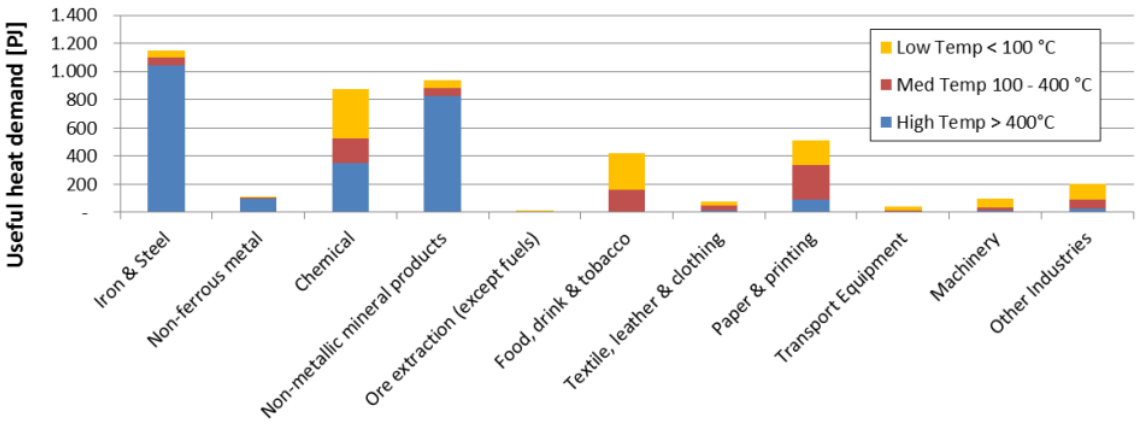

Figure 29. Breakdown of useful heat demand for EU-27 industry for 3 temperature levels for the main industry sectors in Europe [43].

The importance of a sector depends strongly on the country, which means that a huge variety of industrial heat demand exists all over the world. Despite this, the needed temperature and processes within a sector can be assumed to be similar across different countries, allowing the identification of

promising sectors for SHIP integration could be transferable to the global industry even though the data reviewed comes only from a part of it [44].

A key characteristic for a sector to be suitable for the use of SHIP, as it was mentioned before, is the consumption of low and medium temperature heat in their process. Nevertheless, it is important to notice that it is quite normal for industries to consume steam when medium temperature heat is demanded even though lower working temperatures would be enough to reach the process requirements. This fact leads to the conclusion that when assessing the feasibility of introducing SHIP, the temperature that should be looked at is the actual one needed by the process, not the temperature of the heat carrier being used. This operational perspective should be also considered not only for solar thermal integration but also for reducing the current energy consumed by a process [45].

Figure 30 shows the main industrial sectors for integrating SHIP and, what is an important parameter to do this integration, the range of temperature demanded as for the heat supply during operation. The figure shows the most suitable processes inside each sector applying the criteria of looking for those with low-temperature requirement [44].

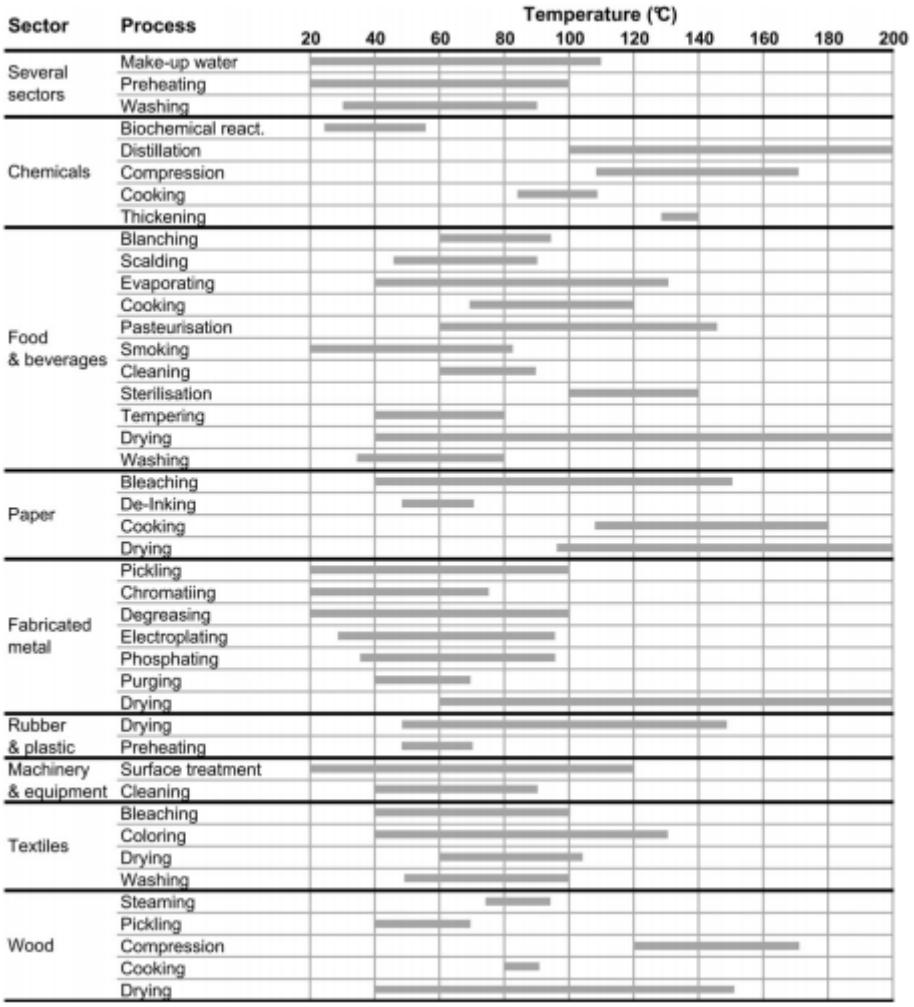

Figure 30. Promising industrial sectors and processes for the integration of solar thermal energy characterized by the range of temperature heat [44].

A Report of IRENA and IEA determined in 2015 that a very high percentage of the low-temperature heat demand is found in the sectors of food, beverage, paper and textile whilst medium temperature

ranges are characteristics for processes in the chemical and plastic industries. Half of the total heat consumption in industrial processes is related to these industries for activities such as drying, cooking, cleaning, extraction and many others under 250ºC [4].

Finally, the sectors which have currently more participation in SHIP integration are depicted in Figure 31, where it is seen the total number of existing solar systems installed and the thermal capacity for industries all over the world. The data showed comes from solar heat systems in industry operating on March of 2020, evidencing that the biggest capacity installed accounts for the mining sector as a very first place, followed by the food and textile industry. The mining sector leads in installed capacity thanks to the Miraah plant in Oman with a thermal capacity of 300 MW_{th} [46] and two large-scale solar plants (34 and 10 MW_{th}) built in Chile for water heating in copper mining and [42].

On the other hand, the food and beverage sector accounts for 46% of the installed systems, demonstrating the huge potential for these sectors in small and medium-sized customers. Another promising sector is the textile industry, with a total of 25 installed plants and 26 MW_{th} (6%) of installed thermal capacity. This information comes from 301 detailed solar systems that can be found in the SHIP (Solar Heat for Industrial Processes) database, an online portal operated by AEE INTEC in Austria [46] [47].

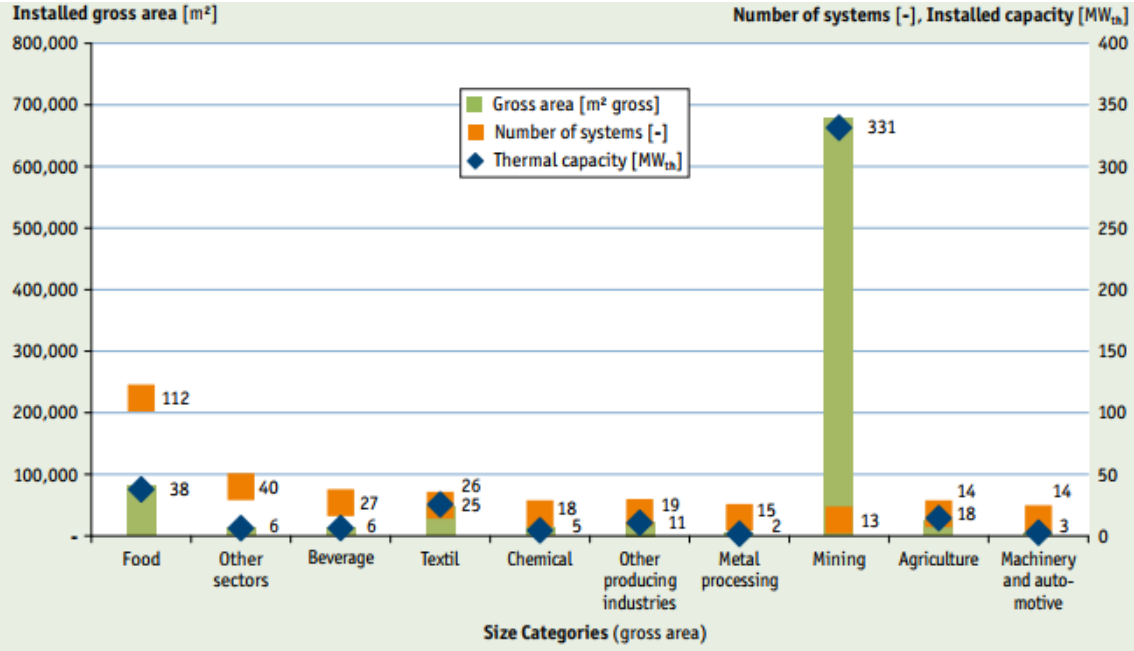

Figure 31. Solar process heat applications in operation worldwide end of March 2020 by industry sector [46].

The potential market analysis for SHIP has been developed by identifying the promising sectors based on two criteria: high global heat demand and low-temperature requirements. Having selected these first conditions, other specifications described in the next paragraph will be considered in further steps of the study for estimating the SHIP potential (see section 5.5.6).

There is a recovery heat waste potential that competes with solar heat and involves those industrial activities which can easily reduce their heat demand thanks to energy efficiency measures; some examples are recovering heat from exhaust combustion gases, installing an economizer for a boiler or using the waste heat from cooling and compressed air. Other limitations for calculating the potential of an industrial sector are that some processes which currently required heat must be partially supplied with electricity due to operational reasons. The space available for implementing solar technologies is also a limiting factor as well as the capacity of roofs for carrying static loads such as solar collectors. As a reference, the most promising sectors for SHIP analysed in the German industry are food and beverages, textiles, paper and chemical [44].

Other studies confirm the potential of the industrial sectors mentioned before, identifying food and beverage, textile, transport equipment, metal and plastic treatment, and chemical as key sectors for SHIP deployment. The most suitable industrial processes include cleaning, drying, evaporation and distillation, blanching, pasteurisation, sterilisation, cooking, melting, painting, and surface treatment [45].

5.3.1 Food and beverage

The food and beverage industry is expanded all around the world and is currently the sector with more installed solar thermal systems. It is characterized by a large heat demand in the temperature range up to 150ºC, where it is found some suitable processes for solar heat integration such are pasteurization of liquid goods at 65 to 100 °C, cooking at 100 °C in meat processing, blanching of vegetables or meat at 65 to 95 °C, drying and evaporation at 40 to 130 °C in fruit and vegetable processing or cleaning of products and production facilities at 60 to 90 °C [44]. The most used solar technologies for these applications are FPC and PTC. This sector is dominant in worldwide SHIP plants thanks to Mexico, US, Greece, India, Spain, and Austria which seem to be growing in this market [39].

The energy consumed during the year 2016 in low and medium temperature processes accounts for 44 EJ (exajoule), being the food and beverage sector a consumer of nearby 3.3 EJ and 2.2 EJ at low and medium temperature heat respectively [16].

The sub-sectors of brewery and diaries are very promising for SHIP integration and almost 90% of its heat demand could be supplied at 100ºC or less temperature. The main processes and their temperature conditions are shown in Table 8.

End-use	Sub-Sector	Process	Max. Operating Temperature (ºC)
Process < 100 ºC	Dairy	Homogenization	75
	Dairy	Flash pasteurization	72
	Brewery	Mashing (pre-heating of brewing water)	65
	Brewery/Dairy	Bottle cleaning	85
	Brewery/Dairy	CIP	90
Process > 100 ºC	Dairy	Sterilization	120
	Brewery	Wort boiling (evaporation of water)	~100

Table 8. Exemplary process temperatures in the brewery and dairy industry [48].

In the case of the brewery industry, thermal energy accounts for about 80% of the energy demanded and the main consumers are wort boiling (25-50%), bottle washers (25-40%) and pasteurization. In the process of malting, hot air is required at 60-80 ºC for drying the barley and stopping the germination of the grains. The water temperature range demanded is between 25 and 125ºC and it could be supplied with flat plates collectors. Dairies often work the whole week with a continuous demand and its most suitable processes for solar thermal application are pasteurization (60-85ºC) and sterilization (130-150ºC). The process of drying milk demands also a high and constant flux of hot air (60-180ºC) [49]. It is worth mentioning the potential of solar air heating in food processing and the tobacco industry [4].

5.3.2 Paper, pulp and printing

As it was mentioned before, 75% of the energy consumption for paper production is estimated to be heated at low and intermediate temperature, providing a great opportunity for implementing solar thermal systems. The HTF supplied by solar technology could be water, steam, air or oil depending on the process. The potential of SHIP in this sector has been assessed by various studies which were especially focused on India [39].

The mot characteristics processes of this industry are named in Table 9 along with the range of heat temperature demand and the common heat transfer fluid used:

Process	Required temperatures (ºC)	HTF
Bleaching	120-150	Water
De-linking	60-90	Steam
Paper drying	90-200	Air, steam
Pulp preparation	120-170	Pressurized hot water

Table 9. Processes with corresponding temperatures and HTF required in a paper industry [50].

The drying process is remarkable due to be by far the highest energy consumer. Drying cylinders are frequently used for this purpose, requiring steam at 130-200ºC. Regarding the cost of energy in the paper industry, by average represents 11% of the total manufacturing costs and can even reach 25%, which indicates the high importance of efficient energy consumption in this sector [44].

Even though this industry is globally extended and that big industrial countries such as the US and China leads its production, it is worth mentioning the great importance of this sector in Uruguay, Finland and Sweden, probably thanks to the primary materials they possess [51].

5.3.3 Chemical

The chemical sector has the largest quantitative potential for the application of solar heat thanks to its enormous heat demand. Even though it requires a great amount of energy at high temperature, the processes that operate with low and medium temperature heat demand half of its heat [4], being suitable for solar technology. The average energy costs for energy accounts for 4-5% of the total manufacturing costs [44].

The amount of energy consumed by the chemical industry considering the world industrial activity in 2016 is about 3.1 EJ for low-temperature heat, and 4 EJ for medium temperature [16].

The organic chemical industry is the largest sub-sector regarding energy consumption and typically uses steam cracking processes to make olefins (ethylene, propylene and butadiene) from naphtha, ethane, propane or other crude oil-derived feedstocks [52]. Furthermore, the production of ammonia and petrochemicals is highly energy-intensive, whereas the subsectors of inorganic chemicals and pharmaceuticals need less energy. The processes defined as the most suitable for using solar heat are cooking (85 to 110ºC), distillation (110 to 300ºC), bio-chemical processes at low temperatures (<60ºC), preheating and polymerization [44].

The International Renewable Energy Agency determined in 2015 the chemical sector as the most promising for SHIP integration, accounting for half of the global industry potential due to the near end-of-life of two-third of the existing capacity by 2030. This fact gives the chance to solar integration in new construction, rising the feasibility of this technology as an alternative heat source [4].

5.3.4 Textile

The textile sector is one of the biggest industries in the world and seems a very interesting option for solar thermal integration in regions such as China and Southeast Asia where it has a great expansion.

Most of the processes involved in this industry are below 100ºC, only colouring needs higher temperatures as is shown in Figure 31. Some important processes at low temperature are, for example, washing at 40 to 90 °C, drying, and a great number of finishing processes like dyeing and bleaching at 70 to 100 °C or desizing at 80 to 90 °C. A study estimate that up to 25 to 50% of the heat consumption in the textile sector could be covered by solar thermal energy [44].

The amount of heat consumed by the textile industry in 2016 for low-temperature heat is about 0.4 EJ and 0.9 EJ for medium temperature, considering the global industrial activity [16].

5.3.5 Mining

The mining industry is not as extended in every country as the industries mentioned before, it depends directly on the natural resources of each region. In this case, SHIP application is particularly interesting for remote mines where solar radiation is a great energy alternative to fossil fuels due to the costs of fuel transportation. These are the cases of dominant mining industrialized countries such as South Africa, Chile, Austria and Germany, where SHIP has already been integrated for cleaning processes and water preheating. Some potential applications for solar heat are not only found in thermal processes but in chemical and carbothermic reduction processes too [39].

The integration of solar thermal energy for water heating could be applied to a process at low temperature in the copper mining industry: solver extraction and electrowinning. This one is characterized by demanding water temperatures between 60 and 90ºC and, in the case of copper mines in the north of Chile, is supplied with solar thermal energy with two of the biggest SHIP plants of the world [42].

It is estimated that the heat consumption in by mining industry in 2016 for low-temperature heat is about 1.1 EJ and 0.7 EJ for medium temperature, considering the world industrial activity [16].

The most important deployment of SHIP in the global industry is the case of the Miraah plant in Oman. Its thermal capacity is equal to 300 MW_{th}, which means that near two-thirds of the total capacity installed in the world. It is the largest solar plant for industrial processes and continues its expansion. The solar plant implemented parabolic through collectors and supply steam for enhanced oil recovery [52] [47].

5.3.6 Conclusion for solar thermal potential in industrial sectors

Five industrial sectors have been selected as promising customers for the deployment of SHIP technology. The potential of the sectors depends highly on the operational temperature range due to the importance of this criterion in the designing and feasibility of integrating SHIP. On the other hand, the amount of heat required under 400ºC by each industry must be considered as current solar technologies can reach this temperature with concentrator collectors and the appropriate solar radiation. Nevertheless, this temperature condition could be quite elevated as other studies have considered 300ºC [44], a fact that will be taken into account when assessing the results.

In Figure 32 it is shown the heat consumption of the most promising sectors and their ranges of temperature, noticing that chemical, food and beverage and paper industries have a great heating demand in low and medium temperature. It is also important to mention that the unique context of each country and the share of energy consumption in its industry for each sector is also considered.

For example, the case of Chile is especially promising in mining even though it does not have a big contribution to global heat consumption, while the textile industry has great importance in countries as China, Turkey, or Viet Nam.

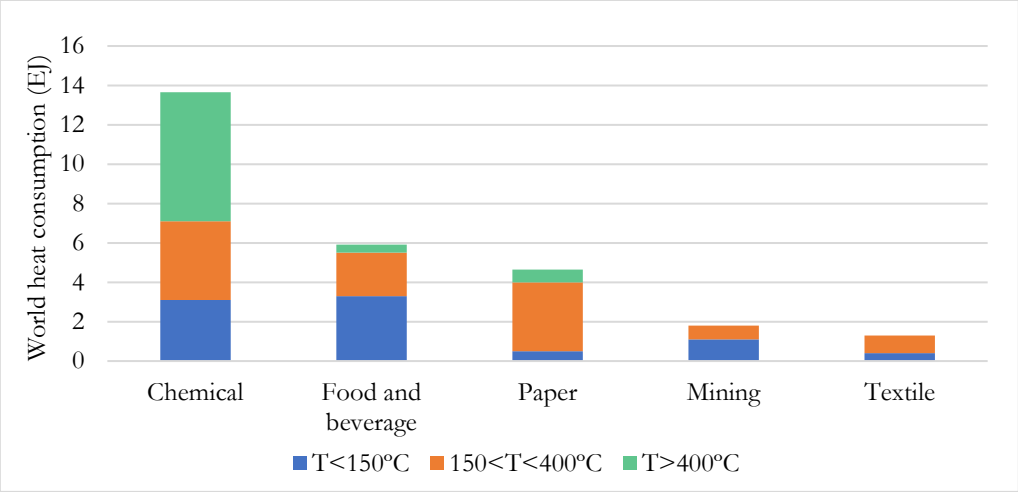

Figure 32. Share of industrial heat demand by temperature level for SHIP potential industrial sectors [16] [53].

For further research, other specific parameters such as operation time for an industrial sector, the current use of renewable sources for heat generation or the roof space for solar collectors installation is key when assessing the potential of SHIP. The potential recovery for waste heat is also an important factor in some sectors; for example, in chemical, food and beverage and paper industries near 7% of the energy in the UK is wasted, making them an important focus for energy efficiency measures [54].

The share of heat for each temperature range in the different industries is estimated based on different studies as well as the ratio between heat and total final consumption. Anyway, it is a general assumption, and the percentages may differ depending on the source of information.

Industrial sector	<150ºC	150<400ºC	>400ºC	TFHC/TFEC
Chemical	22%	30%	48%	0.78
Food and beverage	65%	28%	7%	0.84
Paper	59%	27%	14%	0.75
Mining	60%	40%	0%	0.39
Textile	29%	71%	0%	0.50

Table 10. Share of temperatures ranges for the total final heat consumption (TFHC) in industries and its ratio with respect to the total final energy consumption (TFEC) in selected industries [53] [44] [35].

The literature reviewed confirm these sectors as the most promising; nevertheless, there are other generally mentioned like the machinery industry because of its high energy consumption and the existence of many processes with low and medium heat temperature.

5.4 Solar thermal technology market in industry

The most promising industrial sectors for implementing solar thermal energy has been identified. In addition to this, it is reviewed the current plants and market for solar thermal technology, its main manufacturers and costs.

Figure 33 represents the number of solar systems, capacity and collector's area for 301 SHIP operating plants [46]. Near half of the solar plants use flat plates collectors, which require a lower

initial investment and are generally applied for smaller industries and processes with low-temperature requirements. Nevertheless, parabolic trough collectors are commonly used for bigger projects which require higher temperatures and generally have a bigger solar field. Moreover, the thermal capacity for PTC plants is three times bigger than the one for FPC.

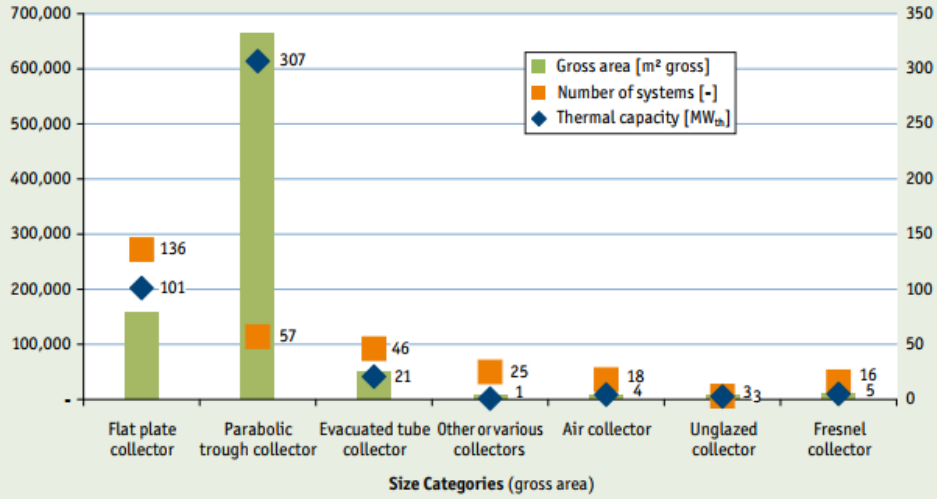

Figure 33. Process heat systems, capacity and gross collector area for the different solar collector technology [46].

Geographically, PTC projects tend to be a more attractive solution in countries with high direct solar irradiation. The case of Mexico is especially interesting as it has 34 currently operating plants of the 57 counted in Figure 33. FPC technology is more extended across the globe and has a large number of plants installed in Europe, region which also leads in ETC (16 plants) [47].

Figure 34. Worldwide operating SHIP plants [47].

Regarding the companies that currently cover the SHIP market in terms of turnkey projects, the most remarkable are located in Mexico and China. The companies with a larger number of turnkey plants at the end of 2019 are listed in Figure 35, where we can also find suppliers from India, Germany, Jordan or Austria. It is also shown the most commercialised type of collectors, which are the FPC and PTC. If it is taken into consideration the companies with more area of collectors sold (above 10,000 m^2), three companies from Chile, Denmark and the US are also remarkable [55]. The case of

Chile is due to its solar plants in the mining industry and for the US is because of the huge plant built in Oman.

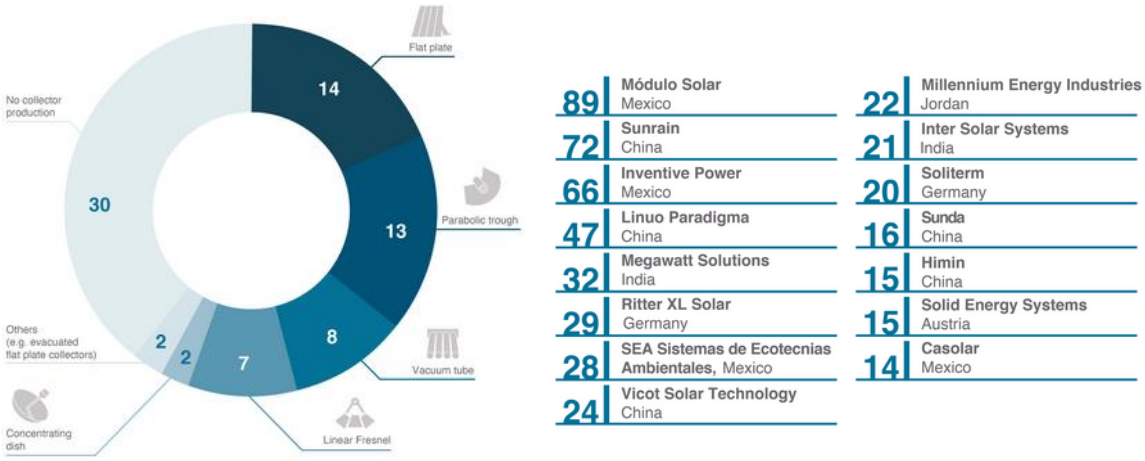

Figure 35. Division of worldwide turnkey SHIP suppliers by technology (left) and list of the suppliers with more projects by the end of 2019 (right) [55].

Finally, some studies have assessed the economic feasibility of solar heat integration in different countries and industrial processes, concluding with the importance of fuel price growth as a key parameter. The payback of various projects resulted in six years approximately; 50-70% of the costs were attached to the solar collectors whereas the rest implicate the installation [14]. Some of the prices for solar collectors in different regions are depicted in Figure 36.

Solar collector type	Location/Country	Cost USD ($/m²collector)
FPC	India	180
CPC	India	333
	China	130
	Europe	450-900
PDR (fixed)	India	113-300
PDR (tracking)	India	300-600
PTC	India	270
	Europe	650
	Mexico	400-629
LFR	Europe	690-900

Figure 36. Costs of different types of solar thermal collectors [14].

5.5 Potential customers and geographical market

Five industrial sectors have been analysed for been the most promising ones in integrating solar thermal technology. In order to reduce the scope of the project and focus the potential market for SHIP, further analysis is done regarding the geographical market of interest. An MCA performed to assess the fundamental aspects of the countries and identify their potential. These aspects englobe the energy policies that are currently pushing companies and societies for developing a more sustainable industry, the solar resource, and the trends of markets in term of renewable energies, industrial sectors growth or suitable business environment. The analysis details are described in section 11.1 Appendix 1: Multi-Criteria Analysis

5.5.1 Geographical market of interest

The multi-criteria analysis based on the criteria described in section 3.2. have been performed for narrowing the geographical scope and determining promising countries where solar thermal technologies have great potential. Most of the data used for this analysis comes from reliable international sources (IEA, OECD), nevertheless, due to a lack of reliable information for some countries only 141 have been considered in the MCA.

Figure 37. Results from the MCA, worldwide countries potential for SHIP integration.

The world map above shows the potential for the integration of solar thermal technologies in the industrial sectors selected. The regions with a darker blue colour represent the most suitable countries, showing that China and the United States are at the top of the ranking. There are zones such as Europe, south and east Africa, some countries of South America and southeast Asia that seems to be a potential region for SHIP implementation.

There are two criteria which higher weight in the country selection: the energy consumed by the most promising industrial sectors regarding solar integration and the solar resource. In the case of energy consumption, it is not only taken into account the total consumption but also the percentage of the energy that is consumed in the promising sectors concerning the total energy demanded by the industry of the country. Moreover, a sensitivity analysis has been made to detect how countries vary their position in the ranking depending on the weight that has been given to this percentage. The results from this sensitivity analysis shows which countries have a big dependence on this criterion and, therefore, the size of their market might not be appropriate to be at the top. This has happened mainly to little countries with big industry in a specific sector.

Figure 38 shows the number of positions that each of the top 30 countries moves when the criterion of energy consumption is changed. The comparison is made between a share of the weight of 50-50 (total energy consumption and importance of the promising sectors in the country) and a share of 90-10. The countries of Netherlands, Jamaica, Jordan and Kenya are initially left out of the top ranking due to their high variability in the analysis.

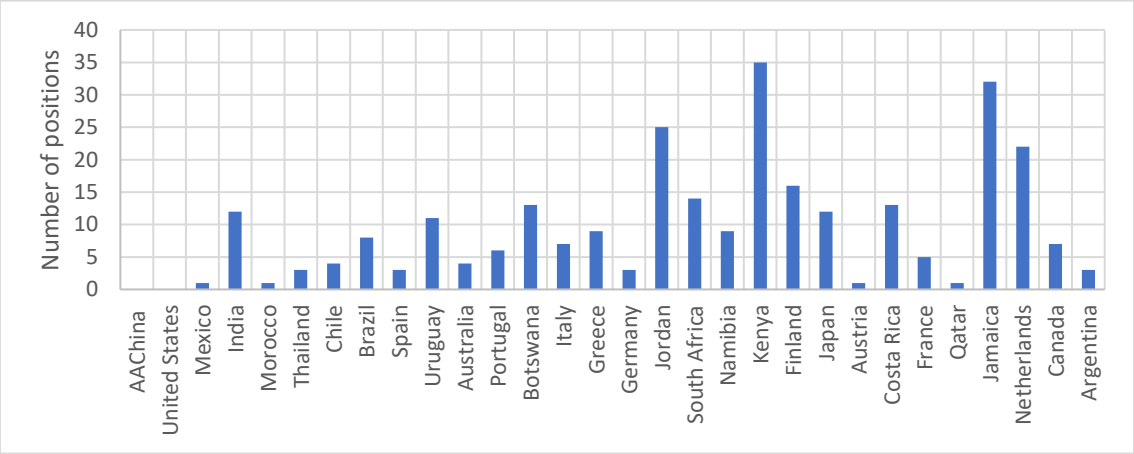

Figure 38. Variability of the countries position in the ranking of SHIP potential integration with the sensitivity analysis.

A classification by continents with the top 30 countries is shown in Table 11 along with the position of each country in the ranking on the left of its name and the value resulted from the analysis on its right. Europe and America dominate the ranking, with 8 countries each.

Asia	Europe	America	Africa	South-East Asia and Australia
1-China (69.8)	9-Spain (37.6)	2-US (61.3)	5-Morocco (39.6)	6-Thailand (39.3)
4-India (41.4)	12-Portugal (36.1)	3-Mexico (44.2)	13-Botswana (35.8)	11-Australia (36.9)
20-Japan (33.3)	14-Italy (35.5)	7-Chile (38.3)	17-SouthAfrica (34.6)	
24-Qatar (32.6)	15-Greece (35.3)	8-Brazil (37.6)	18-Namibia (34.4)	
Jordan	16-Germany (35.1)	10-Uruguay (37.4)	Kenya	
	19-Finland (33.5)	22-Costa Rica (33.0)		
	21-Austria (33.0)	25-Canada (32.4)		
	23-France (32.8)	26-Argentina (32.0)		
	Netherlands	Jamaica		

Table 11. Ranking of the 30 countries with higher potential in SHIP integration resulted by the MCA.

As it is seen, the results show great scores for countries all over the world, so it is decided to analyse in deep the case of the most potential countries for each region as well as the special case of Europe due to the number of countries which stand in the upper part of the ranking even if they do not lead the top 10. European countries have demonstrated better results in terms of sustainable energy policies and ease of doing business, furthermore, the solar radiation criterion has provided an important technical advantage to some Mediterranean countries. America is indeed an interesting continent for SHIP deployment, nevertheless, some countries that resulted in being promising within the MCA do not represent a big market because of their little industrial consumption such as Uruguay and Costa Rica.

5.5.2 Top non-European countries

The trends of industrial sectors consumption and the heat temperature range required are the parameters analysed in Figure 39 for the 10 non-European. in further research for European countries, other factors such as the solar resource, energy policies or technical limitations are detailed.

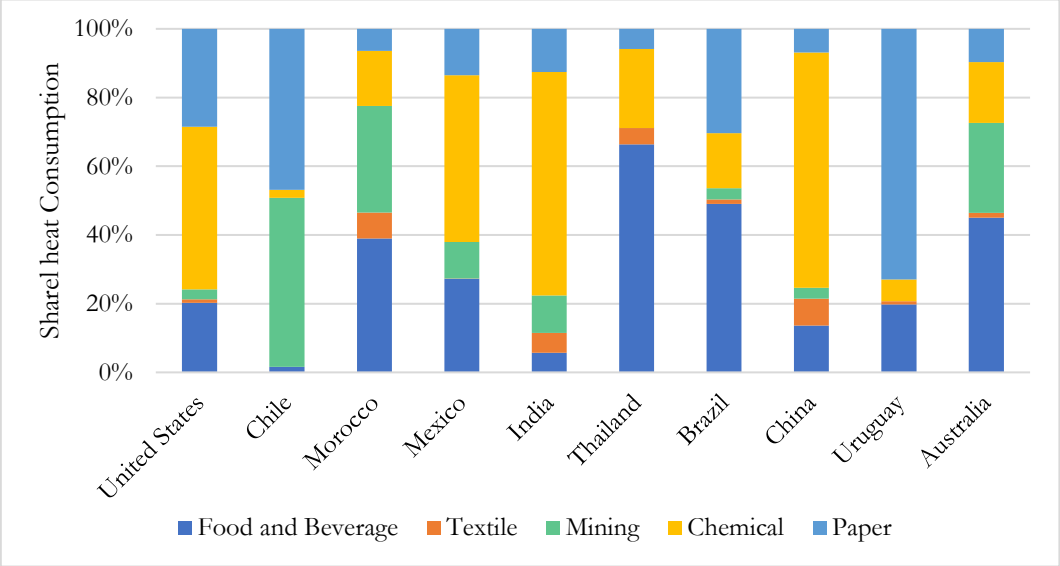

Figure 39. Share of heat consumption between five industrial sectors per country.

The share of heat derived from the total final energy consumption [51] is estimated based on the heat demand characteristics of each sector defined in Table 10. The importance of the chemical industry is noticed in US, Mexico, India and China, which are some of the biggest energy consumers countries in the world. High consumption of this sector implicates that the average heat temperature demand in these countries will be higher, therefore, concentrator technology market might have a big potential in those regions. Mining sector is a key industry in Chile, Morocco or Australia and food and beverage leads in Thailand and Brazil. Textile industry has a lower impact on industrial consumption in comparison with the rest of the sectors, nevertheless, it is appealing due to its low-temperature requirements for some processes that are appropriate for SHIP integration. Its big presence in the Chinese industry entails an important heat consumption.

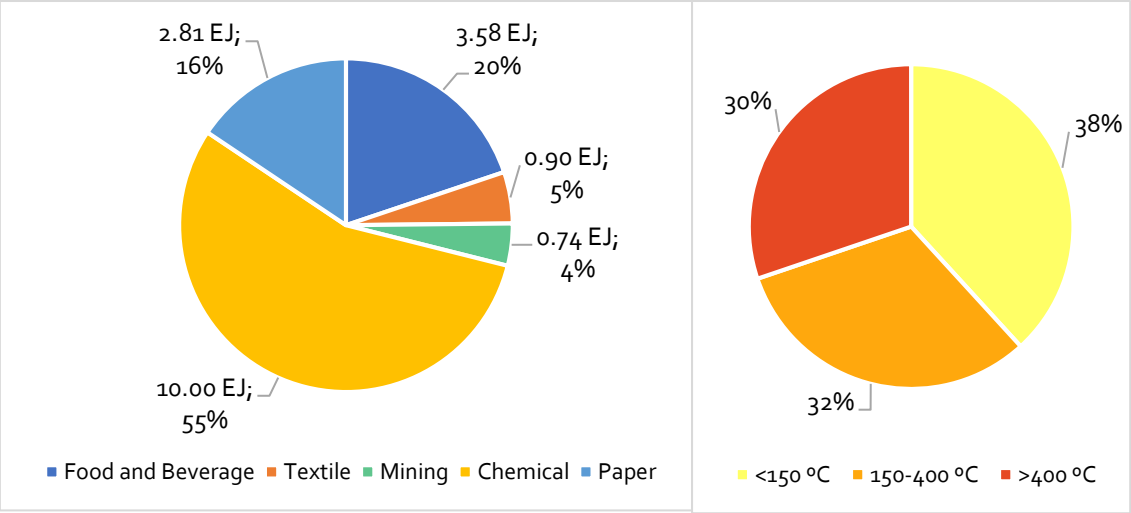

Figure 40. Share of heat consumption in different industries for the top-10 countries of the MCA (left) and share of the temperature range required.

As it is shown in Figure 40, the consumption in chemical industries has a great impact as it is more than half of the total. Even though the deployment of SHIP in this sector is still low due to the high-temperature requirements, it seems to have great potential in the future market [4]. Food and beverage represent also an important share of heat consumption and, in this case, multiple experiences confirm the feasibility and potential in this sector, which makes Brazil a very interesting region for SHIP market. The paper industry is the third with the highest heat consumption and should be considered as well, despite that, the contribution of bioenergy to cover its demand is greater than in other sectors and compete with solar systems.

Finally, Figure 41 depicts the heat consumption for each country divided into industrial sectors. US and China consume ten times or more than the rest of the countries, which means that their market potential should be considered. Knowing that favourable temperature ranges for SHIP integration are low, the demand of countries such as Australia or Thailand depicts great potentials as it is mainly at low temperature. Brazil is without any doubt the third biggest potential market.

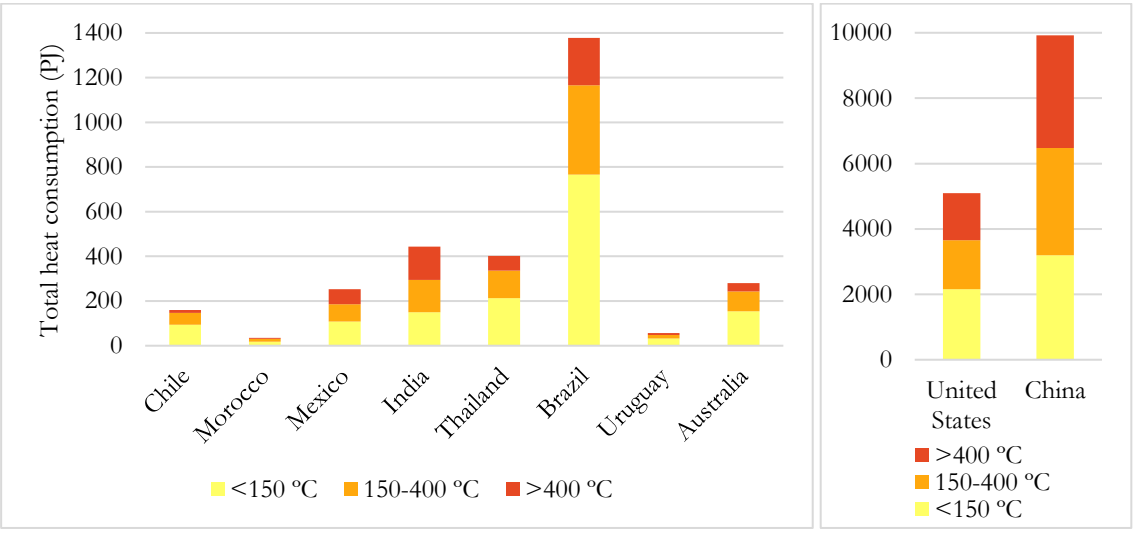

Figure 41. Heat demand in selected industries for the top-10 countries of the MCA and its temperature ranges.

5.5.3 European countries

Europe is determined by the MCA as a potential region for SHIP deployment and the scope of the project is finally limited by this zone. Even though middle and northern countries have the disadvantage of a poor solar resource, the high heat demanded of European industry, the renewable energy policies that have been implemented in the last decade and the business environment makes Europe an appealing place for SHIP deployment.

Figure 42. Results from the MCA of European countries potential for SHIP integration.

One extra criterion has been added to filter the potential for each European country in the MCA: the price of natural gas for industry (or non-householders). This parameter is key to companies for implementing alternative heating systems such as solar thermal collectors. The scores from the MCA presented in Figure 42 (detailed in Appendix 1: Multi-Criteria Analysis) determine that the ten most promising countries are: Spain, Portugal, Finland, Italy, Greece, Germany, France, Austria Netherlands and Sweden. Netherland is considered, even though its high variance results in the sensitivity analysis, due to its high energy consumption in the food and chemical industries as well as its experience in implementing solar thermal systems.

The results from this analysis take into consideration only five industrial sectors, nevertheless, it would be necessary to take into account other important ones such as the machinery industry in Europe for developing a more detailed study of the total potential for SHIP in this region.

5.5.4 Energy policies

A global response to the threat of climate change took place thanks to the Paris Agreement [2] when not only Europe but countries around the world decided to start new policies and invest their resources in reaching the goal of maintaining Earth's temperature below two degrees Celsius. Since then, this common purpose has enhanced governments to stimulate renewable energy technologies as an alternative to fossil fuels for decreasing GHG emissions. Climate change policies go from targets of GHG emissions, carbon pricing and trading programmes to banning or reducing fossil fuels consumption [56].

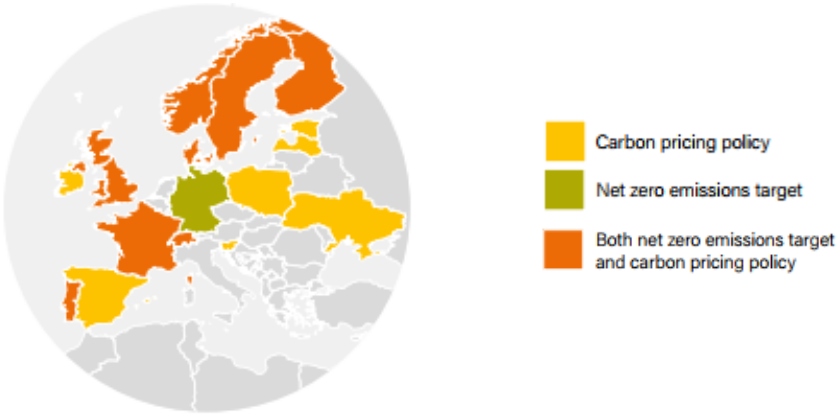

Figure 43. European Countries with climate change policies (selected in [56]) in early 2020.

In 2000 the European Commission created the European Climate Change Programme (ECCP) to help to identify the most environmentally and cost-effective policies and measures that could be taken in Europe for cutting GHG, therefore following the Kyoto Protocol targets. After establishing the 2020 climate & energy package in 2009, new ambitions were decided for 2030: reduce GHG to 40% compared to 1990, improve renewable energy share to 32% and, in the case of energy efficiency, 32.5% [57].

Furthermore, the European Green Deal proposed in December 2019 have designed a set of measures for reaching 2050 with EU as climate neutral. This has changed the path, raising the cut of emissions in 2030 to 55% and proposing the European Climate Law (March 2020) which carries high impacts on the sectors of industry, mobility, energy and buildings [58]. With the Just Transition Mechanism, the EU wants to mobilize at least € 150 billion over the period 2021-2027 to follow the roadmap designed in the Green Deal and help the most affected regions. This huge financing system pretends to create attractive conditions both for public and private entities as well as provide easier access to loans and financial support [59].

An economical incentive for reducing carbon emission was set up in 2005, the EU emissions trading system (EU ETS). It is the biggest carbon market in the world and covers near 45% of the EU's greenhouse gas emissions. The ETS works by limiting the total amounts of emissions that installations covered by a system can generate. To reduce emissions, this limit tends to be reduced. Companies receive or buy emissions allowances in the ETS that must cover all their emissions, having the chance as well of gaining international credits from emission-saving projects. These allowances are trade following the ETS rules [60].

Regarding the energy sector, the Renewable Energy Directive created in 2009 and recast in 2018 establishes the Clean Energy for all Europeans package. New policies are focused on deploying renewable energy as well as changing the electricity market, making it easier for individuals to store and produce renewable. Each Member State is required to create energy and climate plans (NECPs) from 2021 to 2030 [61].

The share of renewable energy as final consumption is a common target for countries around the world but with higher ambitions in Europe (see Figure 44). It is also remarkable the goals established by Brazil or Denmark.

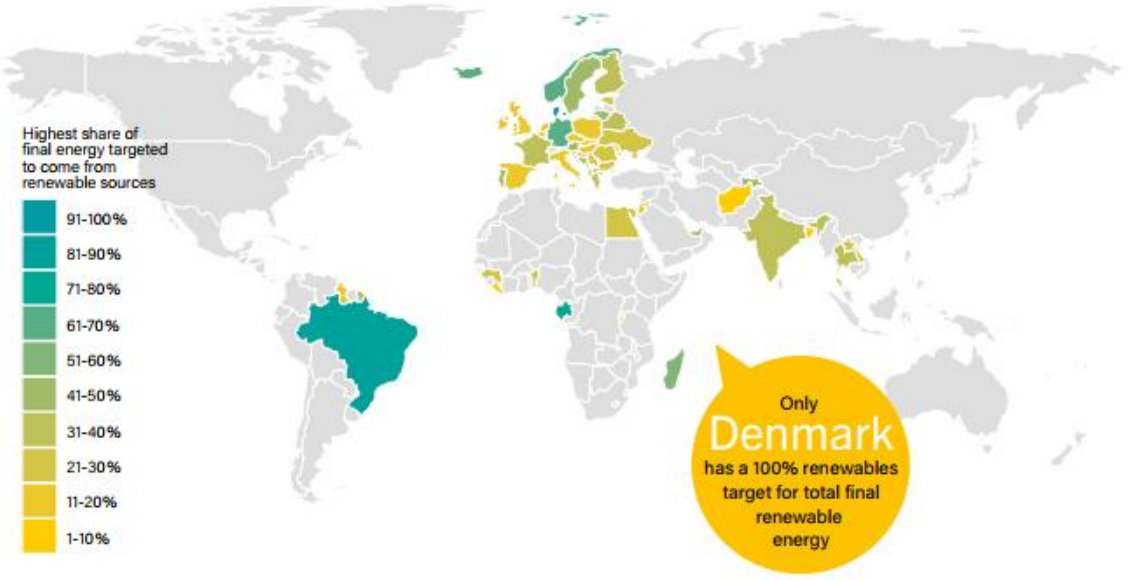

Figure 44. National targets for the share of renewable energy in final energy (end of 2019) [56].

For those ten countries that have been selected as the most attractive in the MCA, it has been made a more detailed review of their policies in Table 12. The status in 2017 of the targets for renewable heat shows that most of the countries already accomplished them in that year. The highest share of renewable heat is achieved by Sweden and Finland where heating demand for spaces is an important energy consumption activity as they have cold climates. Other regions with a higher solar resource such as Italy and Greece have specific goals for domestic solar thermal generation.

Country	Share of renewable heat	Status 2017	Policies in industry
Spain	17.3% by 2020	17.5%	Investment subsidy/grants Tax deductions and exemptions
Portugal	34% by 2020 38% by 2030 69-72% by 2050	41%	Investment subsidy/grants
Finland	47% by 2020	54.8%	Investment subsidy/grants
Italy	17.1% by 2020 Biomass (5,670 ktoe) Geothermal (300 ktoe) Solar water and space heating (1,586 ktoe)	20% 6,320 ktoe 207 ktoe 231.3 ktoe	Task credits
Greece	20% by 2020 30% by 2030 (60% domestic hot water from solar thermal)	26.6%	Investment subsidy/grants
Germany	14% by 2020	13.7%	Loans
France	38% by 2030	21.4%	Investment subsidy/grants
Austria	33% by 2020	32%	Tax deductions and exemptions

Country	Share of renewable heat	Status 2017	Policies in industry
Netherlands	8.7% by 2020	5.9%	Tax credits Feed-in Tariff
Sweden	62.1% by 2020	69%	

Table 12. Energy policies for heating and industry in the MCA selected countries [56].

5.5.5 European solar resource

The solar resource is a fundamental factor for determining feasible locations for solar systems. Solar radiation is scattered and absorbed by atmosphere components that divide it into direct and diffusive irradiance when reaches the Earth surface. The atmosphere characteristics (concentration of clouds, aerosols, water vapour content, etc) of the location where the solar resource is assessed are key to understand how this energy reaches the solar collectors and in which form [62]. As was mentioned in previous chapters, SHIP technologies use global radiation depending on the type of collector that has been implemented; for concentrator systems it has to be considered direct radiation as the major resource, not the diffusive. These facts make the countries near the equator and with the cleanest skies generally more appealing in terms of the solar resource, especially for concentrator systems.

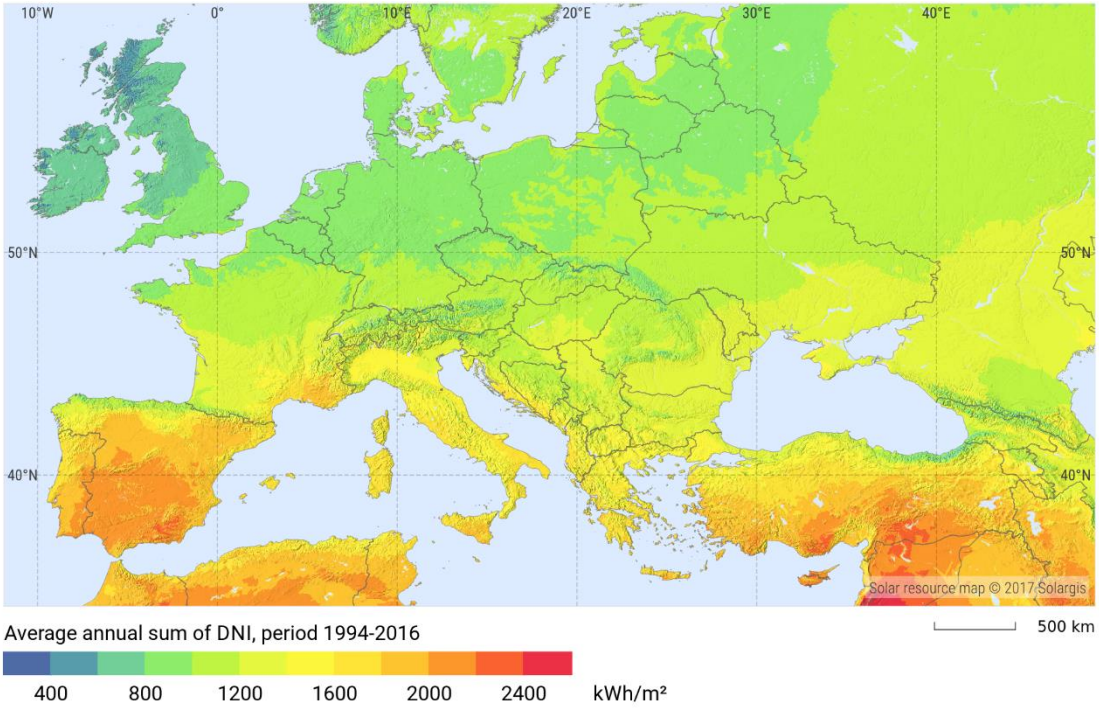

Figure 45. Direct normal irradiation in Europe [63].

In the case of Europe, countries near the Mediterranean region have better direct radiation levels, which makes zones of Spain, Italy, Greece or even France suitable locations for SHIP deployment. There are also emplacements with high altitude that are attractive for their solar resource even in middle and northern countries.

5.5.6 European heating process market for solar integration

In global terms, during recent years the number of solar thermal systems installed in industries has increased, existing 20 SHIP plants with a collector area higher than 1000 m² [43] in 2015 and 43 in 2019 [46]. The leader country in solar capacity in 2015 was Chile due to its solar installations in copper

mining, directly followed by China and US. Nevertheless, the currently largest solar plant integrated into an industry is the one mentioned before in Oman, with a thermal capacity of 300 MWh_{th}, accounting for 68% of the world's total solar thermal capacity. It is used for oil production and generating 6000 tons of steam per day [46].

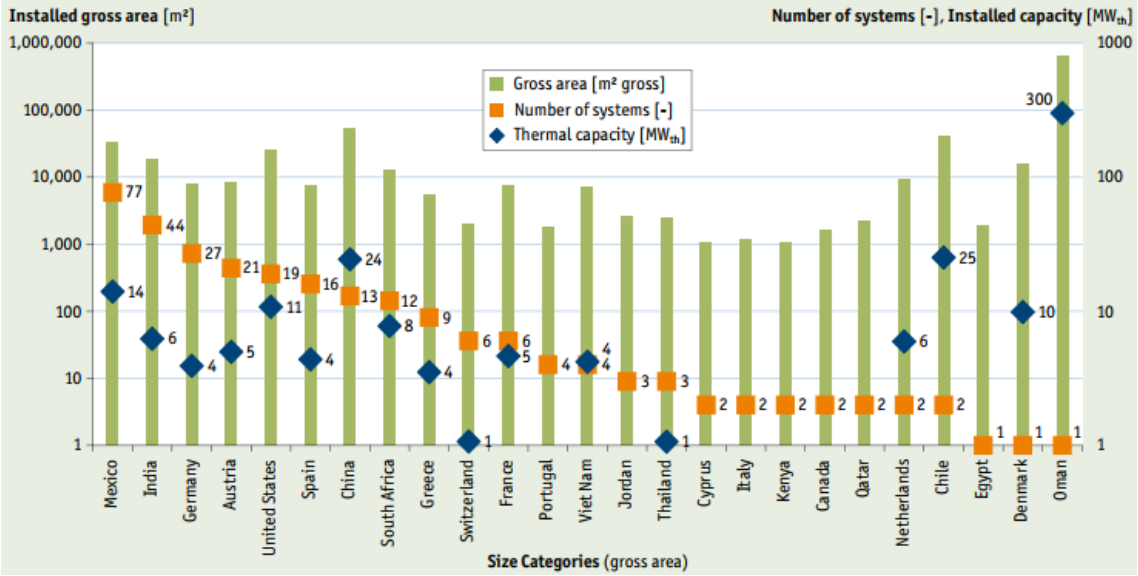

Figure 46. Gross area, thermal capacity. and number of SHIP applications plants for different countries [46].

A review of previous studies [43] has been done in order to analyse which are the limitations of the potential for implementing solar thermal systems in Europe and have a reference for the obtained results. The literature reviewed shows that about 3.4% and 4.4% of the total industrial heat demand could be supplied with solar energy respectively for Spain and Portugal [64]. In the case of Netherlands (Van de pol et. Al, 2001), the target of the analysis was on processes demanding hot water under 60ºC for some industries (food, paper, textile, and laundry) and the results estimated a potential solar integration for 3.2% of the total heat demand. A study made in 2003 in Sweden [65] declared that the low awareness about the possibilities for solar heat makes the situation difficult for implementing this technology, concluding that the overall potential was 1.5-2% of the heat demand. In Austria (2004), a potential of 3.9%, concerning the total heat consumption, was defined after considering the share of renewable and the waste recovery potential in specific industries such as food and beverage, chemicals or rubber and plastic [66]. In 2008 the potential for SHIP in Italy [45] was estimated in 3.9% of the heat demand in industry and an analysis of the available roof space for solar system was performed. One of the most cited studies was written in 2012 for estimating the SHIP potential in Germany. The results show a technical potential of 16 TWh per year, about 3.4% of the heat consumed in processes. This last report considered only heat demand below 300ºC and establishes the food and beverage industry as the most suitable industrial sector, followed by the chemical. Additionally, chemical industries have a big potential for heat recovery that makes it less attractive for solar energy implementation [44].

The theoretical potential for SHIP in the European countries selected is highly dependent on the energy and heat consumption for each of the promising sectors. The most consuming country is Germany with large chemical industry. The cases presenting a lower heat consumption are Austria, Greece and Portugal. Nevertheless, the high solar radiation levels of Portugal and Greece determine them as markets of interest and, in the case of Austria, it is one of the countries with a higher number of solar thermal systems in the European industry.

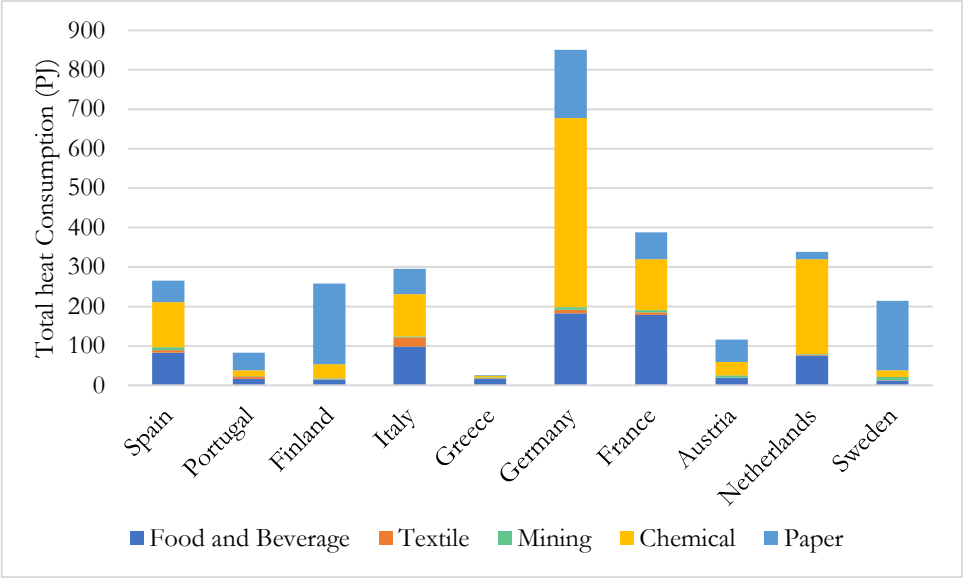

Figure 47. Heat consumption for each country and industrial sector.

The influence of the industrial sectors is key to understand, not only the heat temperature requirements for each country (see Figure 49) but also the type of system and collector that is going to be needed when designing the SHIP integration. The chemical industry has a big share of the SHIP potential in Germany and Netherlands, meanwhile, Portugal, Austria, Finland and Sweden have a bigger share of heat in paper and pulp. In the case of Greece, the country with less heat consumption, its high demand in food and beverage industries makes it a promising country considering the fact that it is the sector with more SHIP plants and greater experience (see Figure 31).

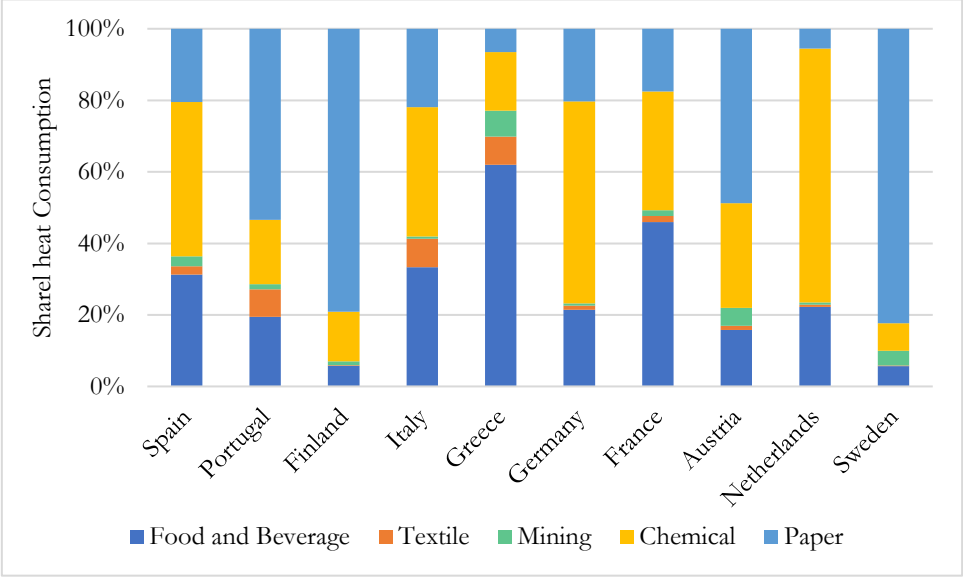

Figure 48. Share of heat consumption regarding the industrial sector for the selected countries.

The sectors of textile and mining have a low contribution to the heat demand of European countries, nevertheless, it does not mean that these industries do not have high importance in other regions such as East Asia in the case of textile or some countries in South America and Africa for mining.

Following the estimations of [67] [35] for the heat share in every industry, the results show that the majority of thermal energy in the ten selected countries is demanded by the chemical sector (41%), followed by paper and pulp (30%) and food and beverage (25%). To estimate how attractive are the processes for each sector regarding SHIP integration, it is also needed to consider the temperature

requirements. In this case, the chemical industry has a higher temperature heat demand than other industries such as food and beverage.

As it was reviewed, low-temperature conditions make it easier for solar thermal to be implemented when the solar resource is not favourable. Almost half of the heat demand is required at low temperatures below 150ºC (44%), meanwhile medium and high temperature shows a share of 30 and 26% of the share demand respectively.

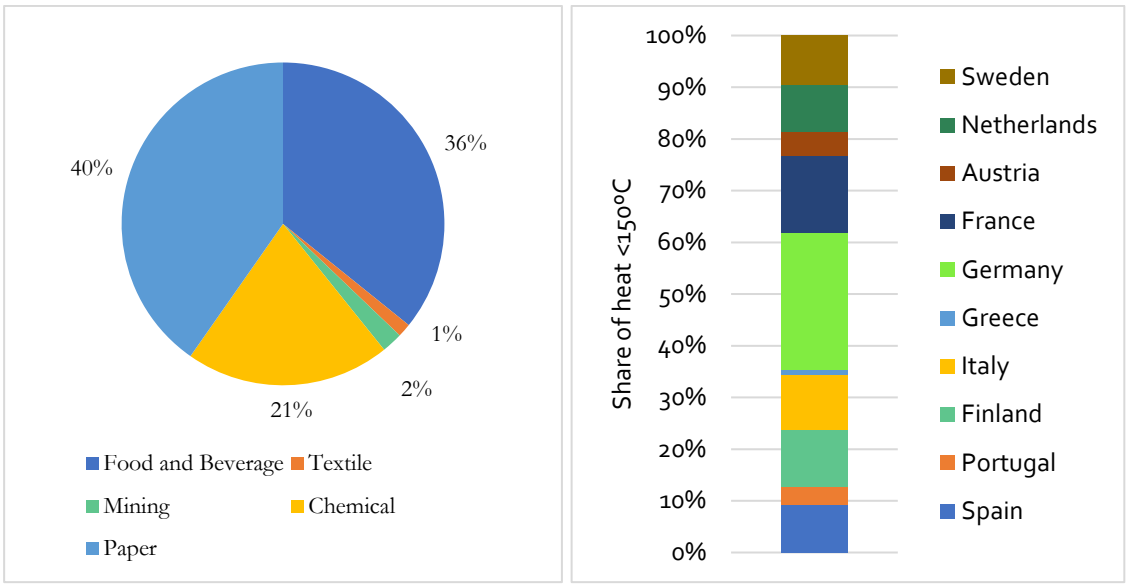

Figure 49. Share of temperature heat below 150ºC by industrial sector (left) and by selected country (right).

Analysing the demand below 150ºC, is it possible to see in Figure 49 how Food and Beverage and Paper and Pulp are leading in heat consumption at low temperature, a key result to understand why most of the SHIP installations have been made in the first one. The pulp and paper industry, even though it represents a great potential market for solar heat, does not have the same deployment of this technology. A possible reason could be that it is not such a globally spread industry and requires a big wood resource which is usually found in countries characterized by cold climates and low solar radiation such as Sweden and Finland. The right figure shows that the countries with higher demands at low temperature are Germany, Spain and France.

The technical potential for solar heat in industrial processes is a complex term that has been developed by multiple studies for different countries and regions. Aiming to estimate this potential, some assumptions have been made following previous reviews mentioned in section 5.3:

- Only processes requiring heat at low and medium temperature are analysed. It should be known that as lower the temperature is required as simple it is to be covered by solar energy.
- Waste heat at high temperature could be recovered with measures of efficiency. The sum waste potential in Europe is 16.7% of its industrial consumption for process heat and countries such as Germany, France, Spain and UK represent 60% of it [54]. Further analysis of the heat recovery potential in each industrial sector should be performed for more precise results.
- The roof space may not be sufficient for solar systems or is not capable to carry the weight of the installation. The assumption of reduction in the potential due to both energy heat recovery and roof availability is 60% [44].
- Solar fraction depends highly on the solar resource and, therefore, on the location. In this case, a solar fraction value of 30% has been assumed [44]. A deeper analysis would require

estimating this solar contribution for each of the ten countries depending on its solar radiation.

- The current contribution of renewable sources for heat supply is considered for deduction SHIP potential, therefore, further research is made to specify the renewable contribution in each industrial sector. Biofuels and waste is the only renewable source considered for this calculations due to the fact that represents the vast majority of renewable heat used in industry [3] whilst solar or geothermal heat contribution are still poor in comparison. The following table shows the conclusions:

	Food	Textile	Mining	Chemical	Paper	EU avg.
Renewable heat (%)	6.0	0.6	3.4	2.5	56.2	13.4

Table 13. Renewable heat share for the different industrial sectors (own calculations with [51]).

The results of SHIP technical potential considering the assumptions made previously are shown in Figure 50. Germany undoubtedly presents the highest potential for the integration of this technology, followed by France. Netherlands, Italy and Spain are also considered big markets for solar heat, depicting similar heat temperature requirements. In addition to this, the estimated heat that could be covered with solar energy in these countries varies between 4 and 5% of the total heat demand. This is a rough calculation but could be validated by the results seen in the literature (3.2-4.4%), considering the variety of scopes defined in those studies and that the maximum heat temperature selected for this analysis, 400ºC, is a bit quite higher.

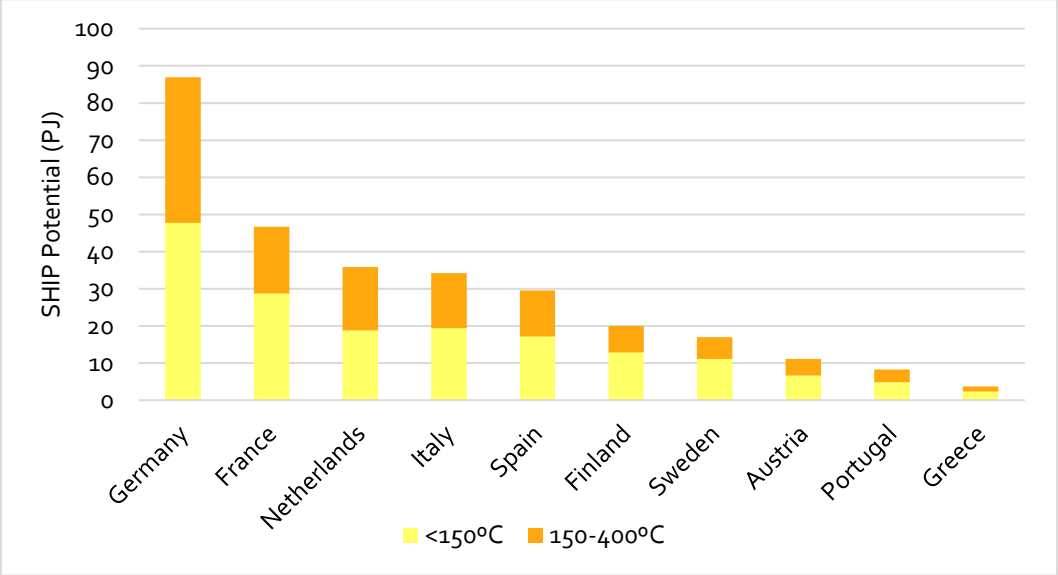

Figure 50. SHIP potential for the selected countries by temperature heat range.

Followed by these first five countries, it is worth mentioning the potential of Finland and Sweden thanks to their huge demand in the paper and pulp industry. As it was mentioned, the difficulty in integrating solar heat in this industry is not just because of the low solar resource, but also the great potential that the paper industry shows in waste heat recovery and the implementation of other renewable energy sources such as biomass. Nevertheless, the potential for SHIP in Sweden was estimated by 1.5-2% of its heat demand [65] and it is needed to be mentioned the processes that could be selected for the integration of solar heat. The most characteristics processes are depicted in Table 9 such as bleaching, de-linking, drying and pulp preparation. In terms of low-temperature requirements, de-linking is the only one within a range of 60-90ºC, while bleaching is also suitable due to this wide range of temperature requirements and only requiring water. Despite this, the main

energy consumer is paper drying, which uses air or steam in the low part of medium temperatures (130-200ºC) and means a great opportunity for the deployment of concentrating collectors [44].

The literature reviewed also generally consider the food and beverages as well as the chemical industries the ones with the highest potential market. Aiming to verify the results of this study, the potential for each sector is depicted in Figure 51. The high share of renewable heat that currently exists in paper and pulp industries has caused a noticeable decrease in its potential for implementing solar energy. Both Food and Beverage and Chemical share the leading place, nevertheless, it should be taken into consideration the difference in temperature requirements. This condition makes the food and beverage industry more suitable for SHIP deployment, especially in short term. Some restrictions that have not been applied for each specific sector such as the waste heat recovery potential may imply an even greater advantage for the food sector since the chemical one has a larger consumption in temperatures above 500ºC [44] and therefore, more possibilities for recovering useful heat.

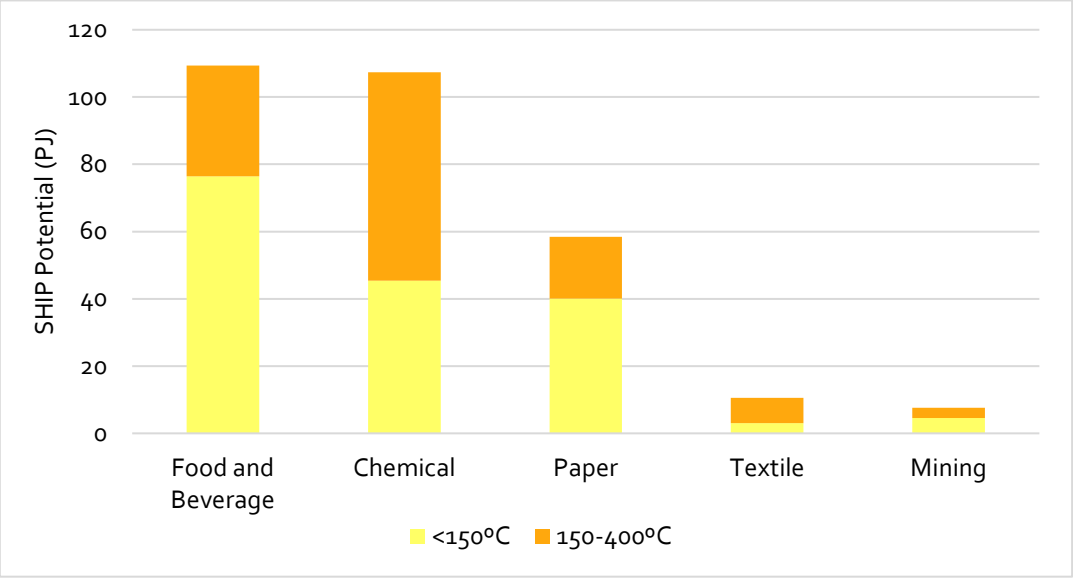

Figure 51. Potential of the promising industrial sectors for European selected countries by temperature heat range.

It must be mentioned that other sectors such as iron and steel or machinery manufacturing could have been considered in the case of Europe due to its big share of heat demand in comparison to textile or mining. Nevertheless, the sector selection was made previously for reducing the geographical scope of the project and was based on global heat consumption and temperature conditions.

5.6 Conclusions for solar heat market and technology

This section is meant to resume the results achieved throughout this study and provide a clear view of the characteristics that a solar thermal system should have to be feasible, as well as the processes and sectors that show the best market potential. These conclusions are needed for justifying the case study selected for the techno-economic analysis following chapters.

An important criterion to assess the potential of SHIP systems is the heat temperature demand. This condition is used, from a technical point of view, to design the solar system and its integration, being more adequate lower temperatures demands as the solar resource and collectors provide a better performance and a simpler design. Moreover, depending on the temperature required the selection of the collector type varies, for example, higher operational temperatures require concentrators and tracking. Looking at the heat demand for processes, its share in the industry is higher for temperatures over 100ºC, where steam is generally required at different pressures. This means that most of the heat demand in industry is supplied in form of steam, varying its requirements of pressure and temperature depending on the load. Moreover, heat at low temperatures heat can be supplied easier than at high temperature through heat with recovery systems and efficiency measures, which makes future solar heat market trends to be focused on higher temperature demands and therefore, concentrator technology (see section 4.1.3. Trends for solar heat process design).

The selection of the appropriate solar collector is based on the five criteria listed in section 2.3.1. "Solar collectors", where the most important consideration regards heat temperature demand. The three concentrator collectors that are used in SHIP applications are PDR, LFR and PTC. These last two have currently more deployment worldwide (Figure 35); their costs and complexity are lower since they only use one axis instead of two, focusing solar radiation in a linear absorber. On the other hand, the concentration ratio, as well as the temperature that those systems can reach, are generally lower than two-axes systems. The PDR has been used for specific applications such as cooking, which has been implemented in various plants in India [4]).

PTC have generally a higher investment but also better performance and require less space than Fresnel collectors [14]. On the other side, LFR provides a good solution not only economically but also in its integration in industrial buildings as it has a lower weight and wind load. LFR are capable of adjusting its power by using variable mirror configuration and its fixed receiver simplifies the hydraulic connections [68]. Regarding temperature requirements, both technologies are used for medium levels (100-400ºC) but LFR is more suitable for the lower part of this range and PTC for the higher [69], being Fresnel technology appealing for SHIP applications and with a renewed interest [4].

The integration concept is key to make solar thermal technology feasible for the industry. Two categories had been described: integration at supply level or process level. The process level requires an analysis of the components and operation of the conventional heating system for designing the solar heat integration: possibilities involve internal/external heat exchangers, intermediate circuits, etc [27]. On the other hand, the supply level has a simpler integration as a standardized approach could be done since the industrial process specifications have less impact. In addition to this, the heat potential for the supply level is greater as the generated solar heat can cover more than one process at the same time as the heat is supplied to the factory grid, for example, steam generated directly send to the steam network.

Steam generation in parallel with the boiler has the largest heat potential for solar heat integration at the supply level. This integration is not affected by the installation of advanced heat recovery systems as it requires heat at medium temperatures [69]. Steam generation could be done direct or indirect depending on whether the steam is produced inside the absorber (direct) or afterwards. This solar integration is further analysed for the case study in the next chapter.

Solar thermal deployment depends on multiple variables that have been discussed throughout this study. The main industrial sectors where this technology could be feasible have been chosen following two main criteria: the temperature range required for heat processes and the total heat consumption. The selected sectors were: Food and Beverage, Paper and Pulp, Chemical, Mining and Textile. Moreover, the industrial processes which could be feasible for implementing solar heat were reviewed for each of the sectors as well as their temperature requirements. Some of these processes are pasteurization, drying, cooking, cleaning, washing, etc.

The geographical analysis for the selection of regions with high SHIP potential is performed through an MCA. The criteria for this purpose were selected based on the drivers for implementing this technology and the heat consumption of the promising industrial sectors. The analysis results in the top countries around the world that have a great SHIP potential, and the selection of Europe as the scope for further research. Multiple factors such as energy policies, natural gas prices, solar resource and experience in SHIP plants have been analysed among other conditions.

The results in European countries shows that Germany, France, Netherlands, Italy and Spain have the biggest SHIP potential, along with the sectors of food and beverage and chemicals.

6 TECHNO-ECONOMIC ANALYSIS

This chapter aims to perform a techno-economic analysis of a certain case of study. This case is in line with the results achieved in previous chapters as it is a Fresnel Direct Steam Generation (DSG) plant located in Spain that provides steam at low temperature at supply level for a factory of the Food and Beverage sector. The plant is modelled and implemented in the software TRNSYS.

At the end of this section, some economic indicators are selected and calculated to assess the economic feasibility boundaries of the system and perform a sensibility analysis of the parameters which have a high impact on the results.

6.1 Industrial process case of study

The case of study is a DSG solar plant built for supplying steam to a factory located in Sevilla, a region in the south of Spain. This solar system is designed by Solatom, a Valencian company dedicated to integrate solar heat in the industry through Fresnel collectors for steam generation, hot water, or thermal oil.

6.1.1 Location

The emplacement of the solar plant is Sevilla, in the southern part of Spain, one of the European countries with higher levels of radiation and the fifth one regarding SHIP potential from the results shown in Figure 50.

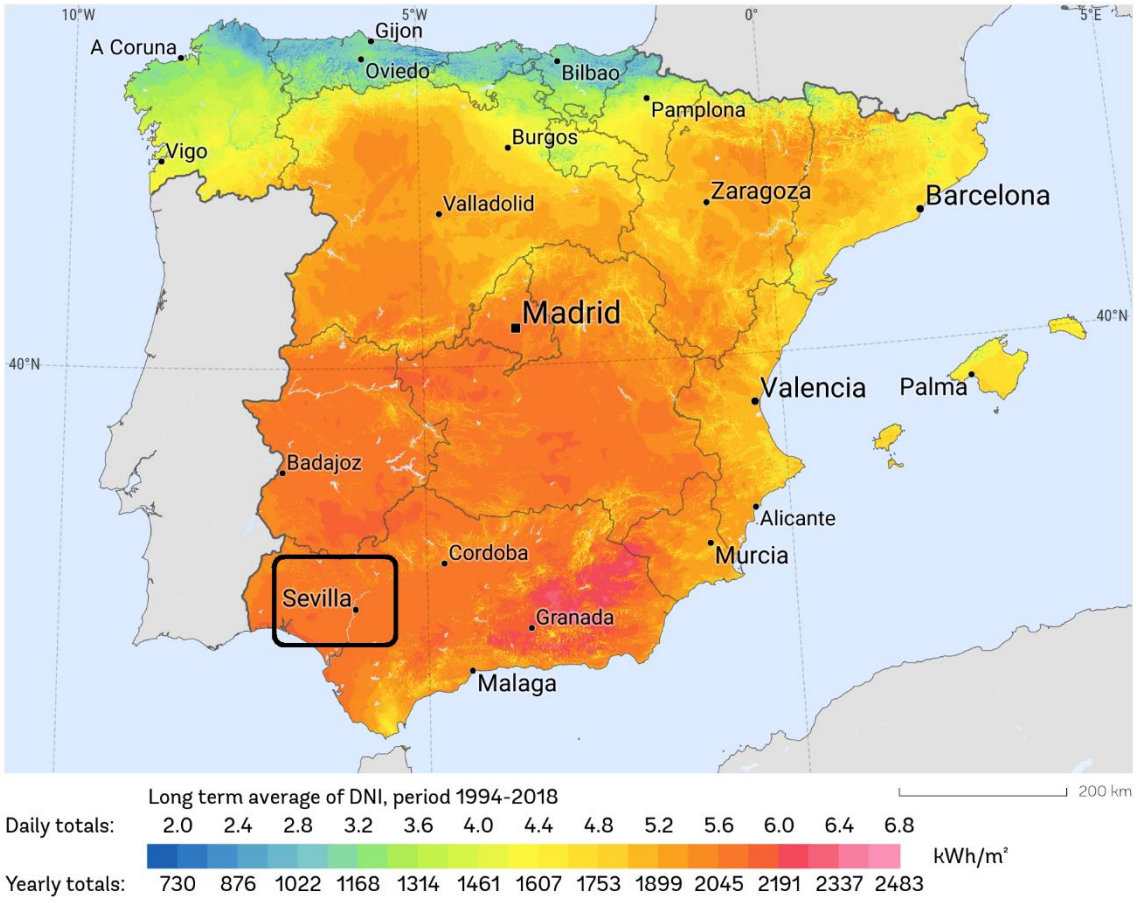

Figure 52. Direct normal irradiation map of Spain [63].

Direct solar irradiation is used for concentrator collectors such as Fresnel; non-concentrators also take into account the diffusive and therefore global irradiation. The region of Sevilla counts with high direct irradiation levels, the value considered for this study is 2208.54 kWh/m² per year.

6.1.2 Industrial sector

A study made in 2017 by Solatom aims to localize the areas in Spain with higher SHIP potential, providing information about four main sectors: Food and beverage, agriculture and livestock, textile, and paper. The first sector was identified as the most suitable for integrating this technology due to the great heat demand, its stable growth, and for being the one with more solar plants in operation.

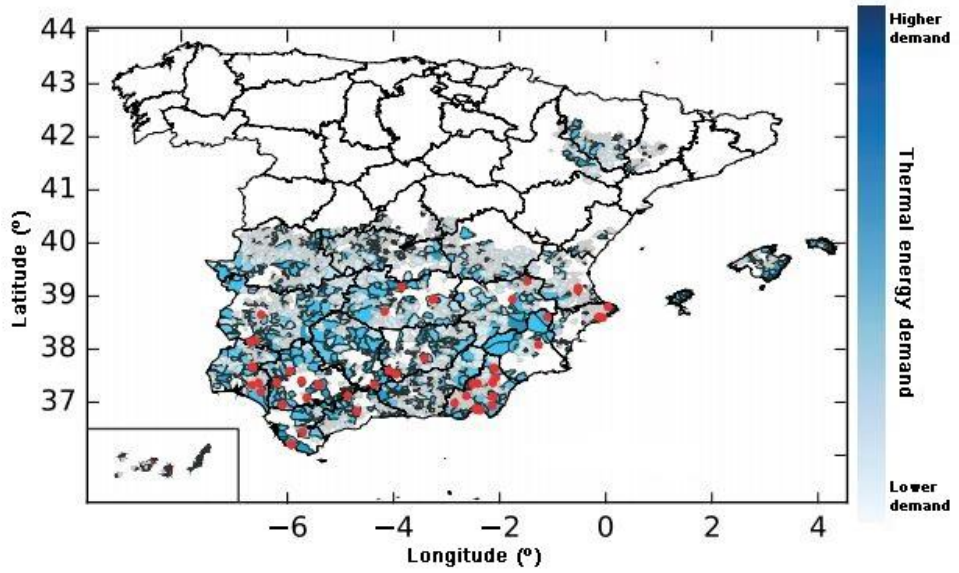

Figure 53. Identified industries and thermal energy demand in Spain for the Food and Beverage sector [70].

The potential analysis filters the regions based on the solar radiation, the access to low-price fuel, the thermal processes for the four sectors and the surface availability of the factories. In addition to this, a validation of the results was made by visiting the locations, providing accurate results of the specific locations where solar heat has a market. These potential customers are represented in the map above as red points. As it is shown, the south of Spain, in particular, the regions of Almería, Sevilla, Cádiz and Huelva, have a high potential for implementing SHIP plants.

This sector is analysed in detail, resulting in the subsectors of preserves and dairy as the ones with the highest interest, as well as the industrial processes of pasteurization, sterilization, scald and boiling [70]. What is more, the work of Solatom in recent years has been providing solar thermal systems to the industrial activities of manufacturing prepared animal feeds, processing and preserving of meat and production of meat products [47].

The SHIP potential assessment commented above is fully in line with the analysis and results obtained in chapter 5: KEY CUSTOMERS AND MARKETS.

6.1.3 Integration concept of DSG

Steam generation with solar concentrated technology is commonly performed through an indirect method, which is to say that a primary liquid (e.g. pressurized water or synthetic oil) is firstly heated up in the solar field and then its thermal energy is transferred to the water. This interaction between the heat carrier and the water is made with a heat exchanger for evaporation (typically kettle-type reboilers).

In this case, the steam is directly generated inside the solar collector absorber tubes (DSG concept is depicted in Figure 54). The result is saturated steam which is delivered at supply level in parallel with the conventional steam boiler. A steam drum is required to separate the water-steam mixture that comes from the concentrating collectors, returning hot water to the solar field and sending saturated steam to the steam line when it reaches the demand temperature and pressure conditions. The liquid level of the drum is maintained thanks to the feed make-up water that goes to the solar system. The integration point of the solar system is the valve in the steam output of the drum, which controls and maintains the required pressure for the factory steam grid. The condense flow in the steam networks is also recirculated to the solar field.

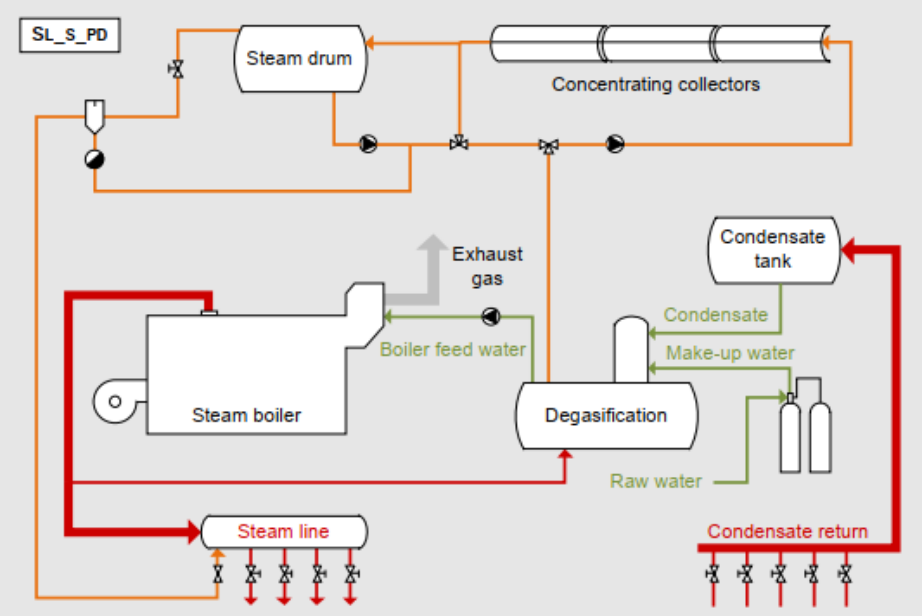

Figure 54. Integration concept for direct steam generation [27].

The performance of this plant is benefited by the lack of a heat exchanger as it directly operates with the final product: steam. Nevertheless, when the solar system is working at a high rate the boiler has to reduce its steam production, causing a negative impact on the boiler efficiency. This fact depends on the efficiency curve of the boiler regarding the load as well as on the ratio installed solar power-boiler capacity and the typical load curve [27] [69].

Some other advantages of non-using synthetic oil in the solar system are the investment reduction in heat exchanger, auxiliaries and storage system as well as in maintenance costs and antifreeze control. Environmental risks such as fire or oil leakage are hence eliminated. On the other side, the cost of pipes and hydraulic components increases due to the higher operating pressure, and the existence of two-face fluid can damage components such as the absorber, requiring an advanced control for the flow and pressure stability [69].

6.2 Solar system

6.2.1 Solar field

The collector selection for the case study is based on the conclusions seen in section 5.6 Conclusions for solar heat market and technology. The main criterion for selecting the collector type is the heat temperature that will be required for the user; that is why the decision should be taken between the CPC and LFR as the steam is required saturated at 158 ºC (6 bars). Even though CPC technology, as was mentioned before, provides better performance with a higher concentration ratio, can achieve

higher temperatures and has a bigger number of installations in industry [14][47], the Fresnel collector has other characteristics that make it suitable for this case study. This collector is not only the most common type of concentrator in the European industries, but also enable easy integration in the industrial building as it has a lower weight and wind load. In addition to this, it is capable to adjust its power by using a variable mirror configuration, which makes it easier for the factory in terms of stable heat supply requirements. Considering the temperature conditions, both collector technologies could achieve medium temperatures but LFR is commonly used for the low part of this range and CPC for higher temperatures due to its performance [69].

LFR has a fixed receiver, which reduces the complexity of hydraulic connections [68], and implies has an optical advantage for DSG as, since the absorber is fixed, the major flux of direct radiation reaches the mirror from the bottom and just a small fraction that is reflected by the secondary mirror hits the top side of the tube. In stratified two-phase flow, the water is found in the lower section of the absorber and receives most of the radiation [69].

Moreover, the solution provided by the company Solatom with their Fresnel FTL20 enhances the deployment of this collector technology thanks to its design and logistics. The FLT20 modules are pre-assembled and pack in factory, and then transported ready to be installed. Each module has a thermal power of 14.5 kW_t and weighs only 26 kg/m^2, making them suitable to be located on roofs.

The solar field of the case study is mainly composed of the Fresnel collectors developed by Solatom. The total area of reflective surface is 1900.8 m^2 and it is structured in 6 loops with 12 modules each one (the area of a single collector is 26.4 m^2).

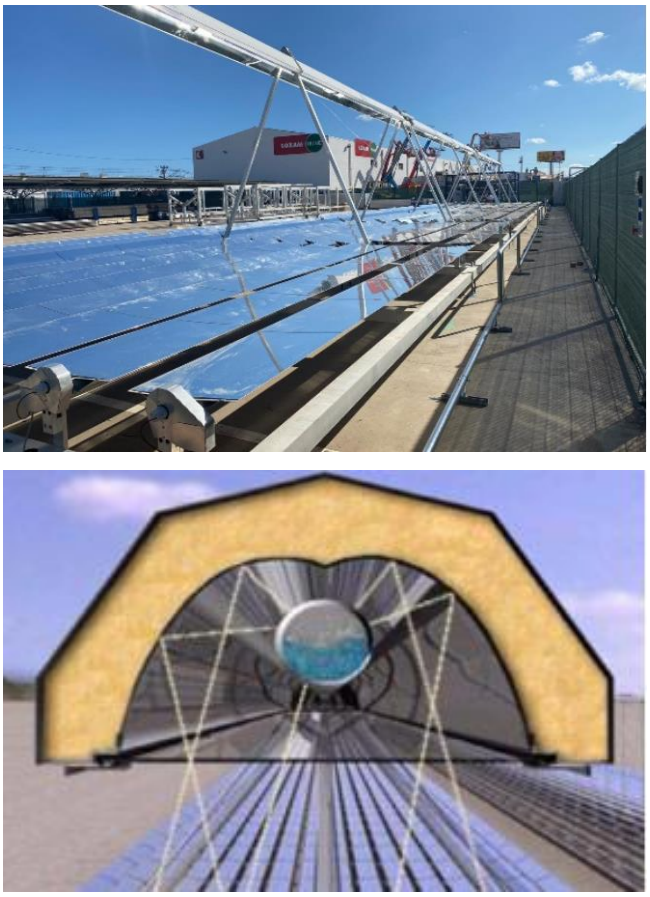

Figure 55.Similar solar field to the case study (top) (source: Solatom [72]) and the secondary mirror with the receiver (bottom) [69].

6.2.2 Steam drum

The steam drum is a key element for DSG, its main function is to separate the biphasic fluid that comes from the solar field to deliver pure steam as the load requires. It also serves for stabilizing the operation of the solar steam production and decoupled the load from the generation source as buffer storage.

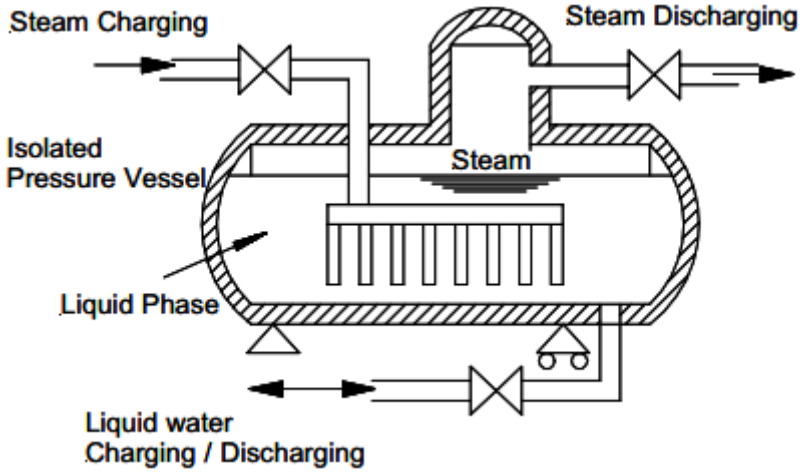

Figure 56. Steam drum scheme [73].

The inlet of the drum is the mix of water and steam coming from the solar collectors. The separation inside the drum allows to send steam at the correct temperature and pressure through a control valve to the steam network and recirculate the liquid water to the solar field. The feed of fresh water is needed by the solar field to maintain the level and it is integrated through a second inlet of the steam drum or by sending it directly to the inlet pump of the solar system.

The horizontal configuration of the drum allows minimising the reaction time of discharge to the load, a better mechanical load distribution (which is especially important when it is installed in a roof) and maximize the energy storage in the water by ensuring that no stratification occurs [69].

Apart from been a phase separator, pressure maintainer and storage buffer, the steam drum has a key application for the everyday operation beginning. The drum serves as a water reservoir that will be used after the shutdown of the plant to fill the two-phase sections with water. This amount of water can be for around 10% of the drum volume [71].

Further research of the steam drum behaviour is performed in next steps of the study in order to clearly define its role in the DSG system, essentially during the start-up of the plant, and model it.

6.2.3 Control system

The goal of the control system in a solar plant is to maintain the operational conditions within acceptable limits. This fact is a challenge due to the disturbances that the energy resource suffers along the day (solar radiation variations, clouds…), demand curve variation, fluid inlet conditions or collector's reflectivity degradation.

In this case, the solar heat supplied does not have to cover the whole thermal demand, which gives the system an advantage in terms of control and lack of thermal storage necessity. When the solar system is not able to satisfy the demand, the pressure falls below the conventional boiler setpoint and it directly works to cover the demand shortage with the related fossil fuel consumption. Three main controllers are used to maintain the DSG system in operation (see Figure 57):

- **Recirculation flow controller:** its function is to maintain the correct flow in the absorber tube for overheating prevention. It is a key control system when the pressure drop varies along the tube due to the two-phase flow dynamics. This mix of water and steam causes instabilities and changes the flow rate, affecting as well to the steam quality at the solar field outlet.
- **Feedwater Controller:** it aims to maintain the water level in the steam drum within acceptable limits. These limits ensure that the water is not high enough to be carried in the steam outlet to the load but with an adequate height to not starve the recirculation pump.
- **Steam Network Pressure Controller:** this controller guarantees the pressure of the steam network at the required demand value. Even though the controller can be linear in the pressure regulation, there are two cases when it should close the valve rapidly. The first one is when there is not enough steam in the drum and the second is when the steam demand is cut-off so the valve closes to prevent overpressure of the steam network.

The following figure does not only show the three points of the system where the controllers collect the information they need (recirculation flow, water level in the drum, and load pressure) but also where are the actuators (recirculation pump, feed pump, and steam valve) which are commanded to make the appropriate changes in the operation. Other important instrumentation is shown as well in Figure 57 which is used for the control and safety of the plant. In the solar field zone it is shown the equation that expresses the total energy yield as the heat achieved by the collectors minus the system losses.

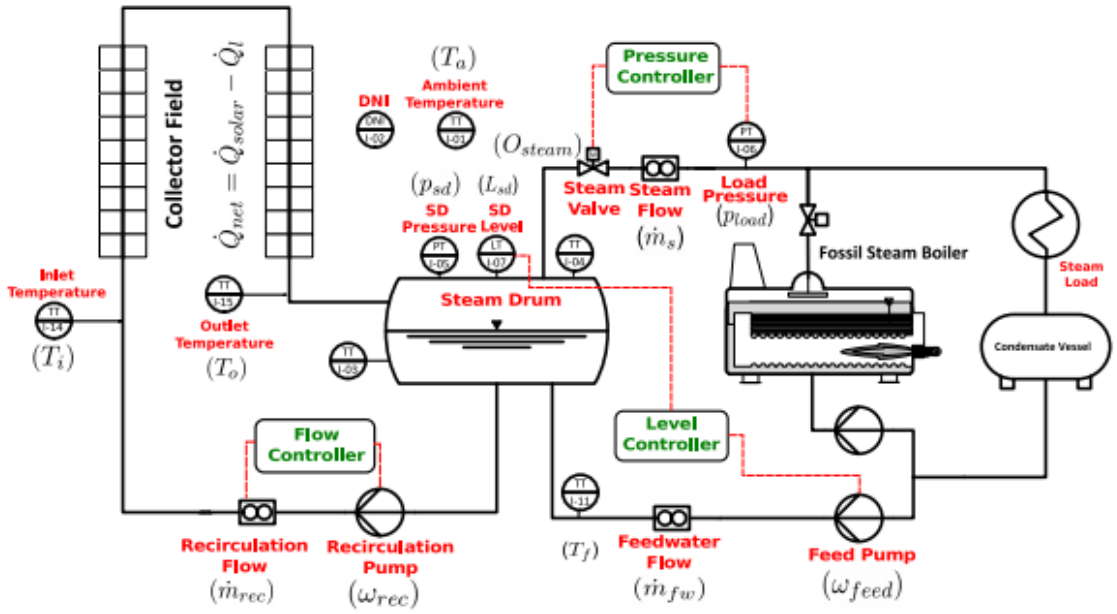

Figure 57. Simplified piping and instrumentation diagram of a solar DSG system in recirculation mode with the three main controllers [68].

The mass and energy balances inside the steam drum are necessary to control properly the operation of the plant. For stable conditions (steady-state), the mass balance is required to maintain the level of liquid by controlling the amount of steam delivered to cover the load ($\dot{m}_{s,out}$) and the feedwater flow ($\dot{m}_{fw}$). The energy balance is performed so the energy extracted from the steam drum as steam output ($H_{s,out}$) should be equal to the net energy provided by the solar field, calculated as and the feedwater input (H_{fw}) and the solar gains minus losses ($H_{solar} - H_{loss,solar}$). These balances of the system are expressed in the following equations:

$$\dot{m}_{s,out} = \dot{m}_{wf} \tag{6}$$

$$H_{s,out} = H_{solar} - H_{loss,solar} + H_{fw} \quad (7)$$

It is possible to calculate the energy balance as it is shown in equation (5).

Slow changes in the system can be "easily" managed. For example, in the case of an increase in the load, the steam controller will open the steam valve at the output of the drum, increasing the steam flow but decreasing the liquid level in the drum. This will be fixed with an increase in the feedwater flow. Problems arrive when solar direct radiation suddenly falls and a rapid pressure drop occurs. That is why model-based control techniques such as the Model Predictive Control (MPC) could be a suitable solution [71].

6.2.4 System behaviour during a day

The control of the steam drum water level and pressure is a great challenge for every DSG plant as the solar resource is discontinuous, and dynamic behaviours of the steam drum occur to address a constant steam pressure in the steam network of the factory.

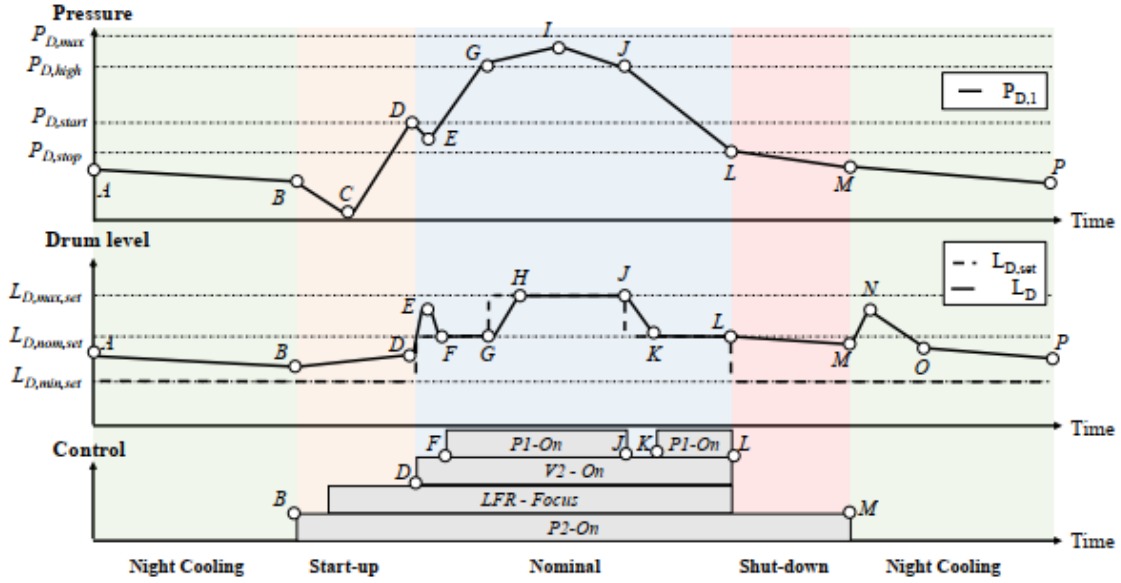

Figure 58. Pressure and steam drum level variations for a characteristic day [69].

A characteristic day of the year is defined by four modes of operation as Figure 58 shows, where the pressure of the system, the water level of the drum and the control actions are divided into three graphs for the 24h of the day. The different modes are described below:

- **Night Cooling:**
  During the night, the liquid section of the system in the solar field and pipes have sensible losses that reduce their temperature while, inside the steam drum which is in saturated conditions, the two-phase section has latent losses that slowly reduce the steam pressure. The drum level decreases as well due to a raising of the water density in the solar field as it gets colder, causing the fed of saturated water from the drum (points O to P and A to B).

- **Start-up:**
  The duration of this phase depends on the state of the collector loop in the morning and therefore the heat losses during the night. The first step is to activate the recirculation pump (P2) to flow saturated liquid that has been stored the whole night in the steam drum to fill the solar field and push into the drum the cold water. This will make the pressure of the

system decrease from point B to C as the temperature of the new mix is also lower. Secondly, the mirrors are focused to harvest solar radiation and start boiling inside the absorber when the temperature reaches saturation and, consequently, the pressure starts rising as steam is collected in the drum.
Finally, a set-point pressure is reached in the steam drum (point D) and the steam control valve (V2) that gives access to the factory load can be open. When this happens, the start-up phase is concluded and there is a little valley in the pressure due to the action of this valve causing the liquid in the absorber to be evaporated or "flash", so an injection of water is required in the system [69]. It is key that the controller should not add cold feedwater during this period so the start-up of the system is done as fast as possible and the thermal balance in the drum is not disturbed [68].

- **Nominal condition:**
  This mode occurs during a major part of the day when enough radiation reaches the solar collectors. The control valve is opened when the pressure in the steam drum is equal to or higher than the nominal one established by the load, triggering a steam flow to the factory. At that time, cold feedwater is pumped (P1) to replace the mass lost so the steam drum level does not fall. The inlet temperature in the collectors decreases thanks to the fresh feedwater flow that is mixed with the recirculated inside the tank, causing the absorber to be mostly filled with liquid and the boiling start point to be moved towards the end of the tube. This phenomenon requires the implementation of advanced control strategies to avoid moving too fast the evaporation start point and harm the tubes.
  During the day, the steam drum has the role of decoupling the load from the steam generation so the system can cover the demand despite solar irradiation variations and the related impacts on the pressure of the solar system. This storage can be maximized by increasing the level point of the drum (point G) and having a steam drum with a big volume and a wide range of operational pressures.

- **Shut Down:**
  When the solar energy transferred to the circulating fluid is not enough to reach the evaporation point, the collectors are unfocused (point L). To keep most of the steam inside the steam drum for the night and have the best conditions to begin the start-up next morning, a few minutes before the shut down a bigger flow rate is circulated to push the hot water and steam inside the drum. The isolation of the drum ensures low thermal losses during the night for the two-phase fluid. This action prevents flashing in the absorber when the pump is stopped during the shut down thanks to the cold water that is injected and, at the same time, the saturated water is stored out of the solar field where heat losses are higher during the night [69].

6.3 TRNSYS simulation

6.3.1 System diagram

Modelling in TRNSYS software is based on the system shown in Figure 54 and Figure 57, where direct steam generation at the supply level is depicted. The blue lines shown in the next figure represents liquid water flows both from the steam drum and the feedwater, orange lines stand for the biphasic flow coming from the solar field to the drum and, finally, the steam separated in the drum and delivered to the steam network of the factory is drawn as a red line.

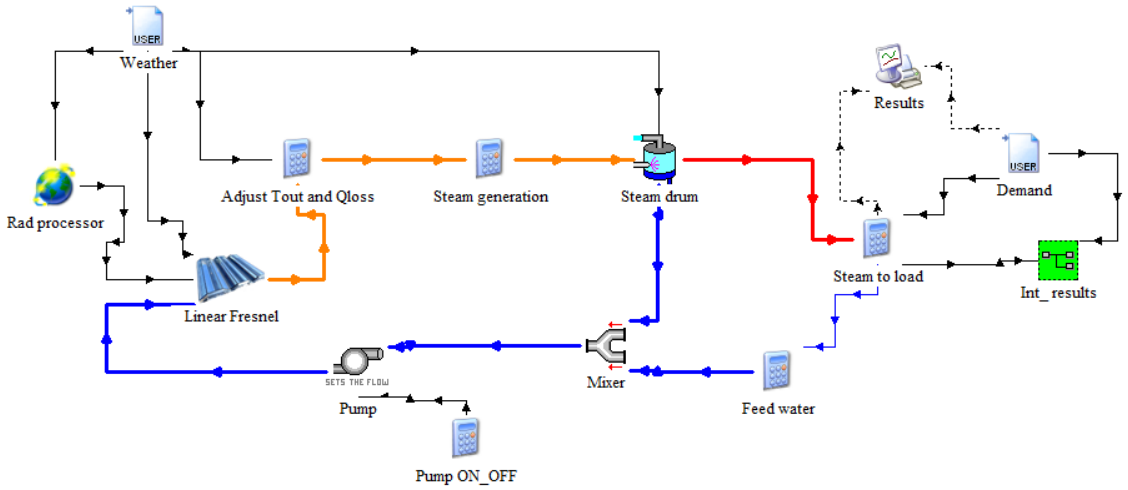

Figure 59. TRNSYS model of the solar array.

Two input files with hourly data for a typical year are required: the thermal demand of the factory and the weather file. This last one provides the information of Direct Normal Irradiation (DNI), global irradiation on the horizontal surface (G_h), relative humidity, ambient temperature and the wind velocity and its direction. A radiation processor is required to interpolate the radiation between hours and simulate the tracking system of the Fresnel collectors. This component provides the radiation that reaches the collectors and its angle of incidence.

The linear Fresnel performance is characterized by the parameters defined in section 6.3.2 and the external file with IAM values (longitudinal and transversal) from the FTL20 provided by Solatom. The "Adjust Tout and Qloss" component is also explained in the next section. The "Steam generation" calculator is used to know the outlet enthalpy from the solar field (h_r) and the steam quality (α_r):

$$h_r = \frac{Q_{gained}}{\dot{m}_r} + h_{rec} \tag{8}$$

$$\alpha_r = \frac{h_r - h_{rec}}{h_g - h_f} \tag{9}$$

Where the enthalpies h_g stands for saturated steam, h_f for saturated liquid and h_{rec} for the recirculation. The flow coming from the receiver is $\dot{m}_r$ and the total heat gained by the solar field is Q_{gained}.

The steam drum separates the two-phase flow recirculating water to the solar field and delivering saturated steam to cover the load. Its characterization is detailed in section 6.3.3. The "Steam to load" component calculates the instant solar fraction whilst the integrated value is calculated within "Int_results". The results are finally plotted and printed.

On the other side, the recirculation flow is mixed with the feedwater using the valve "Mixer". In reality, the feedwater flow (which comes from the plant at 70ºC) is injected into the drum to maintain the water level, nevertheless, due to the design of the drum this injection is so close to the recirculation intake that the total mixed of these two flows is assumed. This fact is explained later, and the calculation of enthalpies is given by equation (18).

Finally, a recirculation pump sets a constant flow of water when DNI is not null. The flow established for the system is calculated based on the criterion that the steam title needs to be below 0.3 at the end of the absorber to avoid strong instabilities. Moreover, the steam title affects the flow pattern

inside the receiver and should be controlled to achieve an annular flow. Other patterns such as stratified flow or dry-out conditions should be avoided in the whole solar field [69]. The pump is designed to provide a constant flow of 6420 kg/h, ensuring that the maximum steam title inside the receiver does not overpass 0.29.

A summary of the components and the specifications of each one is described in Table 14:

Name	Type	Specifications
Rad. processor	16	Single axis tracking parallel to surface Tilted Surface Radiation Mode: Perez 1988 model
Linear Fresnel	1288	Performance parameters Solar field area and number of collectors in series
Steam drum	611	Ideal isolation (no heat losses) Operation pressure: 6 bars
Mixer	595	Temperature, enthalpy, pressure and flow of two inlets
Pump	597	Set the flow to 6420 kg/h

Table 14. Components used to model the DSG plant in TRNSYS.

6.3.2 Fresnel model characterization and validation

The linear Fresnel model provided by the software TRNSYS (type 1228) is not the same as the one of Solatom, the FLT20, which makes it necessary to study how it is possible to simulate properly these collectors in TRNSYS and how are the parameters that characterize the model.

TRNSYS Fresnel is modelled following the Standard EN 12975-2:2006 [74], normative that will be replaced by EN ISO 9806:2013 and at last term by EN ISO 9806:2017 [75]. Therefore, the model selected in TRNSYS is not adjusted to the specifications of the current normative and it is generally used as well for non-concentrator collectors.

The definition of the energy transferred to the fluid inside the receiver is equal for both models:

$$\frac{Q_{gained}}{A} = G_b * IAM_b * \eta_{opt} - c_6 * u * G_b - Q_{th,losses} \quad (10)$$

Where the beam radiation that reaches the surface (G_b) is calculated as:

$$G_b = DNI * \cos(\theta) \quad (11)$$

The area of collectors is expressed with the term A, the direct normal irradiance is the DNI and how it reaches the collectors is defined by the angle of incidence θ and the incidence angle modifier IAM_b. The IAM_b is calculated both for longitudinal and transversal angles in the case of Fresnel collectors. Finally, two more losses are aggregated: optical and thermal. The first one is defined as a non-time dependent efficiency (η_{opt}) related to losses due to an imperfect geometry of the concentrator, tracking errors, etc. An extra parameter, c_6, describes the losses on the optical performance of the collector due to wind velocity u (m/s). Thermal losses ($Q_{th,losses}$) are different in each model as it is described in the next steps.

Thermal losses model in EN 12975-2:2006 for TRNSYS:

$$Q_{th,losses} = c_1 * (T_m - T_{amb}) + c_2 * (T_m - T_{amb})^2 + c_3 * (T_m - T_{amb}) + c_4 * \left(E_L - \sigma * {T_{amb}}^4\right) + c_5 * dT_m/dt \quad (12)$$

In equation (12) the term $T_m - T_{amb}$ is the temperature difference between the average temperature of the fluid inside the receiver and the ambient temperature, E_L is the longwave irradiance (W/m²) and σ accounts for the Stefan-Boltzmann constant (5.67x10^{-8} W/m² K⁴).

The thermal losses are characterized by six fixed parameters described in Table 15; moreover, a literature review of the thermal efficiency curves for various Fresnel has been done to have a range of values that determine the performance of this technology [76] [77] [78].

Parameter	Definition	Range (w/m²)	Average
c_1	Heat loss coefficient for $T_m - T_{amb} = 0$	0.540 - 0.032	0.227
c_2	Temperature dependant heat loss coefficient	0.0032 - 0.00018	0.00065
c_3	Wind dependency coefficient	-	-
c_4	Longwave irradiance coefficient	-	-
c_5	Effective thermal capacity	3.996*	-

Table 15. Thermal losses parameters for a dynamic collector model following the normative EN 12975-2:2006 for TRNSYS.

**The parameter c5 has only been found in one literature source; for that reason it will be further analysed afterwards.*

The parameters which are mandatory to be identified by the normative EN 12975-2:2006 are c_1, c_2 and c_5. Even though a parameter that expresses the gain of diffusive radiation of the collector is also demanded, it is not written in equation (10 as it is noted down in the normative that this value is not always important. What it means by "not always important" is better explained in the most recent normative (EN ISO 9806:2017) where high temperature collectors are better considered; it is accepted that diffusive radiation gains for concentrators could be neglected. The parameters for the model are mandatory or set to zero depending on the concentration ratio, which makes a difference for defining the performance of collectors with Cr above 20. Moreover, for these high concentration collectors, c_2, c_3, c_4, c_6 and the diffusive radiation are set to zero. In this case, it has been analysed multiple Fresnel plants installed around the world for direct steam generation in industrial sectors [47], resulting in a mean concentration ratio near 26 what justifies the assumption that the concentration ratio for a Fresnel collector is above 20. The model approach is the one established by the normative which is used in TRNSYS that takes into account parameters c_1, c_2, c_5. It is neglected the effect of the wind (c_3, c_6) and the longwave radiation (c_4) as it recommends the current normative and other studies [79].

The resulting polynomial model of second order can be correlated with the receiver thermal losses model given by Solatom:

$$Q_{th,loss,r} = 0.00154 * \Delta T^2 + 0.2021 * \Delta T - 24.8 + [(0.00036 * \Delta T^2) + 0.2029 * \Delta T + 24.899] * \left(\frac{DNI}{900}\right) * \cos(\theta) \quad (13)$$

In this case (equation (13), the losses are not calculated regarding the area of aperture of the collectors but the lineal longitude of the receiver. The biggest difference between the models is characterised by the dependence of the Solatom model with the DNI and the angle of incidence on the collector. This second part of the model is created to adjust the heat loss values to other weather conditions that are not the ones at the design irradiation point, in this case, 900 W/m2.

The term c_5, the effective thermal capacity coefficient, is the ratio of its thermal capacity and the area of the collector ($c_5 = Ce / A$). This value is necessary both in the quasi-dynamic and steady-state models, expressing the evolution of the collector temperature along with the changes in the transfer fluid temperature over time. This value is has been calculated following the normative [75]:

$$Ce = \sum_i p_i * M_i * c_{p,i} \quad (14)$$

The effective thermal capacitance is calculated as the sum of the total thermal capacities ($m_i * c_i$) of the constituent collector elements (glass, absorber and liquid contained) weighted by a generic factor p_i. The receiver of the FTL20, a Schott PTR 70, is a stainless-steel absorber with an inner/outer diameter of 6.6/7.0 cm and a glass envelope inner/outer diameter of about 11.5cm/12.0 cm. The values selected for estimating c_5 and the results taking into account a linear area of 1m are shown in Table 16:

Component	p	Density (kg/m³)	M (kg)	c_p (kJ/kgK)	Ce (kJ/K)
Absorber	1	8030	6.862	0.502	3.445
Heat transfer liquid	1	908.59	3.107	4.33	13.453
Glass envelope	0.2*c_1	2000	3.101	0.84	0.124*
Receiver	-	-	-	-	**16.898**

Table 16. Parameters and results for the effective thermal capacity of the receiver (own calculations) [75] [80].

** The glass envelope result will be considered neglectable with respect to the other component, the data used for its calculation is not reliable and the type of glass is not clearly specified.*

Finally, the coefficient c_5 is estimated as 3.840 kJ/m²K in relative terms to the collector's area and considering the simplification made for the absorber as specific parts of the tube such as the extremes has not been taking into account. This value is in the range of the effective thermal capacity in Table 15 used by [76] for simulating a PTC in TRNSYS.

The use of TRNSYS models for Fresnel collectors requires performing an analysis of the possible values for the parameters c_1, c_2 which best fit with the Solatom model. For this purpose, a specific day of the year, the 11th of August, has been simulated in TRNSYS for taking its heat losses curve as reference. The data collected is the DNI, the angle of incidence, outlet temperature from the receiver and ambient temperature.

Having determined the ranges of possible values for the parameters c1 and c2 (Table 15), multiple values have been simulated using the data collected and the two heat losses models using the software Excel. Thanks to the tool *Solver*, varying one parameter the other is calculated with the criterion of reaching the minimum difference between the results of the Solatom and the TRNSYS models. Finally, c_1 and c_2 are estimated as 0.032 W/m²K and 0.000642 W/m²K² respectively and the Fresnel collector is completely characterized counting with a relative error of 5.5%. This error is mainly due to differences at the beginning and the end of the day when the radiation is still low and the temperature of the HTF is not at the operational one.

One of the challenges of using the Fresnel type of TRNSYS to model a DSG system is that it does not take into consideration the biphasic state of the water inside the receiver. As there is no evaporation, the outlet temperature from the solar field does not match with the real temperature which is determined by the pressure of the system and it is in saturation conditions. The solution proposed for using the model provided by TRNSYS and, at the same time, consider a biphasic flow is to limit the outlet temperature of the fluid to its saturation at the pressure of operation, 6 bars. This consideration is made knowing that the system is delivering steam to the steam network of the user which is at 6 bars and that the higher pressures in the steam drum are not considered in this study.

The heat losses of the receiver depend on the mean temperature of the fluid so higher losses are calculated by TRNSYS since the temperature goes high above saturation. That is why limiting the

outlet temperature to the saturation temperature at 6 bars is needed for calculating the real heat losses of the solar field. This consideration is represented in Figure 60:

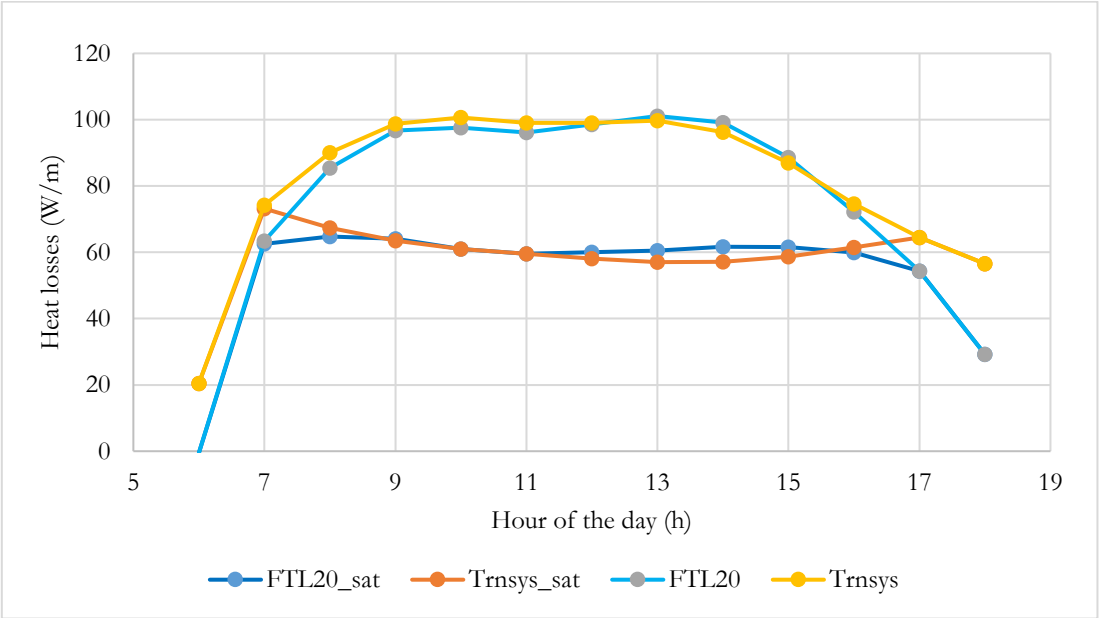

Figure 60. Solar field heat losses curve for both TRNSYS and Solatom models on the 11th of August.

The figure above shows in dark blue the Solatom model and in orange the model created in TRNSYS with a saturation temperature of 158.83ºC (pressure at 6 bars) reached during most of the daylight time. On the upper part of the graph the heat losses of the collectors are simulated without considering any evaporation of the fluid in the solar field as it is modelled by TRNSYS type 1288; the light blue shows the behaviour of the FTL20 Solatom model and the yellow curve the one of TRNSYS, both under the same conditions of radiation and temperatures.

Aiming to correct the value of energy gained by the solar system, an adjustment of the heat losses is performed after the Fresnel component. It sums to the total energy gained the extra losses calculated by TRNSYS which are a result of the difference between the outlet temperature of the Fresnel type and the real saturated one. The adjustment is depicted in the following equation:

$$\frac{Q_{gained,sat}}{A} = \frac{Q_{gained}}{A} + c1 * \left(T_{out,fresnel} - T_{out,sat}\right) + c2 * \left\{\left[\left(\frac{T_{out,fresnel} + T_{in,fresnel}}{2}\right) - T_{amb}\right]^2 - \left[\left(\frac{T_{out,sat} + T_{in,fresnel}}{2}\right) - T_{amb}\right]^2\right\} \quad (15)$$

The term $Q_{gained,sat}$ is the total energy gained in the solar field considering the possibility of having steam and liquid water inside the absorbers, therefore, a saturation temperature at the outlet of the collectors. Q_{gained} is referred to the energy gained if the fluid in the system was only in liquid phase, $T_{out,fresnel}$ depicts the outlet temperature from the solar field without saturation and $T_{out,sat}$ takes into account saturation. The inlet temperature to the collectors is $T_{in,fresnel}$ and the ambient temperature T_{amb}.

6.3.3 Steam drum model

The case of the steam drum modelling is especially challenging as there is no TRNSYS component for this purpose and, as it has been explained in section " 6.2 Solar system", its role decoupling steam generation and demand as well as ensuring adequate pressure levels in the system means a complex task for the controller.

Multiple studies have analysed the dynamics of the steam drum: a model considering the saturated steam as an ideal gas was developed in [81], being quite a simplified approach. Other models, such as the one of [73], are based on a thermal equilibrium between liquid and steam phase even though a great deviation for that equilibrium could happen during charging or discharging of the tank. This model assumes that both phases in contact have the same saturation pressure and temperature. On the contrary, a non-equilibrium model was developed in [82] which calculates separately the thermodynamics parameters of the liquid and steam phase as well as considers finite evaporation and condensation rates. The results provided by the non-equilibrium model differ from the equilibrium one in lower pressures for the accumulator during discharging and higher ones during charging (see Figure 61. Steam accumulator pressure transient during discharging: predictions with equilibrium and non-equilibrium model .Figure 61).

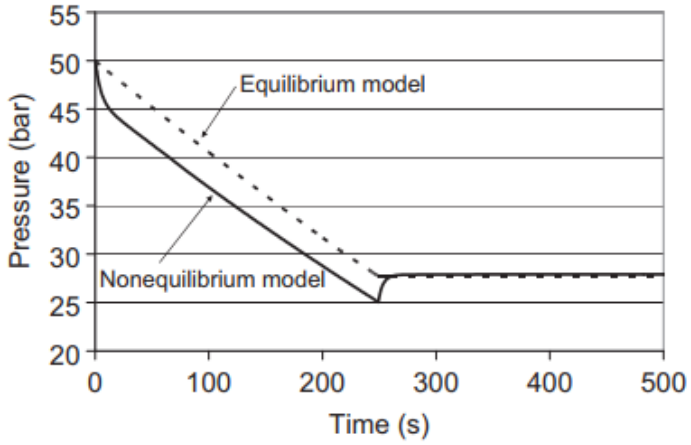

Figure 61. Steam accumulator pressure transient during discharging: predictions with equilibrium and non-equilibrium model [82].

The studies reviewed model the steam drum operation aiming to analyse its dynamic in short timesteps, lower than minutes. The study of transient periods for the drum is usually performed to optimize and ensure proper control of the system, understand the behaviour of the different components and materials under the multiple conditions of an operational day, etc. On the other side, the purpose of this study is to make a techno-economical assessment of this type of technology to evaluate the feasibility boundaries and its market potential. For that reason, the interest of this modelling and simulation is to provide information about the amount of steam produced by the plant and estimate the savings more than analysing the operation and transient performance of the different parts of the system. Consequently, the timestep chosen is longer than the one used for dynamic simulations, an hour, having to face the challenge of characterizing properly a system that has big transient times: the start-up and shut down along the day. The shut down has been defined just as the turn off of the pumps during null values of DNI, while the start-up does affect the amount of steam supplied to the factory as part of it is used to reach the nominal conditions of the plant.

The method applied to perform this task is to estimate how long does it take for the system to finish the transient time, in this case, the start-up, in which the solar system has not reached yet the operational conditions of temperature and pressure. The start-up estimated duration is based on two sources: literature of currently operational DSG plants experience and the results of a dynamic tank model created in TRNSYS. This model aims to verify the duration until the pressure curve reaches 6 bars for different seasons of the year.

The specific use of solar collectors such as Fresnel for direct steam generation is a very recent technology and some of the most reliable and detailed research are the ones made for the pharmaceutical industry RAM in Jordan, [68] and [69]. For that reason, these studies are taken as a reference for validating the assumptions and behaviour of the system modelled in TRNSYS.

The dynamic model of the steam drum has been simplified for the purpose of this study with the following assumptions [68]:

- All the fluid in the solar field is assumed to be saturated even though, for a stratified flow in the absorber, the upper part of the tube could be overheated and the bottom subcooled. When this flow is mixed towards the drum, the resulting deviation is neglectable. Moreover, the whole solar field is considered at the same pressure.
- The recirculation line is always with liquid, there is no evaporation.
- The steam in the drum is always at saturation.
- There is an equilibrium between phases inside the tank so the water inside the tank is also considered to be saturated. There is no temperature gradient between the phases as well.
- The metal is assumed to be always at saturation temperature.

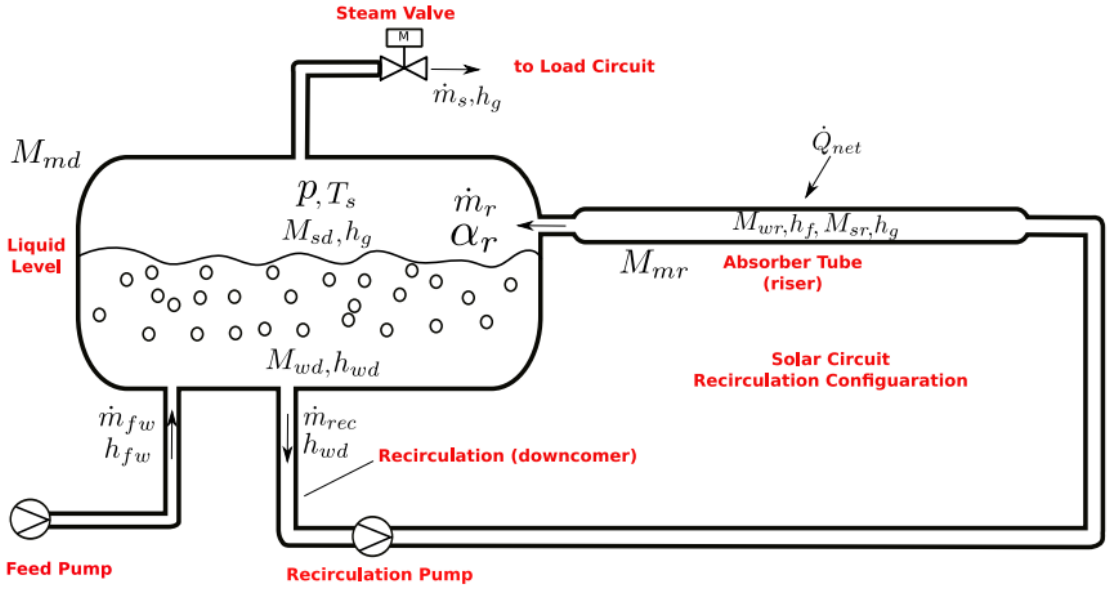

Figure 62. DSG system in recirculation configuration depicting the steam drum and solar circuit with their main modelling parameters [68].

The mass balance in the steam drum is calculated considering the flow in its two inlets, from the receivers($\dot{m}_r$) and the feedwater line ($\dot{m}_{fw}$), and its two outlets, the recirculation line ($\dot{m}_{rec}$) and the steam networking ($\dot{m}_s$):

$$\frac{dM_d}{dt} = \dot{m}_{fw} + \dot{m}_r - \dot{m}_s - \dot{m}_{rec} \tag{16}$$

where M_d is the total mass (kg) of fluid inside the steam drum.

The energy balance in the steam drum is obtained from the first law of thermodynamics considering that the only work is expressed as the variation of the pressure, hence the volume of the tank is constant:

$$M_{sd}\frac{dh_g}{dt} + h_g\frac{dM_{sd}}{dt} + M_{wd}\frac{dh_f}{dt} + h_f\frac{dM_{wd}}{dt} + C_{md}\left(\frac{\partial T}{\partial p}\right)_{sat}\frac{dp}{dt} - V_d\frac{dp}{dt} = \dot{m}_{fw}h_{fw} + \dot{m}_r h_r - \dot{m}_s h_g - \dot{m}_{rec}h_{rec} \tag{17}$$

The term M_{sd} refers to the steam mass and M_{wd} the liquid mass inside the tank. If the steam quality (α_d) is used, these terms are calculated as $M_{sd} = M_d\alpha_d$ and $M_{wd} = M_d(1-\alpha_d)$. The effective thermal capacity of the tank metal body is defined as C_{md}, the pressure p and steam drum volume V_d. The enthalpies of the different flows and phases are represented as h_g for saturated steam, h_f

for saturated liquid, h_{fw} for the feedwater, h_{rec} for the recirculation and h_r for the enthalpy coming from the receivers. Even though h_{rec} could be considered as h_f in a small contained system, it is not the same if the effect of the cold feedwater flow is taken into account as it is fed very closed to the recirculation water intake:

$$h_{rec} = h_f - \frac{\dot{m}_{fw}}{\dot{m}_{rec}}(h_f - h_{fw}) \tag{18}$$

Finally, the control volume of the steam drum is given by:

$$\frac{dM_d}{dt}\left(v_f + \alpha_d v_{fg}\right) + M_d\left(\frac{dv_f}{dt} + \frac{dv_g}{dt}\alpha_d + dv_g\frac{d\alpha_d}{dt}\right) = 0 \tag{19}$$

where the specific volume of the liquid in the drum (v_f) and the steam (v_g).

6.3.3.1 Adaptation of the steam drum model

The previous model has been simplified in this section to be more flexible for its application in TRNSYS and adapted to the purpose of the study, which is to estimate the evolution of pressure during the start-up of the system. The considerations are:

- During the start-up no steam is delivered to cover the load, it is only used to carry the system to the operational conditions, in this case, to a minimum of 6 bars. For that reason, $\dot{m}_s = 0$.
- The contribution of the metal body to the energy balance is not considered as it is done in various studies such as [73] and [82]. In addition to this, this term is directly related to the storage capacity of the drum and, as it will be discussed in section 6.3.4 Interpretation of the model, it does not play an important role in this study

The equations defined previously need to be discretised so they can be implemented in the software. The new exponent n indicates the current time whilst n-1 refers to the previous timestep. The discretization of the equation (23) is shown below:

$${M_d}^n = {M_d}^{n-1} + \left(\dot{m}_{fw} + \dot{m}_r - \dot{m}_{rec}\right)\Delta t \tag{20}$$

Equation (24) has been discretized as follow, clearing the pressure variable:

$$P^n = P^{n-1} + \frac{\Delta t}{V_d}\left({M_{sd}}^n\frac{{h_g}^n - {h_g}^{n-1}}{\Delta t} + {h_g}^n\frac{{M_{sd}}^n - {M_{sd}}^{n-1}}{\Delta t} + {M_{wd}}^n\frac{{h_f}^n - {h_f}^{n-1}}{\Delta t} + {h_f}^n\frac{{M_{wd}}^n - {M_{wd}}^{n-1}}{\Delta t} - \left(\dot{m}_{fw}h_{fw}\right)^n + \left(\dot{m}_r h_r\right)^n - \left(\dot{m}_{rec}h_{rec}\right)^n\right) \tag{21}$$

In this case, the enthalpies inside the tank depend on the pressure of the steam drum, which means that an iterative process is needed to recalculate the pressure and enthalpies at saturation conditions. Anyway, as the timestep selected for the simulation is very little, the enthalpies are calculated directly with the pressure resulting from the calculations of the previous timestep. This error would be greater with a higher timestep so a sensitivity analysis will be performed later in the study to assess the performance of the model.

As the steam generated is kept in the drum, the steam quality increases. It is calculated as follow:

$${\alpha_d}^n = \frac{{\alpha_d}^{n-1}{M_d}^{n-1} + \alpha_r\dot{m}_r\Delta t}{{M_d}^n} \tag{22}$$

A solution that requires more detail and accuracy would use the control volume equation (19) to calculate α_d, nevertheless, it adds a higher level of complexity to the system and requires creating an iterative process in TRNSYS. To simplify the problem, the steam title at the outlet of the receiver for

the duration of a timestep (α_r) has been introduced. For little timesteps this value is calculated more accurately, nevertheless, considering that the radiation data is given per hour, any peak value would be found at lower timesteps duration therefore this parameter would not vary greatly in short times. What this means is that the assumption of considering the value of α_r for calculating the equation (28) should not have a significant error using timesteps way lower than one hour.

6.3.3.2 Literature results for the steam drum dynamic behaviour

The steam drum pressure of a DSG system was measured during a typical day of summer and winter for the RAM solar plant in Jordan. The results are shown in the next figures and provide a good comparison to verify the model created in TRNSYS.

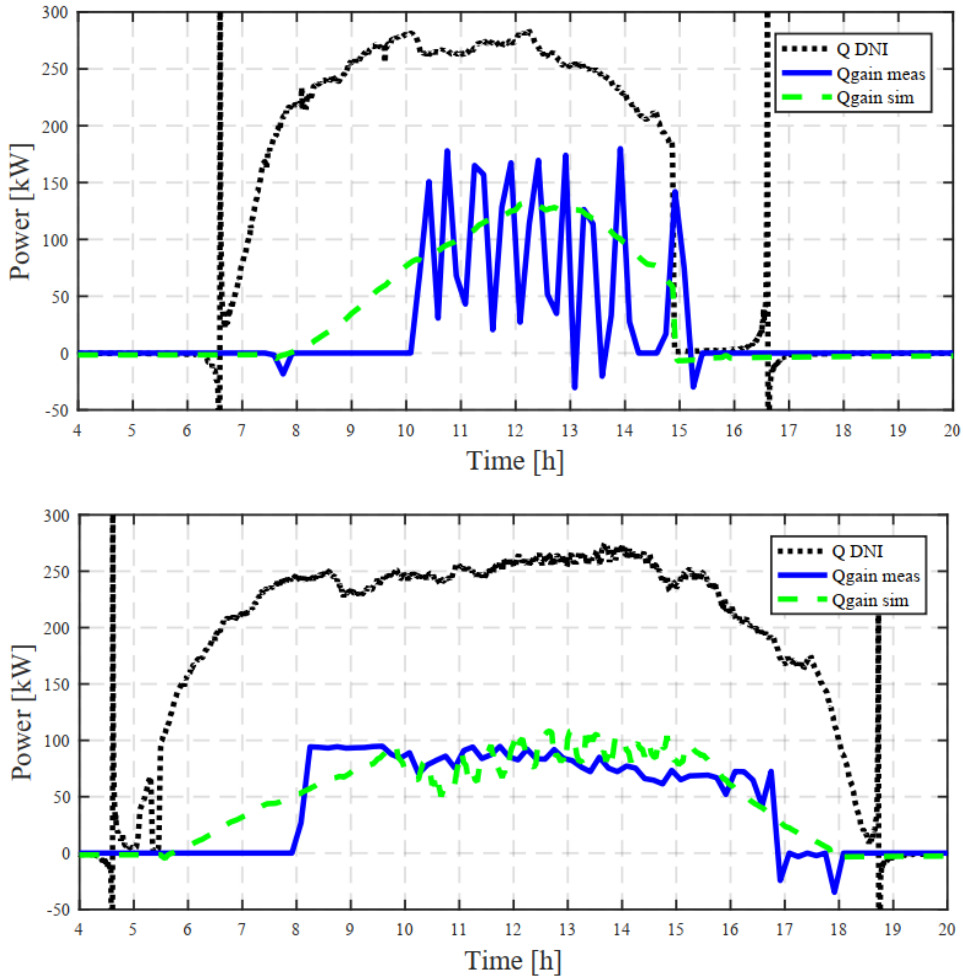

Figure 63. Daily power comparison between a winter day (upper curve) and a summer day (bottom curve) [69].

The previous figure represents the curve of production for the RAM plant during a winter day (2015/12/25) and a summer day (2016/07/03), which gives a clear view of the steam supplied by the steam drum along the day. The difference between the heat gains simulated (green discontinuous line) and the measured net gain (blue continuous line) occurs because the initial gains during the morning are used to compensate night losses and reach the system to the required pressure of operation.

The time required to start delivering steam to the user is nearly two hours since the start-up phase of the system begins. An advantage of the summer day is that the power generated is very stable in comparison with the winter day. This behaviour could be seen through the pressure variation of the

system in Figure 64. The variability in the pressure could be modified thanks to a control strategy to smooth it [69].

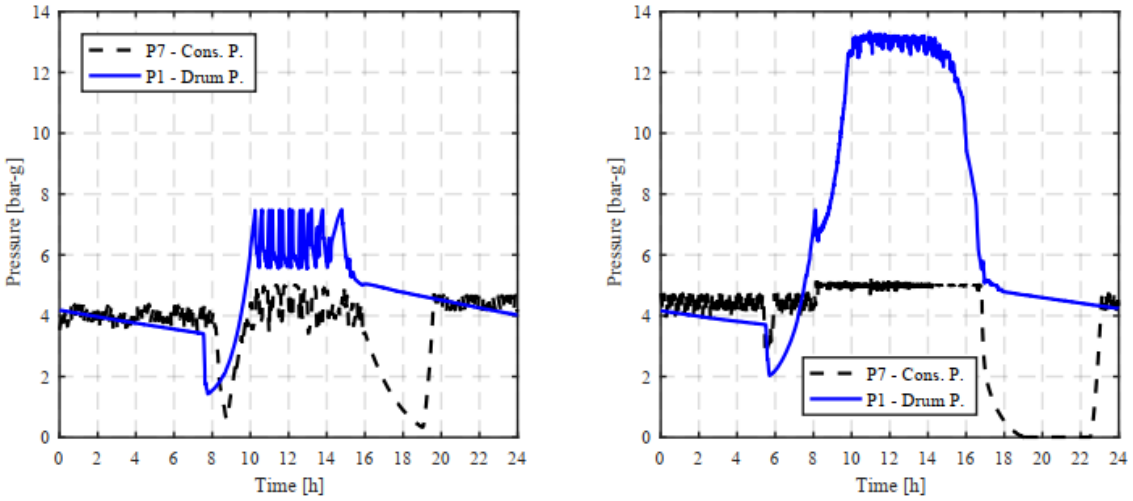

Figure 64. Pressure variation left: 2015/12/25 and right: 2016/03/07 [69].

The storage capacity of the steam drum during summer is shown as an increase of the pressure from the operational point, from 6 barg to 13 barg, contributing to having a more flexible system that is adapted to the steam demand and covers the load for longer times. The blue line in Figure 64 represents the pressure inside the steam drum in bar gauge while the black discontinuous line depicts the pressure on the side of the steam grid. The steam production of the left figure lasts from 10 am to 3 pm whilst on the right starts at 8 am and ends at 5 pm [69].

It is also noticeable that, during the night, the pressure of the system is only reduced by 2 bars from the operation condition thanks to the strategy of keeping the hot water and steam inside the isolated drum. When the recirculation pump gets activated in the morning, a sudden fall of the pressure is seen, a justified behaviour as the liquid in the solar field is colder than the fluid in the drum when both are mixed (see section 6.2.4 System behaviour during a day).

6.3.3.3 Simulation, sensitivity analysis, and results of the steam drum pressure

The initial conditions selected for the simulation of the steam drum pressure are based on the specifications from the case study and the literature review. Aiming to verify the influence of the selected parameters in the results, a sensitivity analysis has been performed. Moreover, due to the simplifications of the model made during the discretization process, different timesteps have been simulated to assess the possible errors.

The most important parameters that contribute to the variation of the drum pressure along time, as was seen in the previous modelling step, are the volume of the tank, its initial pressure, the initial water level, and the feedwater flow. This last parameter may be set to zero for reducing the start-up period. A basic case is defined as follows:

- Tank volume: 4 m^3
- Initial volume occupied by the liquid inside the tank: 70%.
- Initial pressure: 3 bars.
- Ratio of feedwater flow injected in comparison with the steam generation flow: 0%.
- Day: 3rd of July

The values above are selected base on the studies made for the RamPharma Fresnel plant [68] [69]. The steam drum volume may vary depending on the storage capacity that the system demands; in this case, the Hochdorf Plant was also considered as a reference [68].

The timestep analysis is shown in Figure 65 where it is seen that the difference between a big timestep (1h) and a little one (36 sec) is just 6-7 minutes. For the aim of this study where no such duration is problematic, the simplifications made to the discretization of the model are accepted and a timestep of 0.05 hours is selected for simulating the pressure curve of the steam drum during the start-up of the reference day.

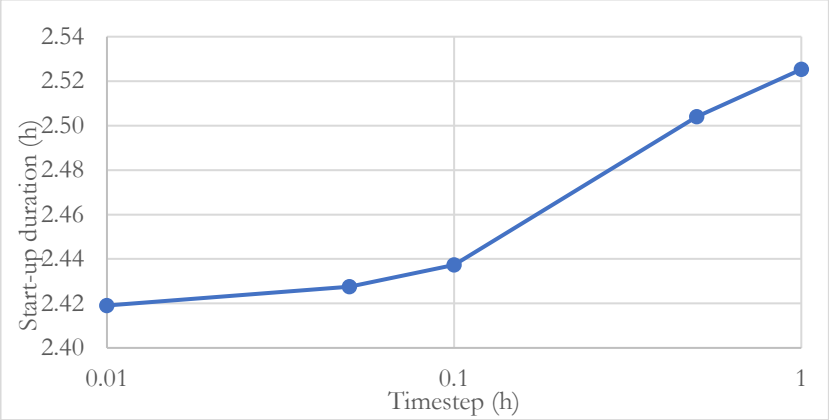

Figure 65. Timestep variation and start-up duration for the basic case.

The parameters selected in the basic case are now analysed to understand their impact on the time duration of the start-up. The only parameter fixed during all simulations is the initial water level inside the tank, which is the one chosen by the RamPharma plant for its nominal operation, 70%.

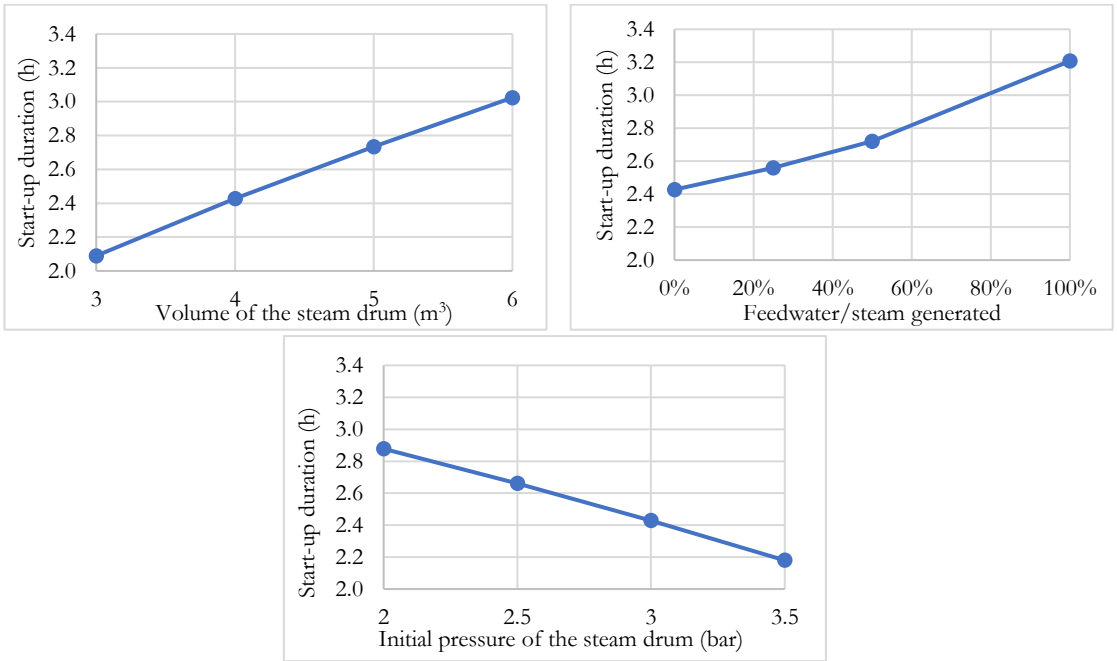

Figure 66.Start-up times from the sensitivity analysis of the steam drum volume (upper left), the ratio of feedwater flow/ steam generated (upper right), and the initial steam drum pressure (bottom).

The three graphs depicted above show how the variation of key parameters of the system and the steam drum affect the time of the start-up, which should be as short as possible. The first graph on the upper left side demonstrates that a tank with big volume difficulties the beginning of the

operation. Nevertheless, bigger tanks have the advantage of a higher storage capacity and higher operational pressures that might be useful in certain applications and give the chance to provide steam when the solar radiation is not enough during a specific time period. For example, in the RamPharma plant, the steam drum is designed to work up to 13.5 barg, even though the steam grid requires 6 barg. This option provides to the steam drum the capacity to work at cover 20 minutes of full load steam production [83].

In the case of the cold feedwater flow, as was mentioned, the best option is not to inject any fresh water during the start-up. However, a minimum water level in the steam drum must be always ensured by the control system. Finally, the duration of the drum pressure seems to be reduced when the initial pressure is higher; an expected result that remarks on the importance of reducing the heat losses over the night.

Finally, the parameters used for the simulation of the plant are those selected for the basic scenario. The results obtained are shown below for two days of the year: a winter day (15/January) and a summer day (03/July).

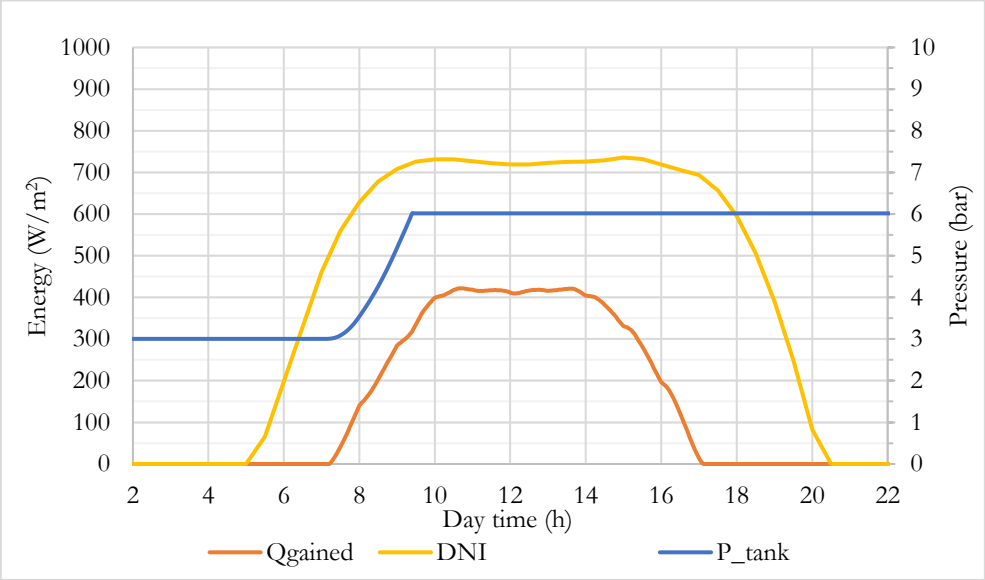

Figure 67. Direct normal irradiation, energy gain and steam drum pressure for a summer day.

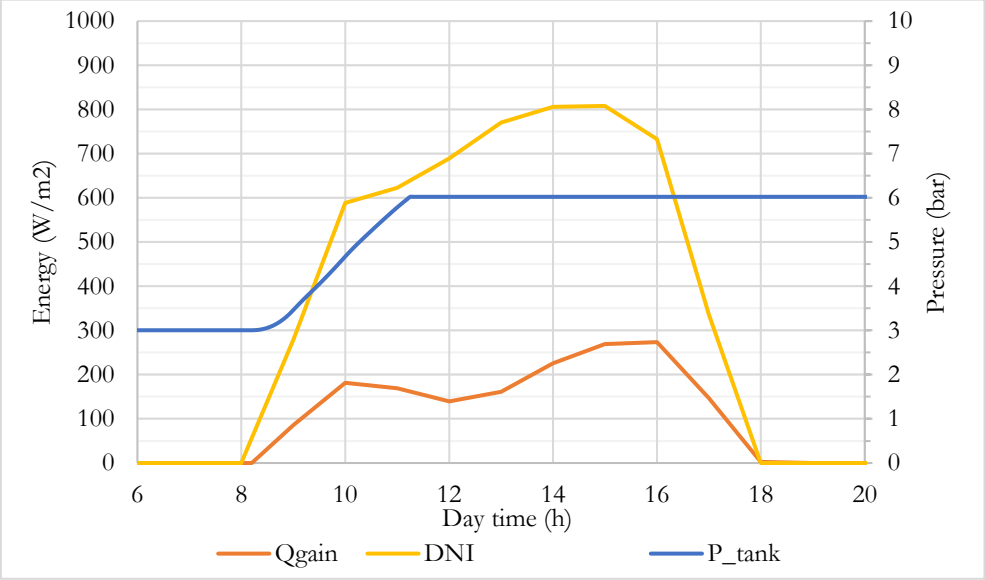

Figure 68. Direct normal irradiation, energy gain, and steam drum pressure for a winter day.

The results show that the pressure reaches the operational conditions (blue line) a bit less than 2h 30 min after the system has gains. At the beginning of the day, the IAM efficiency is zero (it is seen clearly in the summer graph) and it increases along the morning. It is also remarkable that the time need for the system to finish the start-up phase is shorter in summer than in winter, in it is close to three hours for the cold period. These durations obtained in the simulations are just a bit longer than the ones shown in the RamPharma (Figure 64).

In conclusion, the solar system is assumed to begin gaining heat from the Sun after the sunshine and when the angle of incidence allows it. For example, in the case of the RamPharma plant, the recirculation pump begins to work when the DNI is > 200W/m² and the Sun zenith angle is < 80º [68]. The system generates steam and increases slowly the pressure by storing it into the steam drum and recirculating saturated water each time at a higher temperature. When the pressure conditions are reached, the system starts supplying steam to the grid which is at 6 bar and it is shut down at the end of the day when there is not enough radiation to continue producing any steam. The variations along the day of pressure are supposed to be covered by the steam drum, so the pressure does not have great valleys. The start-up period is set to be 2h:30min for spring, summer, and autumn and 3h for winter. As it was commented, the case of RamPharma requires a bit less time (around 2h) but different design parameters have been considered and analysed in this study such as the tank volume, initial pressure, and feedwater flow.

In Figure 69 it is shown the control system designed to start delivering steam to the user when the start-up period is finished. The controller used is the "Start-up clock" (type 980) that measures the time since the collectors start to gain energy in the morning. When that time is bigger than the one established by the component "Season" (type 14) as the start-up duration (2h30min or 3h), the control valve opens to let the saturated steam be consumed by the user to cover its load.

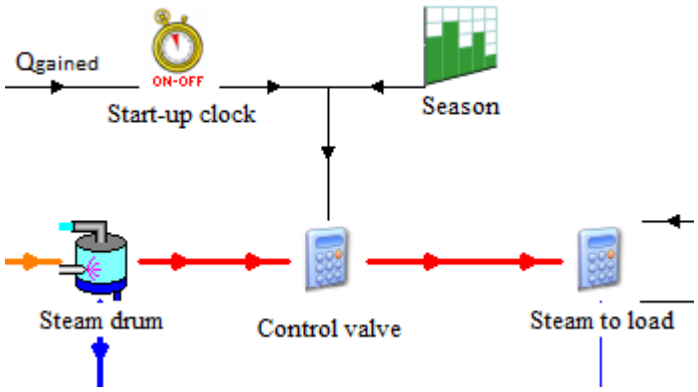

Figure 69. Control system designed in TRNSYS for delivering steam to the user after the start-up.

6.3.4 Interpretation of the model

The developed model tries to provide a simulation of a Fresnel DSG plant as accurately as it is required for the goal of getting the results needed to perform the feasibility assessment in the following chapters. The characterization of the different components has been done thanks to the information provided by Solatom in terms of collector design and operational conditions. A literature review has been conducted to justify the assumptions that are taken and the simulation results.

The two biggest challenges have been the characterization of the collector performance, especially in terms of heat losses. The dynamic of the steam drum was modelled with some simplifications to adapt the model to the TRNSYS tool, performing afterwards a sensitivity analysis to assess the quality of the assumptions as well as the influence of some parameters in the start-up period.

Moreover, the steam drum control and modelling are challenging tasks that are still being researched; in the case of this study, the storage capacity of the drum has just been considered for maintaining the operational conditions, but not as a design parameter. The pressure curves of the steam drum model are only used for estimating the start-up duration. The results needed for the economic analysis are generated with a timestep of 1 hour in the simulations, which makes any dynamic behaviour neglected apart from the start-up phase.

6.3.4.1 Considerations regarding the simulation timestep

The simulation of the solar system model could be done following different approaches. Depending on the time factor, it could be distinguished three simulation methods:

- Steady-state: the model output is assumed to be time independent, and therefore it is not affected by the previous timestep. The conditions are supposed to be stationary [69].
- Quasi-steady state: this approximation for simplifying long-term dynamics represents faster phenomena by their equilibrium conditions, not by their full dynamics. This method required short timesteps but big enough to do not consider fast perturbances on the model results.
- Dynamic: characterized with very short timesteps in simulations, this approach provides a detailed model that represents the transient behaviour of a system and its perturbations within seconds or minutes [84].

In order to better address these concepts, a good example of the difference between quasi-steady state and steady-state could be found in the normative EN ISO 9806:2017, which explain these two possible methods for testing the solar collectors' performance. The difference in the performance model by using the quasi-steady state method is the division of the solar radiation into direct and diffusive and that incorporates the term of effective thermal capacity and, therefore, a transient behaviour of the collector for its losses. On the other side, to accept that a collector is working under steady conditions the testing procedure determines that none of the experimental parameters deviates from its mean value by more than a specific limit, considering a period no lower than 15 minutes.

Moreover, the differences between the quasi-steady and dynamic methods were address in the study performed for the modelling of the Tennessee Eastman process [85]. This process is widely used in the chemical industry and consists of various devices where steam and liquid are found together under different temperatures and pressure, similar to the steam drum studied before. The figure below shows a change in the pressure of a tank or reactor, and which are the results both with the full dynamic model and the quasi-steady state. It is clear that, even though both are similar when the pressure is stable, the fast change behaviour of the tank could only be seen using a dynamic simulation. This dynamic response of the system is key to design and establish the control strategy that needs to be applied.

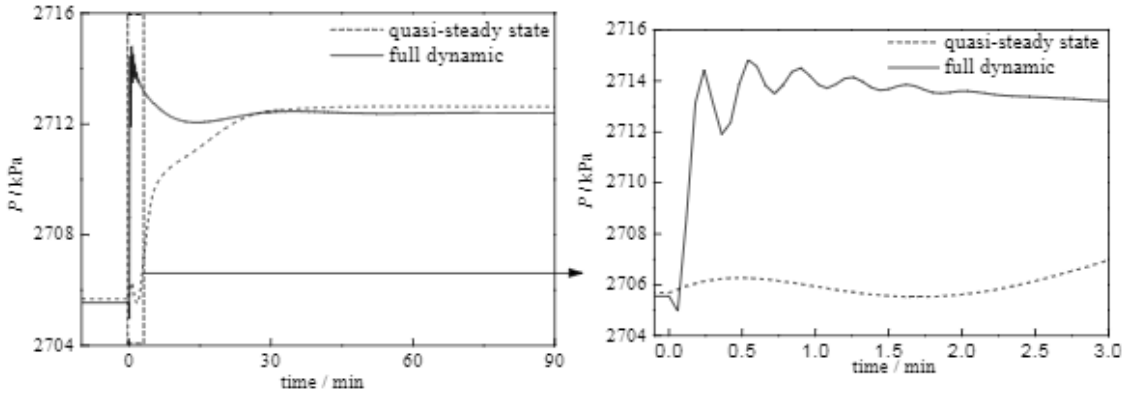

Figure 70. Dynamic response of reactor in quasi-steady state and full dynamic model [85].

The case study was simulated as a quasi-steady state model, selecting a 1 hour timestep with the aim of achieving the required results for performing the techno-economic analysis later on. This consideration was taken as the control system of the plant was not designed for dealing with the perturbances and challenges of a DSG system (explained in detail in section 6.2.3 Control system) regarding the variability of the solar resource. Anyway, this assumption leads to some inaccuracies regarding the plant responses as it was shown in Figure 70, where the dynamic pressure of the tank varies less smoothly than in the quasi-steady results. These fast pressure changes could affect the quality of the steam supply to the user, being the steam drum storage capacity a great factor in terms of dealing with this variability of the solar radiation.

Nevertheless, as the start-up is a critical phase for a DSG system, has been analysed from a dynamic approach the behaviour of the steam drum and the pressure conditions as the bottleneck for starting delivering steam to the user.

6.3.4.2 Considerations regarding the storage possibilities in DSG

One of the main challenges that solar heat has to face in industry is the fact that the demand curve of the factory does not match the solar radiation hours and, therefore, with the renewable heat supply. Moreover, the perturbances created by clouds or other environmental phenomena that make a fast variation on the solar radiation causes various problems for the stability of the solar plant. These two issues could be managed thanks to the use of thermal storage and control strategies.

The types of thermal storage were reviewed in previous chapters (see 2.3.5) and their need is one of the main factors to consider when designing the solar field. In the case of water demand at a temperature below 100 ºC, it is a common procedure to use an isolated storage tank at atmospheric pressure to provide heat when there is not enough solar energy. Nevertheless, the challenge is more complex when the system is delivering steam or other HTF at higher temperatures, which require the use of pressurized water storage or other types of storage materials such as molten salts, concrete, thermal oil, PCM, etc.

In the case of direct steam generation, it is possible to size the solar field in order not to need storage by ensuring that the solar peak does not overpass the demand curve. This design also minimizes the shutdown periods of the solar plant, when it is necessary to defocus the mirrors, and reduces the payback period with the drawback of limiting the solar energy share. In addition to this, the steam supply must be covered as well in parallel with a conventional boiler [86] [87], with the disadvantage that the boiler has its efficiency curve which depends on the load, hence high solar gains may affect the boiler performance [69]. The storage of saturated or superheated steam is generally not economically attractive due to the high investment cost of the pressure vessel in sum to the low volumetric energy density that it provides [88]. The steam storage concept can be suitable for buffer storage applications to compensate fast radiation perturbances, but not for greater periods of time [89]. As it was mentioned, the steam drum capacity for storing depends greatly on the pressure that could be reached by the tank since the steam discharge means a reduction in the pressure and therefore of the saturated water temperature inside the tank.

Moreover, the working days of the factory should be considered as, for small and medium enterprises, it is usual not to work seven days a week. The implication of this fact may enhance the decision of using thermal storage for accumulating solar gains during the weekend [87].

In the case study, the storage capacity of the steam drum is considered only to cover the perturbances caused by clouds and possible solar power peaks, but it has no longer implications. Despite that, it would also be appropriate to analyse if the demand curve could be modified in order to match as much as possible to the solar heat supply.

6.4 Conventional industrial heating system

Nowadays, the most common fuel to cover the heat demand in the Spanish industry is natural gas. This fuel was responsible in 2019 for 8,414 ktep of the final energy consumption in industry and its growth has been positive since 2016 [90]. Regarding the technology for heat generation, the use of boilers is implanted all over Europe and it is the most frequent way of burning natural gas for supplying steam to the factories [35].

The conventional system that generates steam in the case of study is a natural gas boiler with 80% of efficiency. The main advantage is that its operation adapts the generation to the demand, so the load curve is fully covered. The steam production carried out by a boiler in parallel with the Fresnel solar system ensure that, even when there is not enough radiation to cover the demand due to its variation during the day, the boiler is always available. The total heat demand for a year is 4,858.52 MWh and the typical load curve for a day is depicted below:

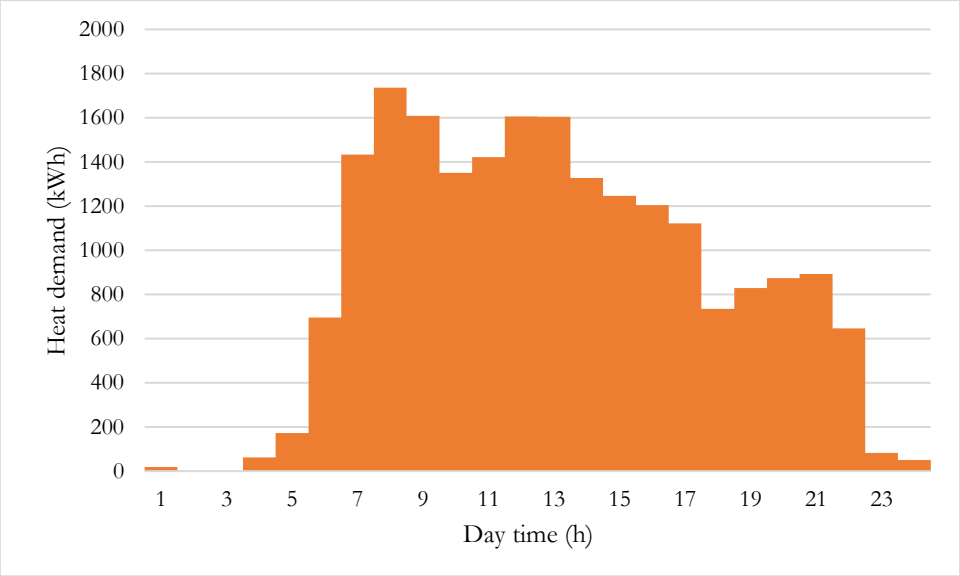

Figure 71. Heat demand curve during a day of summer for the case study.

The heat demand curve varies in size along the year but not in form, being summer and autumn days the ones with higher energy demand. The peaks are found at 8 am and around 2 pm; this second peak is especially suitable to be covered by the SHIP plant. Nevertheless, some parts of the curve may not be covered at any time of the year since they occur during night time.

Natural gas in Spain comes mainly from Argelia and can be bought through multiple commercial agencies, anyway, exist three that cover half of the NG market for the industrial sector: Naturgy, Repsol and Endesa. The first one is the leader in sales for the region of the study case, Sevilla [91]. The price of natural gas differs from householders to not householders; for this second category, large manufactories get better fuel prices than small and medium enterprises (SMEs) like the one in this study. The NG price for European Union countries varies between 35 – 40 €/MWh (all taxes and levies included) for industries with demands in the range of 2.78-27.78 GWh. The selected fuel price for the conventional boiler of the system is the average of the last two years data (from the second semester of 2018 to the first of 2020), which means 36.3 €/MWh [92]. Even though the case study demand is in the range defined before, it is in the lower extreme of that range and may be affected by the difference in prices between little and big industrial companies. For that reason, the sensibility analysis that will be performed to this parameter is necessary as, even NG prices in Europe are quite stable, the final tariff may vary from one company to another regarding its size.

6.4.1 Emission Trading System costs

The European Union Emissions Trading System (EU ETS) allows having a positive economic impact for reducing the emissions of a company. That is why the change from fossil fuels to solar energy has a reduction in the cost for the industry and should be taken into account as a driver for SHIP integration. The ETS works with a unit of GHG emissions, the EUA. A EUA corresponds to the emission of one ton of carbon dioxide or the equivalent amount of gases with higher climate change potential such as perfluorocarbons and nitrous oxide.

Figure 72. Evolution of the EUA price for the past five years [93].

The price of a EUA has been changing over the past decade; for this study, it is chosen 28 €/EUA based on the values depicted in Figure 72. Even though this value is an approximation of the recent years' analysis, the current trends show that it might grow in next years as the EU legislation has become stricter since 2018.

6.5 Techno-economic performance indicators

The feasibility assessment for SHIP integration, not only regarding technical but also economic terms, is performed in a quantitative way with the selected performance indicators. This section describes the indicators that will be used to determine the feasibility boundaries of the case study and understand the limitations and drivers of solar heat technology in industrial processes.

6.5.1 Useful heat output

It is defined as the total amount of heat transmitted to cover the load. This is the purpose of the solar system and, therefore, the main parameter that should be taken into account for assessing the capacity of the system for supplying heat to the industrial process. The sum of the heat generated over a year is defined as the annual yield (H_{net}) [94].

6.5.2 Solar fraction

The solar fraction indicates the share of the total heat load that the solar resource is covering [33]. Locations with higher levels of radiation can achieve higher solar fraction when designing the solar system, as was mentioned before, a usual estimation is 30%:

$$SF = \frac{H_{net}}{H_{load}} \tag{23}$$

6.5.3 Solar system efficiency

The global system performance can be defined as the annual solar to heat efficiency (η_g). This parameter is the ratio between the annual heat output that is supplied to the industry and the total solar energy incident on the solar collector field. Global efficiency is used mainly to compare different solar technologies performance, despite that, as the solar resource is "free", this efficiency is often expressed among the solar yield indicator which serves for calculating other financial/economical parameters [94] [33]. The incident radiation considered in this study is the DNI; with this term, the radiation not harvested by the collectors is also part of the efficiency lost.

$$\eta_{gl} = \frac{H_{net}}{\varphi_{solar}} \quad (24)$$

Other efficiencies for the solar system could be taken into account, for example, the collector's efficiency. This indicator has been already standardized as it is shown in Figure 11 and depends on the type of collector, solar radiation levels, ambient conditions (temperature, wind…), etc.

6.5.4 Capital Expenditures (CAPEX)

The CAPEX is the total investment cost of the project and it is a key indicator for some decision makers even though it does not measure the performance of the solar plant. These costs are divided into direct and indirect. The first one generally refers to the purchase and installation of the equipment whilst the indirect costs are related to the remaining costs incurred in project engineering and development [94].

The costs for the integration of solar heat are the sum of multiple factors and depend strongly on the process temperature level, demand continuity, project size, and the solar resource availability of the location. It is estimated that, for conventional FPC and ETC, investment system costs vary in Europe between 250–1 ,000 €/kW [4]. The investment assumed for the case study will be defined afterwards. It is also common to express the investment value of the collectors in terms of €/m² as it is useful for comparing different solar technologies or solar sizes linking the cost with a physical component, the collector. Nevertheless, this comparison is also affected by installation characteristics: the region where SHIP is implemented, roof/floor space, environmental constraints, size, etc [33].

The costs defined in equation (25) are:

- The investment for the solar field (C_{sf}), which is mainly composed of the collectors.
- Cost of the connection system between the load and the solar field which includes piping (C_{pp}) and the steam drum (C_d).
- Costs for auxiliaries' subsystems such as the electrical and instrumentation (C_{aux}).
- Finally, it is also considered for the total direct CAPEX a contingency cost (C_{cont}).

$$CAPEX_{direct} = C_{sf} + C_{pp} + C_d + C_{aux} + C_{cont} \quad (25)$$

Regarding the cost of the components, the collectors and their installation generally account for 50% of the total investment, piping for 20%, the buffer storage and the possible heat exchange for 11%, and the control system for 5% [4].

6.5.5 Operational Expenditures (OPEX)

The OPEX indicator involves all the ongoing cost for operating and maintenance of the solar system in the industrial plant, as well as the energy consumption. In this case, the solar plant only consumes solar and electrical energy and the costs for the second one are neglected. These expenditures are calculated for a period, generally for a "typical" year. This concept expresses that the estimations are made for a period without unexpected failures or unusual operation [94].

OPEX is quite difficult to calculate because it must take into account parameters such as cleaning the mirrors or a defective piece replacement. Due to this fact, it is commonly taken as a percentage of the CAPEX, with values of around 0.3 to 0.5%. Two types of costs contribute to the OPEX: Fixed costs such as labour, monitoring or maintenance, and variable costs like power consumption or wastes disposal [33].

6.5.6 The Levelized Cost of Heat (LCOH)

This indicator is key to evaluate the cost of heat generated by the solar thermal system. It is a combination of the CAPEX and OPEX over the expected lifetime of the plant and gives a comparison of the costs between different solutions and technologies [33] although their scales and level of investments may be different.

For the calculation of this parameter it is considered the time value of money using the weighted average capital cost (WACC). This value represents the required return on all sources of long-term capital and depends on the typology of the investors, varying according to the project about 2-10% [33].

$$WACC = Eq_{\%} * IRR_{eq} + Debt_{\%} * i_{debt} * (1 - T_{corp}) \quad (26)$$

Equation (26) considers one side the equity share of the investment ($Eq_{\%}$) and its rate of return (IRR_{eq}) and, on the other side, the debt share ($Debt_{\%}$), its interest rate (i_{debt}), and the corporation tax (T_{corp}). The OPEX is calculated as shown in equation (27), where the term System Degradation Rate (SDR) is known as the system degradation rate and affects the heat yield. H_{net} can be assumed as the first year net output heat [94].

$$LCOH = \frac{CAPEX + \sum_{n=1}^{N} \frac{OPEX_n}{(1+WACC)^n}}{\sum_{n=1}^{N} \frac{H_{net} * (1-SDR)^n}{(1+WACC)^n}} = \frac{Lifetime\ Cash\ Outflows}{Lifetime\ Heat\ Yield} \quad (27)$$

Some typical values for solar thermal that can be used as a reference are [33]:

- Lifetime years: 20 to 25 years.
- Degrad (SDR): 0.5%/year.
- WACC: 4%

6.5.7 The Net Present Value (NPV)

This concept is a financial performance indicator used for the comparison of the profitability between projects. It is the sum of the discounted cash-flows along the lifetime of the plant and calculates the future income at present time to help decision making. Equation (28) shows the calculation of the NPV:

$$NPV = -CAPEX + \sum_{n=1}^{N} \frac{C_{flow}}{(1+d)^n} \quad (28)$$

The discount rate (d) is used for applying the time value factor and can be considered equal to the WACC [94] The cash flow is named as C_{flow} and the expected lifetime for the plant t [94]. The term n is the specific year in the lifetime.

6.5.8 The Internal Rate of Return (IRR) and Payback

IRR is calculated as the interest rate value that would make the NPV of the project equal to zero. That depicts the maximum interest rate that a project can handle before having a negative financial outcome and, therefore, not suitable for investors. A high IRR in a project demonstrates its feasibility even though a high interest rate value is selected [94].

On the other hand, the payback period is defined as the years a project needs to start generating profit. In SHIP, this time arrives when the sum of the yearly fossil fuel savings for not using the conventional heating system is higher than the solar plant costs (CAPEX+OPEX), resulting in a positive accumulated cash flow. This indicator not only shows the risk for choosing projects with long term benefits but also helps companies with liquidity problems to select projects with a fast investment return [33]. Moreover, two different payback periods can be distinguished: the simple one which does not consider any time factor such as the discount rate or the inflation, and the discounted payback which does. The second one is recommended when risk is an important issue for investors [95].

6.5.9 Cost and fuel savings

The savings for the integration of solar systems are mainly derived from working with a free energy resource, as it is solar radiation, instead of purchasing fossil fuels for heat generation. In addition to this, for the savings calculation only the maintenance costs of the solar system are considered as the conventional system is assumed to be the same in both scenarios since the boiler keeps working in parallel to the solar system. The calculation of fossil fuel saving is also necessary for estimating the positive environmental impact of the solar system, expressed in savings for the EU ETS. The term C_{BAU} represents the costs for the current BAU scenario (Business-as-usual), and C_{solar} the costs for the proposed new one with solar generation.

$$C_{BAU}{}^{n} = C_{fuel} + C_{ETS} \quad (29)$$

$$C_{solar}{}^{n} = C_{fuel,solar} + C_{ETS,solar} + OPEX_{solar} \quad (30)$$

Moreover, an inflation rate (i) is considered due to the expected growth in natural gas prices for the following years [96]. This growth is modelled for the cash flow as an annualization over the lifetime of the plant as follows:

$$C_{fuel} = Q_{fuel} * Price_{fuel} * (1+i)^{n} \quad (31)$$

Where Q_{fuel} is the amount of fuel consumed by the boiler and $Price_{fuel}$ its price.

6.5.10 GHG emissions savings

The integration of renewable sources as an alternative to fossil fuels leads to a reduction in emissions for industrial activity. This environmental benefit can be calculated as equivalent CO_2 reduction by knowing the amount and type of fossil fuel that has been removed (F_{saved}) from supplying the heat demand for the process.

$$GHG_{saved} = F_{saved} * CO_{eq,factor} \quad (32)$$

The conversion factor of fuel consumption to CO_2 ($CO_{eq,factor}$) is defined for different types of fuel in Table 17.

Type of fuel	CO_{eq} emissions (g/kWh)
Light fuel oil	300
Heavy fuel oil	320
Natural gas	234
Propane or butane gas	274
Coal	384

Table 17. Conversion of fossil fuel consumption to CO_2 equivalent emission [33].

6.6 Technical and economic model input

The parameters applied to the model are collected from the case of study data or assumed based on the literature reviewed and previous research. The cost rates used for estimating the CAPEX are compared with the real plants of Mafrica in Spain (CAPEX=780€/ kW_{th}), Nuova Sarda Industria Casearia in Italy (CAPEX=850/ kW_{th}) [47] and the cost data used for the economic analysis of a Fresnel plant in Sevilla [97]:

Parameter	Value
Heat demand	4,858.52 MWh
Solar annual yield	1,134.17 MWh
Year DNI accumulated	4,196.67 MWh
Solar field cost	410 €/kW_{th} (~58%)
Steam drum cost	65.65 €/kW_{th} (~9%)
Piping costs	30 €/m^2 (~8%)
Auxiliaries cost	5%
Construction, engineering and contingencies costs	20%
CAPEX	740,000 €
OPEX	0.5%
EU ETS price	28 €/$tCO_{2,eq}$
NG price	36.3 €/MWh

Table 18. Parameters selected for the techno-economic analysis.

Parameter	Value
Inflation rate NG	2% [98]
Lifetime	25 [99]
Equity share of the investment	20%
Interest rate for equity	13.5%
Interest rate for debt	3.5%
Debt share	80%
WACC	4.66%
Degradation	0.5%

Table 19. Parameters values selected for the financing study.

.

7 RESULTS AND DISCUSSION

This chapter describes the results achieved after the simulation of the Fresnel plant over a year and its techno-economic assessment. It aims to depict the performance of the solar system, understand its behaviour and discuss the results. On the other side, the economic analysis is not limited by the study case, which establishes the reference scenario, but also a sensitivity analysis is performed to the parameters that most affect the economic feasibility of the solar system. Therefore, the assessment of the favourable conditions for integrating this technology and its main drivers is achieved.

7.1 Case study results

In this section, the results from the case study are shown, not only the energy performance but also its economic analysis. The Fresnel plant operation has been simulated for a whole year, providing the results of the heat transferred to the user steam network, which is its main purpose.

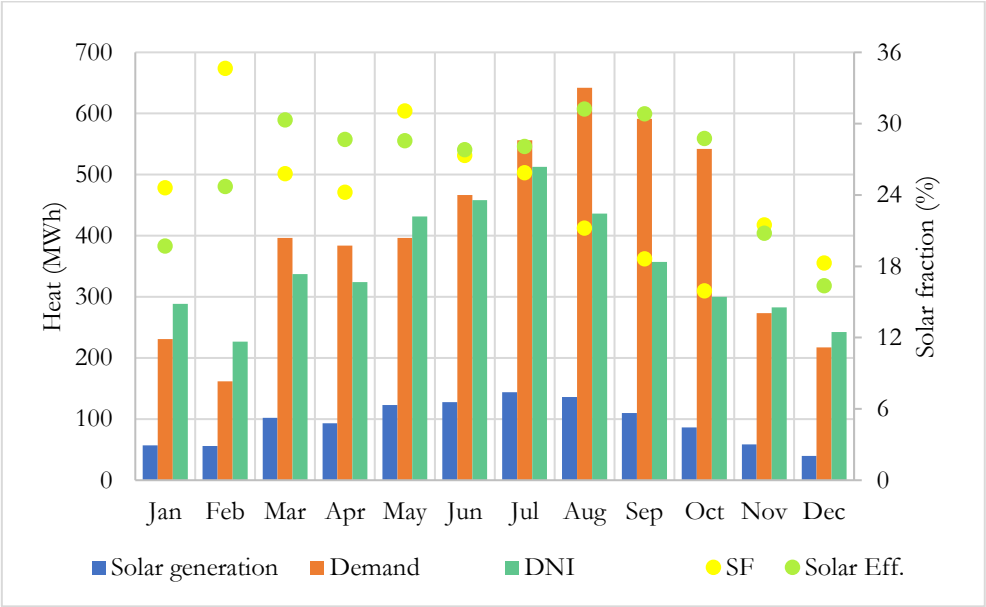

Figure 73. Energy performance values and indicators of the solar plant per month.

Figure 73 shows the total energy performance values of the solar DSG plant for each month. The orange columns represent the heat demand of the factory, which follows the daily profile depicted in Figure 71, increasing during the first part of the year until August and decreasing since then. The maximum achievable beam radiation is the DNI (grey columns), nevertheless, it is not harvested entirely due to being a one-axis tracking system, its optical losses, and the heat losses. Considering that also part of the heat is used to bring the system to the operational conditions during the first part of the morning, the final steam supplied (blue columns) that cover the load represents between 20 to 30% of the DNI (see the green points). In the case that it is considered for the performance calculations the beam radiation that reaches the collectors instead of the DNI, the solar system efficiency over the year is 31.1%. The solar field efficiency calculated as the ratio between the beam radiation that reaches the collectors and the heat transferred to the HTF is 40.2%.

The solar fraction is represented in yellow for each month and depicts an average value of 24.1% over the year. During the period between August and October the heat demand of the factory is higher than the solar radiation, which makes it impossible for the system to reach high solar fraction values even though the system efficiency is the highest of the year. On the other hand, in months

such as January and February with low demands, at certain hours of the day the solar system can achieve the complete coverage of the steam load, presenting values of solar fraction higher than the system efficiency. During a few hours, the solar generation overpasses the demand, nevertheless, it is assumed that the steam drum can store that excess, as it is just for very occasions in those two months.

The economic savings that make the solar DSG plant a profitable business are a consequence of the fuel saved by using solar energy and the reduction of the emissions which are costly in European Union countries. The next graph shows how these savings evolve over the year and the emissions difference between the BAU and the new solar system which means as well a reduction of the environmental impact.

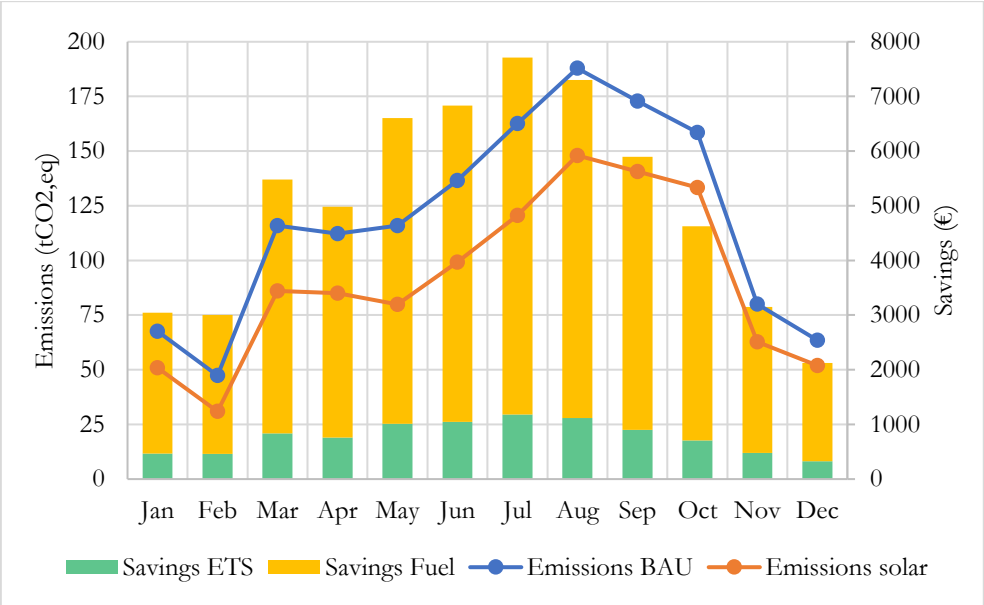

Figure 74. Emissions of both BAU and solar plant, and the related economic savings for fuel and ETS.

During periods with high levels of radiation, the cut on emissions can reach values of 40 tonnes of $CO2_{eq}$. Even though this reduction only means 15.3% of the total economic savings, this extra value added to clean energy projects has served to promote the integration of solar in industry and may have a bigger impact in the future if the price per ETS keeps growing.

The economic indicators that characterize the performance of the new scenario with solar heat are shown in Table 20. Techno-economic indicators for the base case with solar heat integration.Table 20. The net present value of the project, considering a lifetime of 25 years, is positive since the year 16-17. Nevertheless, the simple payback is almost 4 years lower than the discounted one, which means that the project starts providing profits after year 13 if no time factor is considered. These results are set as the base case scenario for the solar heat plant, nevertheless, multiple influential factors may not be accurate because they are selected from the literature reviewed, such as the CAPEX, and others may vary unexpectedly along with the duration of the lifetime of the plant. For that reason, it is needed a sensibility analysis to understand what parameters are the most important ones in terms of estimating the feasibility of the project and consider future possible trends of external variables such as the natural gas price or the costs of emissions.

Techno-economic indicator	Value
Solar fraction	23.3%
Solar efficiency	26.3%
LCOH	50.6 €/MWh_{th}
Simple Payback	13.0 years
Discounted Payback	16.7 years
Net Present Value	259,743 €
IRR	7.6 %

Table 20. Techno-economic indicators for the base case with solar heat integration.

The LCOH value is more elevated than the cost of natural gas, which is a result that reflects the reason why the payback period takes longer than in other solar projects. From a financial point of view, the IRR shows that, if the value of the money was decreasing at a rate above 7.6%, the benefits of the project would not be positive so as the NPV. Therefore, it sets a limit for the investors.

7.2 Sensitivity analysis

The sensitivity analysis is made to estimate the techno-economic boundaries for the integration of this type of technology. The methodology applied for this section is to vary the base case study parameters within the ranges of values that have been decided based on the literature review.

Firstly, two technical aspects have been considered for the analysis: the start-up duration of the solar plant that was estimated in previous chapters, and the energy source that replaces the natural gas, the solar radiation. Then, the parameters related to the cost of the plant, the CAPEX and OPEX, are assessed to see their impacts on the feasibility of the project. Finally, financial and external aspects are analysed: the WACC, the NG price and inflation, and the ETS costs. The parameters and their range values used for the sensitivity analysis are described in the following table:

Parameter	Base value	Analysis range
DNI	Weather data	41-156 %
Start-up time	3h (winter), 2.5h (rest)	1.5-2.5 h
Demand curve	7 days/week	6 days/week
CAPEX	740,000€	+-20 %
OPEX	0.5%	0-1%
NG price	36.3 €/MWh	20-80 €/MWh
NG inflation	2%	0-4%
Discount rate	4.66%	2-8 %
EU ETS cost	28 €/$tCO_{2,eq}$	0-100 €/$tCO_{2,eq}$

Table 21. Parameters and values selected for the sensibility analysis.

Is considered that the prices of NG in Europe are between 30 and 50 €/MWh, hence, the results for the LCOH analysis could be compared with this range of values [100]. Aiming to consider other costs such as the ETS (6.55€/MWh) and the losses due to the boiler efficiency (80% in this case), the range

has been modified to 45-70 €/MWh, so it serves as a visual reference for the graphs and can be compared with the LCOH of the solar steam. This price range will be depicted as a clear blue region in the next graphs. Applying the same logic, the price at which the company buys the NG could be modified from 36.6 to 53.6 €/MWh.

7.2.1 Solar resource and location

The solar resource of the location in Sevilla has a direct normal irradiation value of 2,208.54 kWh/m²year, which makes a total of 4,196.67 MWh/year. The importance of direct irradiation relies on the amount of steam that can be produced; it is a key technical parameter even though it is not determinant for deciding if a solar plant is feasible or not and its potential market (see section 5.5: Potential customers and geographical market). The analysis performed varies the DNI base case on a percentage, and also provides examples of regions with radiation levels within that range to have a location reference for the results:

Location (country)	DNI [kWh/m²year]	Variation of DNI [%]
Amsterdam (Netherland)	905	-59
Munich (Germany)	1101	-50
Ginevra (Switzerland)	1373	-38
Napoli (Italy)	1605	-27
Atenas (Greece)	1795	-19
Windhoek (Namib)	1977	-10
Amman (Jordan)	2500	+13
Mexicali (Mexico)	2815	+27
Calama (Chile)	3451	+56

Table 22. Solar radiation resource for different locations and its variation regarding the case study in Sevilla (own calculations) [63].

Solar radiation level affects the payback period as is seen in Figure 75. For DNI values lower than 1750 kWh/m² the expected payback period increases exponentially, which means that the return on the investment may take longer than the lifetime of the project and, therefore, it is not a profitable business. Moreover, as higher the DNI is as lower is the difference between the discount and the simple payback, decreasing the years by half from locations with 2000 to 2500 kWh/m².

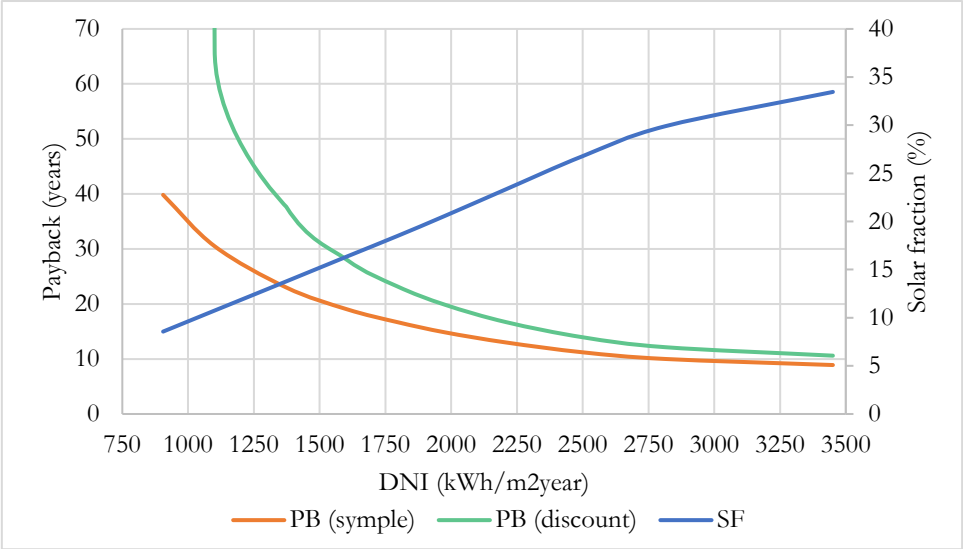

Figure 75. Simple and discounted payback and solar fraction curves under different DNI values.

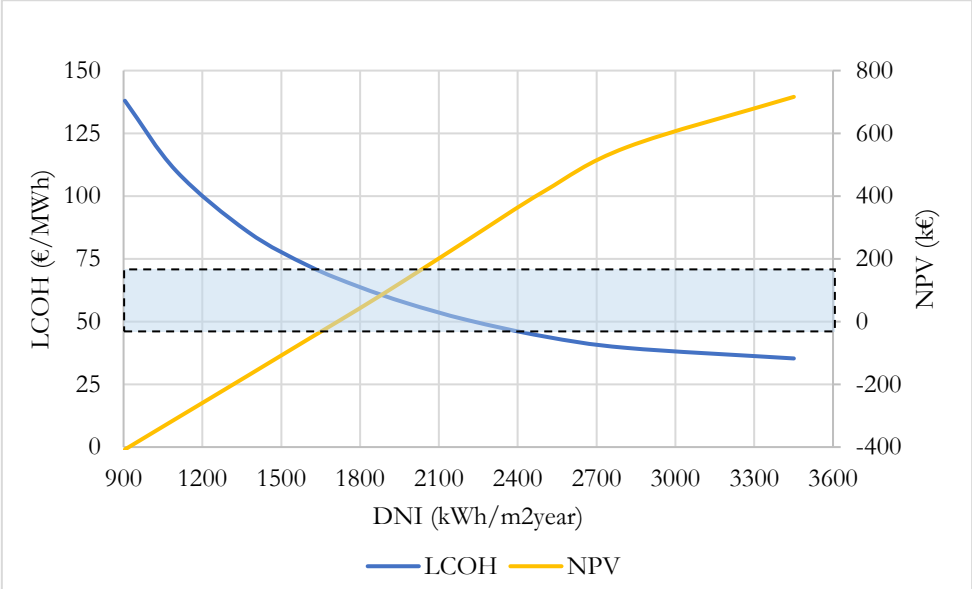

Figure 76. LCOH and NPV under different DNI values visualizing the cost range of NG in Europe.

The LCOH varies extremely with solar radiation, as well as the NPV. Figure 76 shows these results after analysing the DNI for multiple locations, providing the conclusion that the system has an NPV positive just above 1750 kWh/m²year, and seems suitable regarding the LCOH for values of radiation above 2250 kWh/m²year considering the current prices of NG. The NG cost range is achieved by LCOH values above 1650 kWh/m²year, which is a positive result in favour of the SHIP potential. However, it should not be forgotten that this analysis is made for a 25 year lifetime of the project, the years needed for the LCOH to have similar values as the NG have to be taken into account as is seen in detail in Figure 78.

The LCOH curve depicts an exponential behaviour; its cost grows rapidly for low radiation conditions, making it more difficult to deploy this kind of technology in northern countries. On the other hand, it has been proved that in the previous analysis of SHIP potential that other drivers are key to address the feasibility of solar heat such as enabling policies, high NG prices or ease of doing business environment.

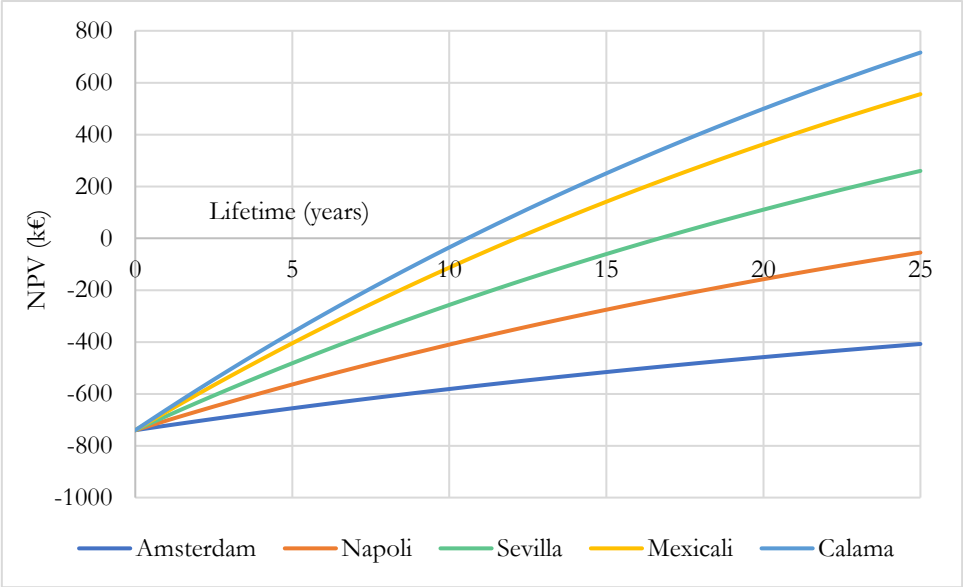

Figure 77. NPV curves for the case study lifetime under different radiation conditions.

The decision of investing in a project is influenced by the NPV curve. It shows not only the cash flow and time dependency during its lifetime but also when the project start been profitable. The figure above depicts how the location, and thus the solar radiation, have a great influence on the economic analysis of the project as varies the inclination of the NPV curve. In the case of the locations with higher solar radiation, the discounted payback tends to be 10 years while the cases of Napoli or Amsterdam require longer times than the 25 years, the expected lifetime of the plant.

7.2.2 Start-up duration

The duration of the start-up period determines when the plant is ready to deliver steam to the user at the correct conditions. Since the duration of this phase has been discussed and estimated in previous steps of the study, it is key to assess the effect of this duration on the economic boundaries and its impact on the results. As it was mentioned, the start-up is a very important phase for every solar DSG plant and requires optimization techniques to reduce it as well as an advanced control strategy.

Duration (summer-winter) (h)	H_{net} variation	Solar fraction variation	Simple Payback	Discounted Payback
2/2.5	+12.6%	26.3%	11.4	14.3
1.5/2	+15.4%	26.9%	11.1	13.8

Table 23. Techno-economic indicators for a reduction in the start-up duration.

Based on the experience with the RamPharma plant, the start-up duration of the DSG plant could be near 2 hours depending on night losses and other variables such as the operational conditions, steam drum level, size, etc. For that reason, the plant has been simulated for lower start-up times, assuming that better conditions, control systems and a more detailed study of the specific behaviour of the case study could improve the performance of the plant during this phase.

Three scenarios have been simulated: the base case (2.5/3h), a second one with a reduction of half-hour both for winter and the rest of the seasons (2/2.5h), and a third case with another half-hour reduction (1.5/2h). The results show clearly that the first reduction implies a notable increase in the yield (+12.6%) while the shortest start-up duration does not have a proportional increase on the yield

(+15.6%). This result may show that there is a minimum time that the system needs until it starts generating steam at 158ºC, regardless of whether the steam generated is used to reach the operational pressure or it is directly consumed by the user. For that reason, the assumption made of selecting a start-up duration to consider the dynamic of this phase has a limited error based on the minim time that the plant requires to reach 158 ºC.

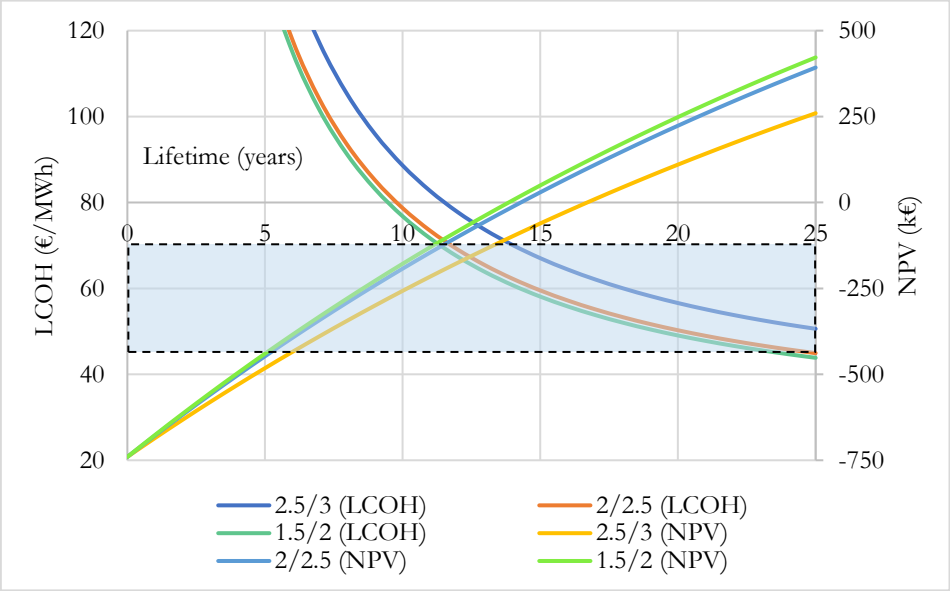

Figure 78. LCOE and NPV curves along the lifetime of the plant for different start-up durations.

The graph above shows, for the whole lifetime of the project, how the LCOH and the NPV evolve for different start-up durations. It can be seen the difference between the base case and the second scenario, and how the LCOH could compete with the NG prices after the year 12. It is also shown that, even though the LCOH curves are parallel between the three cases, it does not occur the same with the NPV; the tilt of the shorter start-up durations make the curve have better results as the lifetime passes.

7.2.3 Demand curve

The demand curve varies a lot from one factory to another, especially if the solar integration is at process level as the demand depends on the specifications of that process. In this case, the integration at supply level gives more flexibility to the solar plant as it is a complement to the steam boiler generation and it delivers the solar steam to the grid of the user, which will be later consumed in the process that requires it at the time.

In this case, the analysis is not related to the shape of the demand curve, but its duration along the week. In many SMEs is it found that Sunday is not a working day; for that reason, companies such as Solatom in Spain must consider that the solar plant only delivers steam six days of the week, instead of the whole time. As the simulation made for the case study is for a typical year and it does not specify the days of the week, an estimation is made by reducing the steam and demand by one septime over the year. The results are shown in the next table:

Economic indicator	Values for the new case: 6/7	Variation (%)
LCOH	59.0 €/MWh_{th}	+17
Simple Payback	15.3 years	+18
Discounted Payback	20.7 years	+24
Net Present Value	109,212 €	-58
IRR	5.9 %	-22

Table 24. Economic indicators for the case of six working days per week and its variation with respect to the base case.

The results show that, even though the technical indicators such as the solar fraction or the solar field efficiency remain constant because both demand and steam generation has been reduced equally, the economic analysis depicts an important change. The simple and discounted payback periods have increased 2.3 and 4 years respectively, whilst the NPV shows the biggest variation with respect to the base case as it has decreased by more than a half.

This calculation proves the importance of the working times of the factory and how it should be considered. To include these considerations during the design of the solar plant is necessary for an adequate dimensioning of the utility and achieve a more positive results in techno-economic analysis.

7.2.4 CAPEX and OPEX

Changes in the CAPEX and OPEX must be analysed as the selected ones are generic data based on literature and are not calculated for the specific case in detail.

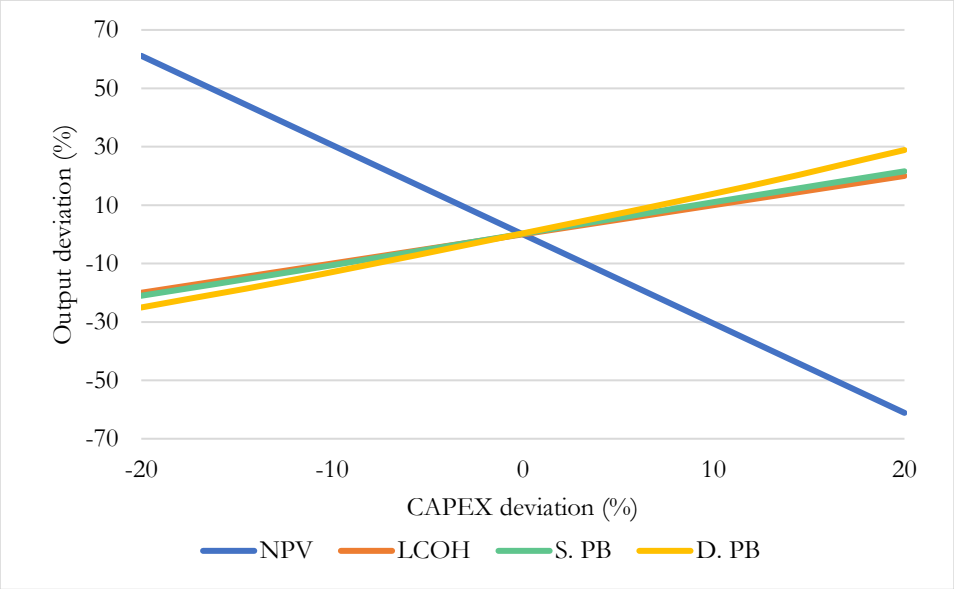

Figure 79. Sensitivity analysis for economic indicators under CAPEX deviations.

A deviation in the CAPEX of +-20% means an investment cost within the range of 592,000 to 888,000 €. The resulted outputs for various economic indicators show that this variation can change the LCOH and the payback by 30%, reaching LCOH values of 40.5 €/MWh; a very competitive price in comparison with the range of prices established for the NG. Furthermore, the most affected indicator by changing the CAPEX is the NPV. It means that this value can vary 60% just by reducing

20% the investment, which means that any saving in the construction of the plant and its components is a great improvement in the feasibility of the project.

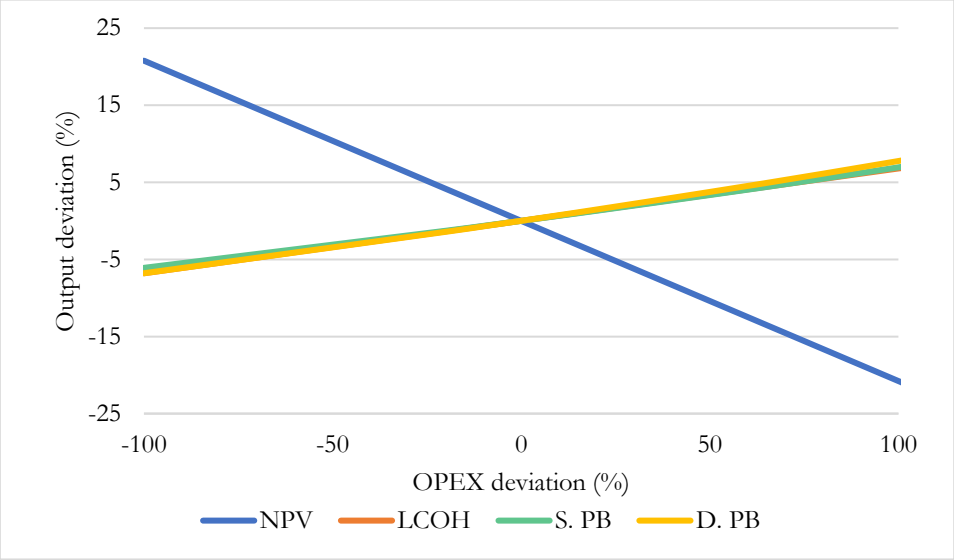

Figure 80. Sensitivity analysis for economic indicators under OPEX deviations.

As it is depicted in the figure above, the impact of the OPEX on the economic results is not remarkable in comparison with the results from CAPEX variations. The deviation of the OPEX required to visualize an influence on the results is 100% of its value, which means the range of 0 to 1% of the CAPEX. As it happened before, the most affected indicator is the NPV, which varies 20% in the extremes. Even though it is assumed that the cost of maintenance and operation for the plant is regular over the years, it may increase as the components get older and need to be replaced. However, this fact is partially considered in the calculation of the LCOH as a degradation factor that decreases the total yield along the lifetime of the project.

7.2.5 NG price and inflation

The natural gas price is one of the main drivers for investing in solar heat technology. This price can vary with the location if the industry is in a region with difficulties accessing it or are far from the extraction. Another factor that increases the NG price is the size of the company since an SME do not have the same conditions as a big company. Moreover, the natural gas price tends to vary over time and it is expected to grow by 2%/year.

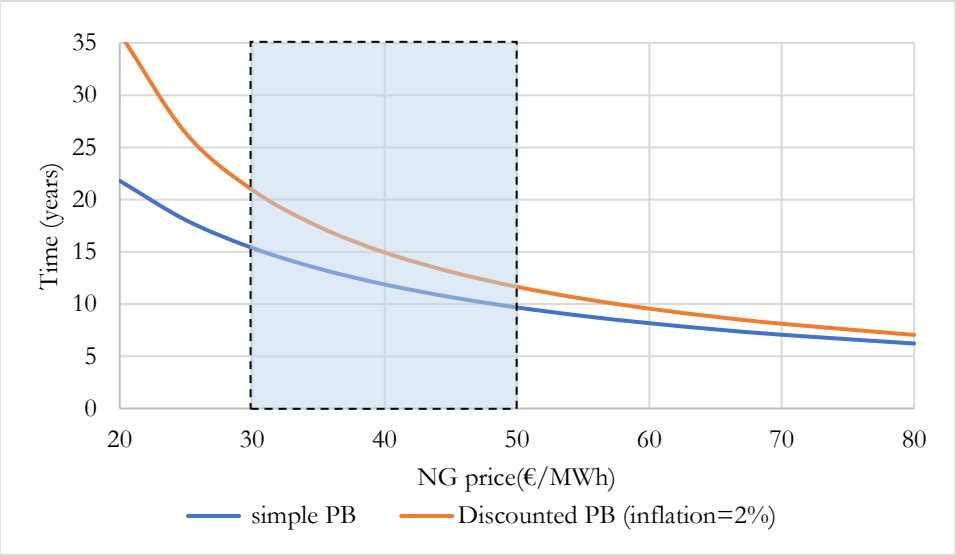

Figure 81. Sensitivity analysis of the payback periods based on a variation of the NG price.

The blue region in Figure 81 shows the range of prices for NG in Europe, nevertheless, the fuel used may vary as well as its price so higher values may be found for SME industries. For example, fuel oil prices such as 63 €/MWh could be found as an acceptable value for SMEs [101] and have payback periods between 5 and 10 years, way more attractive for industrial users. It is remarkable as a feasibility boundary that prices above 50 €/MWh present payback periods lower than 10 years.

In addition to this, the discount payback differs from the simple for low NG prices, what makes integrating solar heat technology in countries with low NG prices, such as the US, or projects with high discount rate a less feasible option due to the time factor.

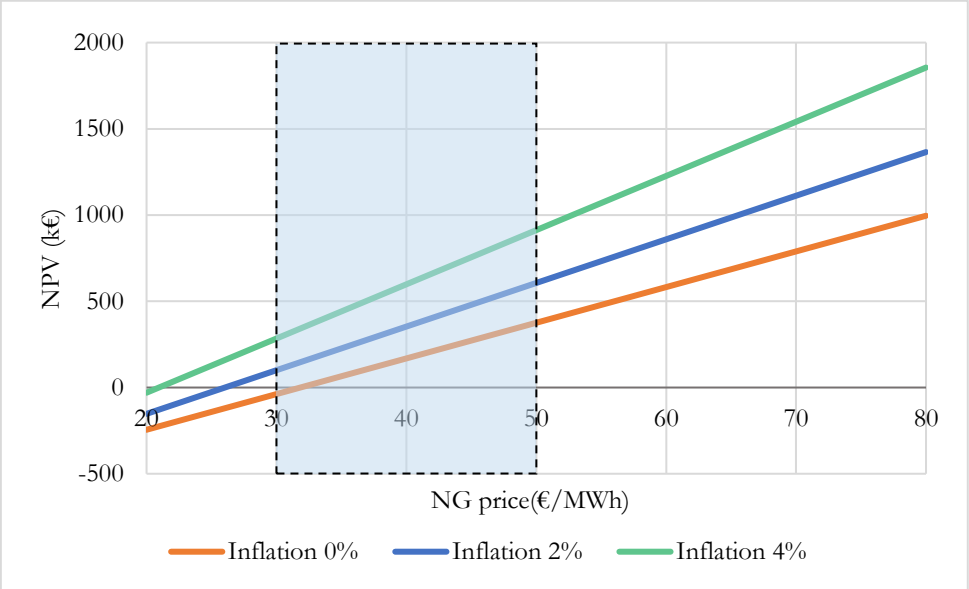

Figure 82. Sensitivity analysis of the NPV under different NG prices and inflations.

In the graph above three different inflation values are considered. This inflation is difficult to be predicted but is necessary to be studied in order to anticipate future trends of the NG market. All the scenarios with NG prices below 20 €/MWh do not generate any profits so the solar plant should not be constructed. On the other side, for the range of European NG prices, it is depicted that NPV is positive, especially if the inflation is counted. It is shown on the left side of the graph that, as expected,

when the NG price grows the inflation has a greater impact on the final NPV hence the high costs of the fuel make the solar savings increase with respect to the BAU scenario.

7.2.6 Discount rate analysis

In this case, the discount rate selected was assumed to be the same value as the WACC, which is used for the LCOH calculation. This is the weighted average capital cost and is useful for the company to measure the influence of the time factor and decide whether invest money in the project. The great impact of this parameter on the NPV can be seen in Figure 83, where it is reduced by 110% for high discount rates. Moreover, the NPV can be negative for discount rate values of 8% and above. On the contrary, the expected profits with low discount rates make the NPV more than double its value, reaching LCOH and discounted payback periods about 25% lower.

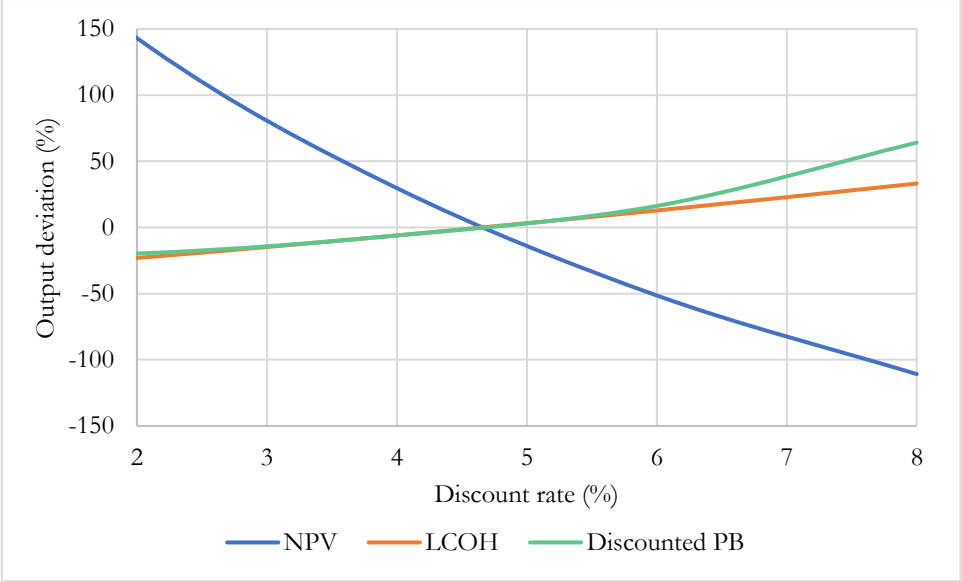

Figure 83. Sensitivity analysis for economic indicators under different discount rates.

Both the LCOH and discounted payback shows a similar reduction for low discount rates, however, for higher values, the payback starts increasing and getting above the lifetime of the solar plant. The range of LCOH seen in Figure 83 is 31-67 €/MWh, still a competitive price for the solar heat with respect to fossil fuels considering the 25 years analysis period.

7.2.7 EU ETS

The cost for generating GHG emissions was not a driver to implement solar technologies until the price of the EU ETS rose in 2018. Knowing that this change was made by the EU to accelerate progress towards the 2030 goals and that the sustainable development goals will require to cut way more emissions than the ones of today's world, it is necessary to study different scenarios where the pollution caused by burning natural gas have a bigger share of the industrial costs.

The ETS trends have been analysed by multiple organizations and the expected price range for a EUA is 56-89 €/tCO_2 by the year 2030 [102], making fossil fuels a more costly option for supplying heat in industry each year. As it is shown in Figure 84, the total price of NG will be increased by this penalty for pollution and, considering the costs for 2030, the ETS impact will be between a quarter and a third of the total NG cost in less than ten years, a significant share. If the conventional efficiency of 80% for heat generation is considered, the cost of producing an MWh of heat with NG increases

a 20%. This new price is shown as the orange line and causes solar plants to be a more feasible option as a competitive LCOH is achieved in a shorter time.

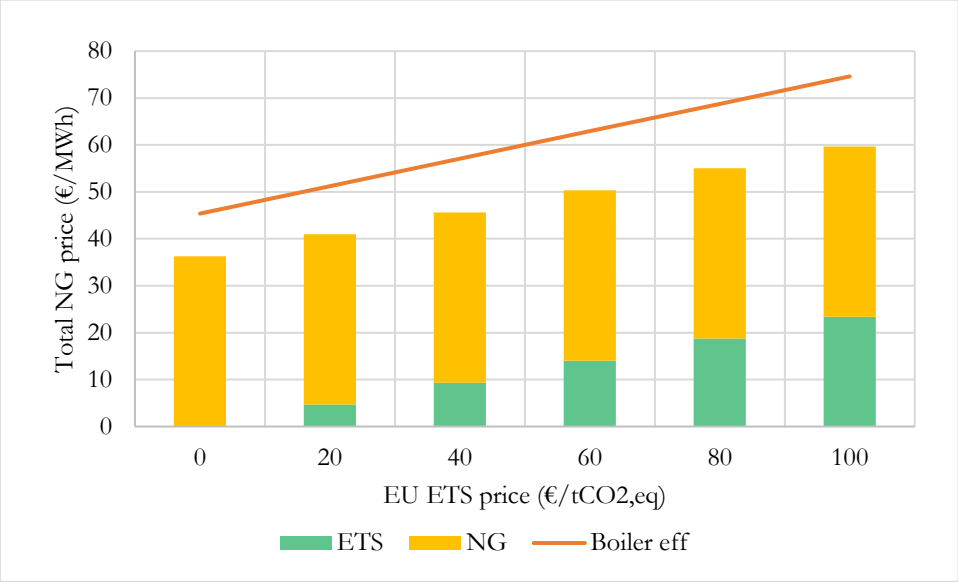

Figure 84. Total NG Price considering the ETS cost and boiler efficiency under different ETS prices.

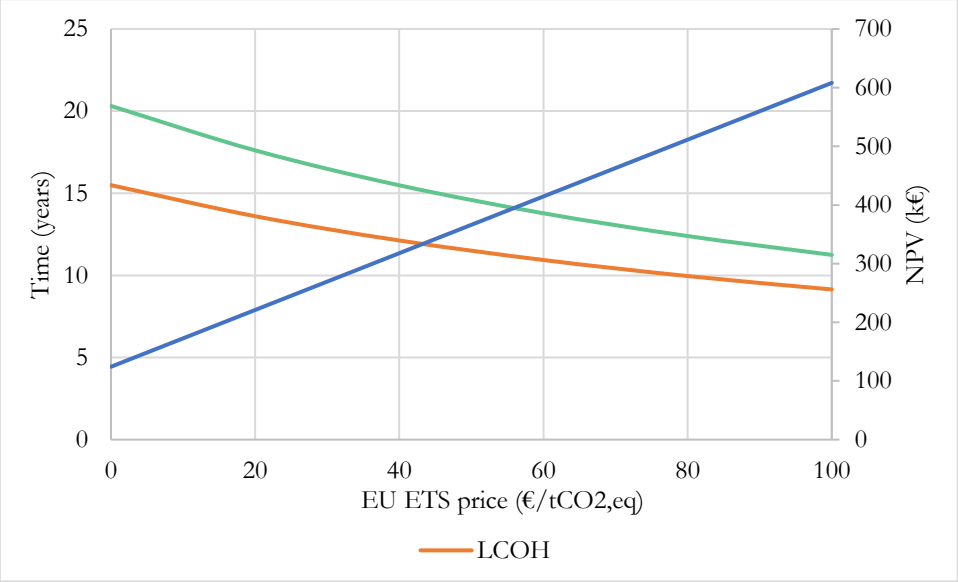

Figure 85. Sensitivity analysis of the payback periods and the NPV under different ETS prices.

The figure above shows how the payback periods could be reduced by 4 to 6 years approximately just counting on the growth of the ETS costs. The NPV is benefited as well by this increment and, even though a 0 €/tCO$_2$ price would not imply a negative NPV, the ETS contribution to make the solar plant a profitable business is remarkable.

7.2.8 Case scenario with suitable conditions for SHIP integration

The previous analysis is performed to assess how the techno-economic indicators are affected by the input parameters of the SHIP plant and what are the main drivers for achieving a feasible project. As a result, suitable conditions for solar heat deployment based on the case study can be achieved with

favourable levels of DNI, investment, NG prices and the cost of emissions. These conditions are described in the next table based on cost estimations made by Solatom and its developed simulation tool [101]. Changes have been proposed in terms of CAPEX, fuel price and inflation for an SME. The rapid growth in the EU ETS price is also considered.

Parameter	Value
CAPEX	600,082 € (315.7 €/m²)
OPEX	0.5%
Fuel price	58 €/MWh
Fuel inflation	3.5%
Discount rate	4.66%
EU ETS costs	35 €/$tCO_{2,eq}$

Table 25. New values for economic parameters with Solatom references for an SME.

Economic indicator	Value
LCOH	41.03 €/MWh_{th}
Simple Payback	6.6 years
Discounted Payback	7.2 years
Net Present Value	1,249,346 €
IRR	17.8 %

Table 26. Economic indicator results for the new case of an SME based on Solatom references.

The new results provide an example of how this technology could be a profitable investment for industries where the fuel is bought with prices high above the ones that big companies get. Moreover, the resulted LCOH is very competitive with fossil fuels prices and the new payback periods make the option of integrating solar heat in industry a less risky option.

Even though this study has been made assuming that the conventional fuel used for generating steam is natural gas, it is possible to conclude that higher prices of the fuel are needed to achieve feasible results for implementing solar heat systems, therefore, other types of fuels should be considered as well. The case of fuel oil is especially interesting as its price is higher than the NG, about 58 €/MWh as it was referenced from Solatom data, hence representing factories that use this fuel as a suitable market for solar heat. This fact may also be motivated by the lack of infrastructure that could easily send NG to those industries.

7.3 Results feedback to the market analysis

The results from the case study do not only provide an assessment of the feasibility of SHIP systems and the driving conditions for this technology to be deployed, but also is a useful tool for tuning the Multi-Criteria Analysis performed in previous steps of the study.

The criteria and weights selected for determining which is the solar heat potential market for a country were based on the literature reviewed, the discussions with the expert on the field and the supervisor of the study Rafael Guédez Mata, and the useful tool of the Pairwise comparison matrix (see section 11.1 11.1Appendix 1: Multi-Criteria Analysis). Nevertheless, as the weights selected for each criterion

are fundamental for calculating the MCA scores, it is necessary to perform an iterative process to provide feedback to this analysis from the results achieved in the case study. The main drivers for achieving positive indicator values in the case study are mainly the solar resource, the price of the conventional fuel, the emissions tax cost from the ETS and the plant costs presented in the CAPEX.

As the MCA directly affects to the countries selected as potential markets, the variations on the weights related to the NG price and the solar resource might affect the TOP 10 European countries list that was established. Moreover, the specific share of renewable energies on the different industrial sectors described in Table 13 is also applied to the heat consumption values to provide more accurate results.

By including the share of renewable energies in the MCA Finland and Sweden are the only ones affected as the paper and pulp industry is responsible for most of their industrial heat consumption, and this sector has a great share of renewable energies due to the biomass potential for their waste. Finland has moved down in the ranking two positions while Sweden is out of the top 10.

Finally, the NG price weight has been increased 5% and the solar resource 5.7% reducing as well proportionally the weights for the rest of the criteria.

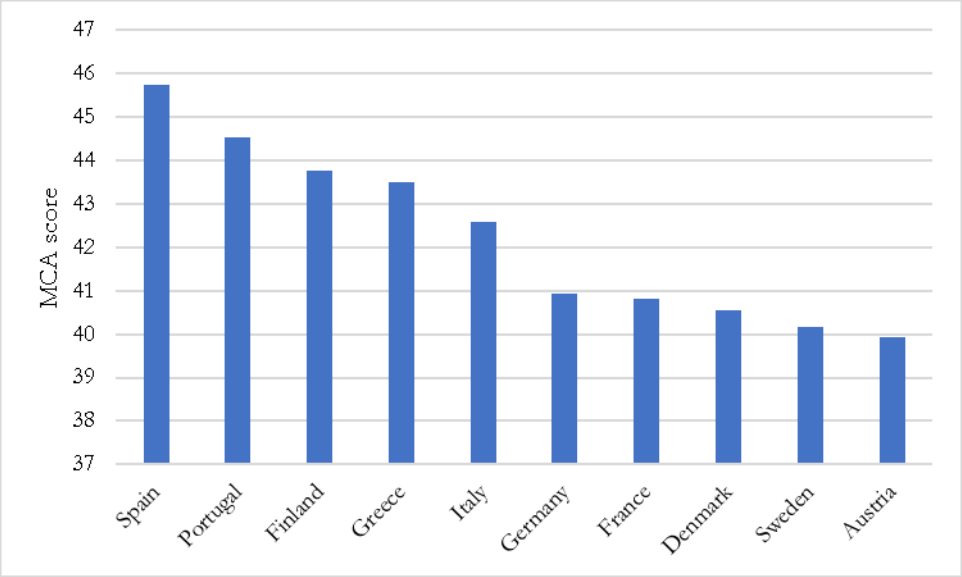

Figure 86. MCA scores for the top 10 European countries after modifying criteria weights.

As it is shown in the above figure, by increasing these two criteria the results do no change greatly the top 10 European countries. The main variation is that Denmark has raised and Netherlands disappeared, what is a consequence of the high prices for natural gas that Denmark shows

In conclusion, it is especially interesting the importance of these two factors, the solar resource and fuel price, for creating feasible conditions. Taking into account the location of the factory, it should not be forgotten the availability of fuel, that is why this kind of technology is succeeding in been integrated where the NG infrastructure does to reach the factory and other types of fuels such as fuel oil are used in the conventional heating systems.

8 CONCLUSION

The objectives of the project have been achieved as the thesis has been completed with the following conclusions:

- The current background of environmental and energy crisis and the huge heat demand in industry at low temperature has been described as drives for the implementation of solar thermal technologies aiming to reduce emissions in this sector.
- Solar thermal technologies, their integration, and main design parameters have been reviewed through literature.
- The most promising industrial sectors and processes have been identified based on the heat demand and temperature requirements.
- An MCA has been performed to determine the SHIP potential market based on geographical boundaries.
- A case study has been selected, based on the previous market assessment, and modelled in TRNSYS. The system characterization is a Fresnel direct steam generation plant located in Sevilla (Spain) based on the information provided by the company Solatom.
- A techno-economic analysis has been performed on the case study and the feasibility boundaries have been assessed through a sensibility analysis. The main driver conditions for the SHIP deployment have been hence analysed.

The urgency to reduce GHG emissions for fighting climate change as well as the global high dependency on fossil fuels for energy supply have allowed renewable energies to take a step into the energy market. The industrial sector not only has a big contribution to the global emissions but also a low share of renewable energy for covering the heat demand. Knowing that most of the energy consumption in industry is heat and that half of it is at medium-low temperature (below 400 ºC), it is a great market for the integration of solar thermal technologies.

The current state of deployment of solar heat systems does not have a notable impact on industry despite having a greater expansion in other sectors such as buildings. The necessary technology for SHIP integration exists and a study of the market potential has been assessed in order to enhance its deployment.

The integration of solar heat could be done both at supply and process level, providing hot air, water, steam, or oil to industrial activities such as pasteurization, drying, cooking or cleaning. With the criteria of high heat demand and low-temperature requirements, five promising sectors have been analysed: food and beverage, paper and pulp, chemical, textile and mining. Steam generation at the supply level has been considered as one of the most promising systems taking into account its integration advantages and the potential of direct steam generation plants.

The potential market has been geographically determined by performing an MCA; countries all over the world have been assessed considering their heat consumption in the selected sectors and other conditions that enhance the techno-economic SHIP feasibility such as solar radiation levels, favourable energy policies, previous experience in SHIP plants, ease of doing business environment, etc. The price of natural gas has been also considered after selecting Europe as a suitable market for solar heat technologies.

The SHIP market has been addressed by estimating the potential heat demand that this technology could cover considering limitations such as the competitiveness with other renewable heat sources, the expected heat recovery potential, the solar fraction, and roof space availability in factories. The results show that the five countries with bigger potential are Germany, France, Netherlands, Italy, and Spain, while the sectors with the most potential market are food and beverage, and chemical.

A case study has been selected based on the previous conclusions: a direct steam generation plant with Fresnel collectors in Sevilla, south of Spain. The company which has provided the necessary information for characterizing the system is Solatom, which has been working in the last years implementing solar heat systems in the meat industry in Spain. The plant has been modelled using the software TRNSYS, taking special consideration in the Fresnel performance, the dynamic steam drum behaviour and its influence on the plant start-up duration.

The results achieved through the techno-economic analysis show that parameters such as solar radiation, conventional fuel prices and EU ETS prices have a major impact on economic indicators including the payback period or the NPV. A sensitivity analysis shows that locations with radiation values above 1750 kWh/m² have positive values for NPV, and above 2250 kWh/m² the cost of generating solar heating (LCOH) is under European natural gas prices. In addition to this, fuel prices above 50 €/MWh depict payback periods under 10 years. The future trends indicate a favourable scenario for the deployment of SHIP technology as European policies are causing rapid growth in the ETS price and the investment cost as well as the risk for the investor may decrease while the experience with solar heat in industry expands. Moreover, this technology seems like a suitable alternative for SMEs since they have higher fuel prices compared to big companies. This could also apply to industries in locations with difficult connection to natural gas suppliers but with high radiation levels.

In addition to this, regions near the equator such as Latin America, Africa or South Asia with high radiation level show a big technical potential for SHIP that has been affected due to high rates of corruption, low values of the ease of doing business indicator or low experience and investment in this technology. Nevertheless, countries from these zones such as Mexico, Chile or India has proved that the deployment of this technology could be enhanced with supportive policies that promote renewable heat, along with international cooperation to share experience and knowledge. Solar heat in industrial processes is a feasible alternative (or a complement) to conventional systems under certain conditions that have been analysed in this study, helping to reduce the dependency of the industrial sector on fossil fuels and reducing the GHG emissions towards the sustainable development scenario.

9 FURTHER RESEARCH

This section aims to suggest new research paths that could be followed to keep a further analysis of solar heat in industry. The first research suggestions are related to the potential market analysis:

- The heat potential of other industrial sectors such as iron and steel or machinery.
- The evolution of the promising countries in growing economies with high radiation levels.
- Appropriate policies to enhance SHIP technologies in locations with difficult connections to fuel suppliers.

Moreover, some suggestions are made in order to improve the results of this work and help to provide more accurate results for further research:

- The creation of a TRNSYS model for a steam drum capable to simulate pressure variations with dynamic behaviour.
- The incorporation of advanced control strategies into the system.
- A comparison between different tools for solar direct steam generation modelling.

10 BIBLIOGRAPHY

[1] United Nations, "Policy Brief 15, interlinkages between energy and climate," UN, 2018.

[2] United Nations, "What is the Paris Agreement?," [Online]. Available: https://unfccc.int/process-and-meetings/the-paris-agreement/what-is-the-paris-agreement. [Accessed 15 10 2020].

[3] IEA, "Renewables 2019 Market analysis and forecast from 2019 to 2024," IEA, París, 2019.

[4] IEA-ETSAP and IRENA, "Solar Heat for Industrial processes. Technology Brief," 2015.

[5] IEA-SHC, "Solar Heating & Cooling Programme," IEA, [Online]. Available: https://www.iea-shc.org/. [Accessed 15 10 2020].

[6] United Nations, "UN Report: Nature's Dangerous Decline 'Unprecedented'; Species Extinction Rates 'Accelerating'," 06 05 2019. [Online]. Available: https://www.un.org/sustainabledevelopment/blog/2019/05/nature-decline-unprecedented-report/. [Accessed 25 03 2021].

[7] IEA, "Global CO2 emissions in 2019," 11 02 2020. [Online]. Available: https://www.iea.org/articles/global-co2-emissions-in-2019. [Accessed 25 03 2021].

[8] IEA, "Data and statistics," 16 11 2020. [Online]. Available: https://www.iea.org/data-and-statistics?country=WORLD&fuel=CO2%20emissions&indicator=CO2BySector. [Accessed 25 03 2021].

[9] United Nations, "THE 17 GOALS," [Online]. Available: https://sdgs.un.org/goals. [Accessed 25 03 2021].

[10] IEA, "World Energy Model," 10 2020. [Online]. Available: https://www.iea.org/reports/world-energy-model/sustainable-development-scenario. [Accessed 25 03 2021].

[11] A. Prag, *The IEA Sustainable Development Scenario,* Katowice: IEA, 2018.

[12] IEA, "World Energy Outlook 2020," IEA, Paris, 2020.

[13] IEA, "Renewables 2020, Analysis and forecast to 2025," IEA, Paris, 2020.

[14] M. H. N. R. L. Kumara, "Global advancement of solar thermal energy technologies for industrial process heat and its future prospects: A review," *Energy conversion and management,* vol. 195, pp. 885-908, 2019.

[15] C. Philibert, "Renewable Energy for Industry," OECD/IEA, París, 2017.

[16] Solar Payback, "Solar heat for industry," 2017.

[17] S. K. e. al, "Traditional Biomass Energy," in *International Conference for Renewable Energies*, Boon, 2004.

[18] M. K. K. M. P. Siddharth Suman, "Performance enhancement of solar collectors—A review," *Renewable and Sustainable Energy Reviews,* no. 49, pp. 192-210, 2015.

[19] R. D. L. V. F. A. L. Evangelisti, "Latest advances on solar thermal collectors: A comprehensive review," *Renewable and Sustainable Energy Reviews,* no. 114, 2019.

[20] R. M. e. al, "Performanceofevacuatedflatplatesolarthermalcollectors," *Thermal science and engineering progress,* no. 8, pp. 296-306, 2018.

[21] G. V. e. al, "Solar thermal collectors," in *Solar Hydrogen Production*, Academic Press, 2019, pp. 151-178.

[22] J. J. e. al, "Chapter 12- Concentrating Solar Power," in *Advances in Renewable Energies and Power Technologies*, Elsevier, 2018, pp. 373-402.

[23] A. B. e. al, "Modeling and design of solar heat integration in process industries," *Journal of Cleaner Production,* no. 170, pp. 522-534, 2018.

[24] L. L. H. X. F. G. Alva G, "Thermal energy storage materials and systems for solar energy applications," *Renewable Sustainable Energy Rev.,* no. 68, pp. 693-706, 2017.

[25] S. H. R. L. H. Mads Troldborg, "Assessing the sustainability of renewable energy technologies using multi-criteria analysis: Suitability of approach for national-scale assessments and associated uncertainties," *Renewable and Sustainable Energy Reviews,* no. 39, pp. 1173-1184, 2014.

[26] S. Kalogirou, "The potential of solar industrial process heat applications," *Applied Energy,* vol. 73, p. 337–361, 2003.

[27] B. M. e. al, "Task 49 -Solar Process Heat for Production and Advanced Applications: Integration Guideline," IEA SHC, 2015.

[28] D.-I. B. Schmitt, "Classification of industrial heat consumers for integration of solar heat," *Energy Procedia,* vol. 91, pp. 650-660, 2016.

[29] R. S. A. S. S. Mekhilef, "A review on solar energy use in industries," *Renewable and Sustainable Energy Reviews,* vol. 15, pp. 1777-1790, 2011.

[30] A. K. Om Prakash, "Historical Review and Recent Trends in Solar Drying Systems," *International Journal of Green Energy,* no. 10(7), pp. 690 -738, 2013.

[31] B. P. S. F. J. F. Zhiyong Tian, "Analysis and validation of a quasi-dynamic model for a solar collector field with flat plate collectors and parabolic trough collectors in series for district heating," *Energy,* no. 142, pp. 130-138, 2018.

[32] G. B. e. al, "Chapter 6 - Solar Thermal Collectors," in *Solar Hydrogen Production*, Academic Press, 2019, pp. 151-178.

[33] France's Alternative Energies and Atomic Energy Commission, "D2.3 Key Performance Indicators to evaluate the integration of solar heating in industrial processes," European Comission, 2018.

[34] IRENA, "A background paper to "Renewable Energy in Manufacturing"," IRENA, Abu Dhabi, 2015.

[35] T. F. e. al, "Mapping and analyses of the current and future (2020 - 2030) heating/cooling fuel deployment (fossil/renewables)," European Commission, 2016.

[36] Office of Energy Efficiency & Renewable Energy, "Energy Efficiency Vs. Energy Intensity," U.S. Department of Energy, [Online]. Available:

https://www.energy.gov/eere/analysis/energy-efficiency-vs-energy-intensity. [Accessed 14 11 2020].

[37] European Union, JRC scientific and policy reports: Heat and cooling demand and market perspective, Luxembourg: EU, 2012.

[38] U.S. Energy Information Administration, "International Energy Outlook 2016," Washington DC, 2017.

[39] S. F. e. al., "Solar process heat in industrial systems – A global review," *Renewable and Sustainable Energy Reviews,* vol. 82, pp. 2270-2286, 2018.

[40] C. B. A. G. Juergen Fluch, "Potential for energy efficiency measures and integration of renewable energy in the European food and beverage industry based on the results of implemented projects," *Energy Procedia,* no. 123, pp. 148-155, 2017.

[41] M. H. e. al, "Solar process steam for pharmaceutical industry in Jordan," *Energy Procedia,* no. 70, pp. 621-625, 2015.

[42] G. Q. e. al., "Analyzing the potential for solar thermal energy utilization in the Chilean copper mining industry," *Solar energy,* vol. 197, pp. 292-310, 2020.

[43] B. M. Pierre Krummenacher, "IEA SHC Task 49: Solar Process Heat for Production and Advanced Applications, Methodologies and Software Tools for Integrating Solar Heat," IEA, 2015.

[44] B. S. U. J. K. V. C. Lauterbach, "The potential of solar heat for industrial processes in Germany," *Renewable and Sustainable Energy Reviews,* no. 16, pp. 5121-5130, 2012.

[45] R. B. S. D. Claudia Vannoni, "Potential for Solar Heat in Industrial Processes," Solar Heating and Cooling Executive Committee of the International Energy Agency (IEA), 2008.

[46] M. S.-D. Werner Weiss, "Solar Heat Worldwide: Global Market Development and Trends in 2019, Detailed Market Data 2018," AEE INTEC, Austria, 2020.

[47] "Database for applications of solar heat integration in industrial processes," AEE INTEC, [Online]. Available: http://ship-plants.info/. [Accessed 6 10 2020].

[48] S. B. W. Z. Holger Müllera, "Development of an evaluation methodology for the potential of development of an evaluation methodology for the potential of," *Energy procedia,* no. 48, pp. 1194-1201, 2014.

[49] S. Kalogirou, "The potential of solar energy in food-industry process heat applications," 2006.

[50] A. K. S. e. al, "Potential of Solar Energy Utilization for Process Heating in Paper Industry in India: A Preliminary Assessment," *Energy Procedia,* no. 79, pp. 284-289, 2015.

[51] IEA, "World energy balances, IEA World Energy Statistics and Balances (database)," 2020. [Online]. Available: https://doi.org/10.1787/data-00512-en . [Accessed 20 10 2020].

[52] IRENA, "Global Renewables Outlook: Energy transformation 2050," International Renewable Energy Agency, Abu Dhabi, 2020.

[53] Solar Payback, "Solar Heat for Industry: South Africa," Berlin, 2017.

[54] M. P. e. al, "Industrial waste heat: Estimation of the technically available resource in the EU per industrial sector, temperature level and country," *Applied Thermal Engineering,* no. 138, pp. 207-216, 2018.

[55] Solar Payback, "Suppliers of Turnkey Solar Process Heat Systems," [Online]. Available: http://www.solar-payback.com/suppliers/. [Accessed 16 11 2020].

[56] REN21.2020, "Renewables 2020 Global Status Report," Paris, 2020.

[57] European Union, "EU Action, Climate strategies & targets," EU, [Online]. Available: https://ec.europa.eu/clima/policies. [Accessed 4 11 2020].

[58] European Union, "European Green Deal," [Online]. Available: https://ec.europa.eu/info/strategy/priorities-2019-2024/european-green-deal_en. [Accessed 04 11 2020].

[59] European Union, "The Just Transition Mechanism: making sure no one is left behind," [Online]. Available: https://ec.europa.eu/info/strategy/priorities-2019-2024/european-green-deal/actions-being-taken-eu/just-transition-mechanism_en. [Accessed 04 11 2020].

[60] European Union, "EU Action, EU Emissions Trading System (EU ETS)," [Online]. Available: https://ec.europa.eu/clima/policies/ets_en. [Accessed 04 11 2020].

[61] European Union, "In focus: Renewable energy in Europe," [Online]. Available: https://ec.europa.eu/info/news/focus-renewable-energy-europe-2020-mar-18_en. [Accessed 04 11 2020].

[62] N. J. e. al, "2 - Principles of CSP performance assessment," in *The Performance of Concentrated Solar Power (CSP) Systems*, Elsevier, 2017, pp. 31-64.

[63] Solargis, "Global Solar Atlas," 2019. [Online]. Available: https://globalsolaratlas.info/download. [Accessed 21 10 2020].

[64] S. H. e. al, "POSHIP -The Potential of Solar Heat for Industrial Processes," 2001.

[65] P. Kovacs, Solenergi i industriell processvärme : en förstudie av svenska möjligheter, Sweden: Borås, 2003.

[66] M. T. e. al, PROMISE - Produzieren mit Sonnenenergie: Potenzialstudie zur thermischen Solarenergienutzung in österreichischen Gewerbe und Industriebetrieben, Wien: Studie im Auftrag des Bundesministerium für Verkehr, Innovation und Technologie, 2004.

[67] Solar Payback, "Calor solar para la industria: México," Solar Payback, 2018.

[68] M. M. Mokhtar, "Control of Solar Thermal LinearFresnel Collector Plants in SinglePhase and Direct Steam Generation Modes," Karlsruher Institut f¨ur Technologie (KIT), Doctoral Thesis, Karlsruhe, 2019.

[69] A. Frein, "Modeling, optimization and experimental evaluation of Solar Direct Steam Generation for integration into industrial heating processes," Politecnico di Milano, Department of Energy, Milano, 2017.

[70] Solatom, "Who is Who, Estudio geolocalizado del potencial de aplicaciones de calor solar de proceso en media temperatura," Solar Concentra, 2017.

[71] M. M. e. al, "Direct Steam Generation for Process Heat using Fresnel Collectors," *International Journal of Thermal & Environmental Engineering,* vol. 10, no. 1, pp. 3-9, 2015.

[72] Solatom, [Online]. Available: https://www.solatom.com/. [Accessed 20 11 2020].

[73] M. E. Wolf-Dieter Steinmann, "Buffer storage for direct steam generation," *Solar Energy,* vol. 80, p. 1277–1282, 2006.

[74] EN/TC 312, *EN 12975-2:2006 Thermal solar systems and components - Solar collectors - Part 2: Test methods,* Brussels: CEN, 2006.

[75] Technical Committee ISO/TC 180 "Solar, *EN ISO 9806:2007 Solar energy - Solar thermal collectors - Test methods (ISO,* Brussels: CEN, 2007.

[76] Z. Tian, "PhD Thesis: Solar heating plants with flat plate collectors and parabolic trough collectors," Technical University of Denmark, Lyngby, 2018.

[77] NREL, *System Advisor Model Version 2020.11.29,* Golden, CO: National Renewable Energy Laboratory, 2020.

[78] A. S. Alfaro, "Degree Project: Análisis de colectores solares de media potencia," University Carlos III, Madrid, 2016.

[79] L. V. R. L. -M. A. G. D. P. F. Sallaberry, "Heat Losses Model for Standardized Testing of Receiver Tubes for Parabolic-Troughs," in *AIP Conference Proceedings 2033, 030016*, 2018.

[80] A. K. T. e. al, "Structural analysis of absorber tube used in parabolic trough solar collector and effect of materials on its bending: A computational study," *Solar Energy,* no. 163, pp. 471-485, 2018.

[81] P. N. D. a. I. E. V. D. A. Shnaider, "Modeling the Dynamic Mode of Steam Accumulator," *Automation and Remote Control,* vol. 71, no. 9, p. 1994–1998, 2010.

[82] B. M. S. P. V. D. Stevanovic, "Dynamics of steam accumulation," *Applied Thermal Engineering,* vol. 37, pp. 73-79, 2012.

[83] M. B. e. al, "First year of operational experience with a solar process steam system for a pharmaceutical company in Jordan," *Energy Procedia,* no. 91, pp. 591-600, 2016.

[84] M. E. G. D. L. T. Van Cutsem, "Combined detailed and quasi steady-state time simulationsfor large-disturbance analysis," *Electrical Power and Energy Systems,* vol. 28, p. 634–642, 2006.

[85] B. C. e. al, "Dual-time scale based extending of the benchmark Tennessee Eastman process," *Computer Aided Chemical Engineering,* vol. 44, pp. 529-534, 2018.

[86] A. Häberle, "19 - Concentrating solar technologies for industrial Process Heat and Cooling," in *Concentrating Solar Power Technology*, Philadelphia, Woodhead Publishing, 2012, pp. 602-619.

[87] S. Hess, "3 - Solar Thermal Process Heat (SPH) Generation," in *Renewable Heating and Cooling*, Philadelphia, Woodhead Publishing, 2016, pp. 41-66.

[88] C. P. e. al, "Thermal energy storage evaluation in direct steam generation solar plants," *Solar Energy,* vol. 159, pp. 501-509, 2018.

[89] D. L.-N. e. al, "Combined storage system developments for direct steam generation in solar thermal power plants," in *ISES solar world congress*, 2011.

[90] MITERD/IDAE, "Balance de energía final," 2021. [Online]. Available: http://sieeweb.idae.es/consumofinal/. [Accessed 15 03 2021].

[91] Comisión Nacional de los Mercados y la Competencia, "Informe de supervisión del mercado de gas natural en España," Madrid, CNMC, 2020.

[92] Eurostat, "Gas prices for non-household consumers - bi-annual data (from 2007 onwards)," 11 03 2021. [Online]. Available: https://ec.europa.eu/eurostat/databrowser/view/nrg_pc_203/default/table?lang=en. [Accessed 16 03 2021].

[93] EMBER, "EUA Price," [Online]. Available: https://ember-climate.org/data/carbon-price-viewer/. [Accessed 27 11 2020].

[94] R. Guédez, "A Techno-Economic Framework for the Analysis of Concentrating Solar Power Plants with Storage," KTH Royal Institute of Technology, Department of Energy Technology, Doctoral, Stockholm, 2016.

[95] D. J. P. a. T. H. Walter Short, "A Manual for the Economic Evaluation of Energy Efficiency and Renewable Energy Technologies," NREL, Colorado, 1995.

[96] N. Sönnichsen, "Statista," 27 01 2021. [Online]. Available: https://www.statista.com/statistics/252791/natural-gas-prices/. [Accessed 18 03 2021].

[97] D. S. J. G.-H. S. S.-D. C. Marugán-Cruz, "Solar multiple optimization of a DSG linear Fresnel power plant," *Energy Conversion and Management,* no. 184, p. 571580, 2019.

[98] A. J. Melling, Natural gas pricing and its future, Europe as the Battleground, Washington: Carnegie Endowment for International Peace, 2010.

[99] G. C. D. Cocco, "Energy and economic analysis of concentrating solar power plants based on parabolic trough and linear Fresnel collectors," *Power and Energy,* vol. 229, no. 6, pp. 677-688, 2015.

[100] R. G. e. al, "Levelized cost of heat for linear Fresnel concentrated solar systems," *Energy Procedia,* no. 49, p. 1340 – 1349, 2014.

[101] SOLATOM, "Ressspi," 2018. [Online]. Available: https://www.ressspi.com/. [Accessed 25 03 2021].

[102] F. Watson, "Analysts see EU carbon prices at Eur56-Eur89/mt by 2030," 03 12 2020. [Online]. Available: https://www.spglobal.com/platts/en/market-insights/latest-news/coal/120320-analysts-see-eu-carbon-prices-at-eur56-eur89mt-by-2030. [Accessed 24 03 2021].

[103] Frankfurt School-UNEP Centre/BNEF, "Global Trends in Renewable Energy Investment 2020," Frankfurt School of Finance & Management gGmbH , Frankfurt and Main, 2020.

[104] The World Bank Group, "GDP (current $)," [Online]. Available: https://data.worldbank.org/indicator/NY.GDP.MKTP.CD. [Accessed 21 10 2020].

[105] Eurostat, "2.3 From where do we import energy and how dependent are we?," European Union, [Online]. Available: https://ec.europa.eu/eurostat/cache/infographs/energy/bloc-2c.html. [Accessed 21 10 2020].

[106] The World Bank Group, "Ease of Doing Business Scores," [Online]. Available: https://www.doingbusiness.org/en/data/doing-business-score. [Accessed 22 10 2020].

[107] Transparency International, "Corruption Perceptions Index," Transparency.org, [Online]. Available: https://www.transparency.org/en/cpi/2019. [Accessed 21 10 2020].

[108] IEA, "IEA Natural Gas Information Statistics," [Online]. Available: https://www.oecd-ilibrary.org/energy/data/iea-natural-gas-information-statistics/world-natural-gas-statistics_data-00482-en. [Accessed 28 10 2020].

11 APPENDIX

11.1 Appendix 1: Multi-Criteria Analysis

The MCA performed in this study has the aim of selecting the most appealing regions for the integration of solar heat systems in industry. The criteria used for this purpose have been chosen after a review of the solar field and the characteristics that make these systems technical and economically feasible. The main sources of this analysis are international databases such as the IEA and OECD. The first step for this selection process is the specification of the criteria selected based on this review (Table 27, Table 28, Table 29). Normalization is applied to maintain the values of the criteria between 0 and 100 in order to have a proper comparison between them. This normalization is made based on the higher value scored by a country, which has 100 points and becomes the reference for the rest. Some criteria have a specific scoring method that is explained in its definition described in the table. The pairwise comparison matrix (Table 32) is used for defining the weight of each criterion. This matrix is a useful tool to compare the importance of each criterion with regard to the others and based on the author experience.

The calculation of the final MCA's score for each country is made using the following equation:

$$Country_{Score} = \sum_{i} Criteria_i * Weight_i \qquad (33)$$

Finally, a last criterion is applied for the European countries as it is the selected region with higher market potential. The price of natural gas of each country is considered as described in Table 30.

Criteria	Definition and source	Weight
TFEC in five industrial sectors: **- Chemistry.** **- Food and beverage.** **- Paper, pulp and printing.** **- Textile and leather.** **-Mining.**	Aims to size the potential market. The total final energy consumed in promising industrial sectors for SHIP integration comes from the database of "OECD energy balances" [51]. Each sector has the same weight.	29.7 % (5.9 %/sector)
Sector national impact for five industries: **- Chemistry.** **- Food and beverage.** **- Paper, pulp and printing.** **- Textile and leather.** **-Mining.**	The measure of the impact or importance that one of the selected sectors have inside a country industry is calculated as the TFEC this sector consumption regarding the total consumption of the country industry [51]. Each sector has the same weight. $Sector\ national\ impact = \frac{TFEC_{Sector}}{TFEC_{Industry}}$	7.4 % (1.5 %/sector)

Table 27. MCA potential industrial sectors criteria group, definition, source and weight.

Criteria	Definition and source	Weight
Solar resource	Solar energy is the source of heat for this technology so its availability in the country is a basic technical criterion to assess SHIP potential [63]. The average global horizontal radiation is considered for each country.	22.9%
Renewable energy policies	Countries with policies that promote a transition from fossil fuels to renewable sources are taken into consideration. The score depends on the application by the country of three possible types of policy, each one with the same impact on the score: Renewable heat and cooling, solar thermal, and renewables in industry (Table 12) [56].	8.6%
Investment trends in renewable energy	Public and private investment in renewable projects indicates how likely is for a country to host these technologies. Half of this criteria (4% of the weight) takes into consideration the total investment in renewables in 2019 and the other half the ratio of the investment by the GDP of the country. This last one is necessary to consider how big is the investment in comparison with the economy of the country [103] [104].	8.1%
Experience in SHIP	The number of solar heat systems in industry that are currently operating is an indicator of the experience that the country has in SHIP projects and, therefore, it is keener to implement them [47].	7.5%
Dependence rate on natural gas imports	Solar energy used in industry provide energetic independence thanks to the reduction of fossil fuels consumption. Countries with high imports and low production of natural gas tend to rely on alternative sources as a solution for their external dependence [51] [105]. This parameter is calculated as follows: $$NG\ Dependence = \frac{NG_{imports} - NG_{exports}}{Total\ NG\ inland\ consumption}$$	1.93%
Power consumption in industry	Electrification of industrial heat is a trend that partially competes with solar heat. High power consumption in the industry of a country indicates a less available market for SHIP [51].	1.93%

Table 28. MCA Energy situation and resources criteria group, definition, source and weight.

Criteria	Definition and source	Weight
Ease of Doing Business	This indicator shows how much the regulatory environment for local entrepreneurs in an economy has changed over time in absolute and relative terms with respect to other economies. It is calculated considering multiple economic indicators that evaluate how easy is to start a business, get credit, trade across borders, etc [106].	9.7%
Index of Perceived Corruption (IPC)	IPC ranks countries from 0 to 100 by their perceived levels of public sector corruption, according to experts and business people [107].	2.3%

Table 29. MCA macro-environmental context criteria group, definition, source and weight.

Criteria	Definition and source	Weight
Natural gas price	High natural gas price is considered an important driver for companies to start using alternative energy sources such as solar. NG prices for non-householders are selected for the year 2019 [108].	5%

Table 30. MCA extra criterion for European countries.

The weights of each criteria were decided based on the results provided by the "Pairwise comparison matrix". As it is seen, the matrix compares each criterion of the right column with all the rest which are displayed in the top line. A value between 2 - 9 is given if the criterion is more important than the one with which it is being compared to, and values between 1/9 and 1/2 on the contrary. If both criteria are equal in importance, it is valued as a 1. The consistency ratio of the matrix is equal to 1.9%, lower than 6%, the accepted limit.

Pairwise comparison matrix

	C1	***C2***	***C3***	***C4***	***C5***	***C6***	***C7***	***C8***
C1	1	5	2	5	8	5	9	5
C2	1/5	1	1/3	1	2	1	4	1
C3	1/2	3	1	3	5	4	7	3
C4	1/5	1	1/3	1	2	1	4	1/2
C5	1/8	1/2	1/5	1/2	1	1/3	2	1/3
C6	1/5	1	1/4	1	3	1	5	1
C7	1/9	1/4	1/7	1/4	1/2	1/5	1	1/5
C8	1/5	1	1/3	2	3	1	5	1

Table 31. Pairwise comparison criteria.

On this second table it is shown the weights results after applying the comparison matrix and the definition of each of them:

Criteria	Description	Weights
C1	Energy consumption in potential sectors	37.1%
C2	Investment trends in RE	8.1%
C3	Solar resource	22.9%
C4	Experience in SHIP	7.5%
C5	NG external dependence	3.9%
C6	Energy policy (RE, Solar, RE industry)	8.6%
C7	Index of Corruption	2.3%
C8	Ease of doing business	9.7%

Table 32. Criteria weights result.

11.2 Appendix 2: Example of an industrial process integration using the Pinch analysis

The process consists of a food packaging line, in which ingredients are heated, cooked, and filled into jars. The jars are previously washed in a washer. The product is concentrated by evaporation during the cooking process. The available utilities are steam and cooling water respectively [27].

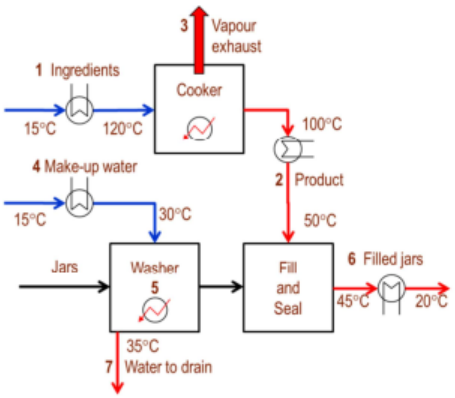

#	Name	T_{in} [°C]	T_{out} [°C]	Flow [kg/s]	c_p [kJ/kg^{-1}K^{-1}]	Heat rate [kW]
1	Ingredients heating	15	120	4.0	3.0	1260
2	Product cooling	100	50	3.6	2.8	500
3	Vapor condensation	80	79	0.4	1000	400
4	Washer make-up water	15	30	1.8	4.18	112.9
5	Washer lye bath holding	80	84	17.9	4.18	300
6	Filled jars cooling	45	20	6.0	2.0	300
7	Washer water to drain	35	20	1.5	4.2	94

Figure 87. Process flowsheet (left) and the corresponding list of process heat sources and heat sinks (right) of the food packaging line example process [27].